X-651-71-191
PREPRINT

NASA TM X- 65558

AIR-SEA INTERACTION IN THE TROPICAL PACIFIC OCEAN

LEWIS J. ALLISON
JOSEPH STERANKA
ROBERT J. HOLUB
JOHN HANSEN
FREDRIC A. GODSHALL
CUDDAPAH PRABHAKARA

MAY 1971

GSFC

GODDARD SPACE FLIGHT CENTER
GREENBELT, MARYLAND

X-651-71-191
PREPRINT

AIR-SEA INTERACTION IN THE TROPICAL PACIFIC OCEAN

Lewis J. Allison
Joseph Steranka
Robert J. Holub*
John Hansen*
Fredric A. Godshall**
Cuddapah Prabhakara

*Air Weather Service Member, U.S. Air Force
**National Oceanic and Atmospheric Administration

Goddard Space Flight Center
Greenbelt, Maryland

AIR-SEA INTERACTION IN THE TROPICAL PACIFIC OCEAN

ABSTRACT

An atlas of 3-monthly sea surface temperature anomalies in the eastern tropical Pacific Ocean was produced for the period 1949 to 1970.

Sea surface temperature anomalies along the U.S. and South American west coasts and eastern tropical Pacific, appeared to be oscillating in phase from 1949 to 1970. Similarly, the satellite-derived cloudiness for each of four quadrants of the Pacific Ocean, 130°E-100°W, 30°N-25°S were also pulsating in unison.

The sea surface temperature anomalies were found to have a good degree of correlation both positive and negative with the following monthly geophysical parameters.

(a) Satellite-derived cloudiness
(b) strength of the North and South Pacific semi-permanent anticyclone
(c) tropical Pacific island rainfall
(d) Darwin surface pressure.

Several strong direct local and cross – equatorial relationships were noted. In particular, the high degree of correlation between the tropical island rainfall and sea surface temperature anomalies ($r = +0.93$), permitted the derivation of sea surface temperatures in the tropics back to 1905.

The air-sea interactions indicated in this study could be potentially valuable in the prediction of the seasonal behavior of the tropical Pacific ocean and the atmosphere above it.

PRECEDING PAGE BLANK NOT FILMED

AIR-SEA INTERACTION IN THE TROPICAL PACIFIC OCEAN

INTRODUCTION

An understanding of the interaction of the tropical oceans with the atmosphere is important for the solution of problems concerning the varied time-period changes in the oceans and atmosphere. (Zipser, 1969, U.S. Committee for the GARP, 1969, Rasool and Hogan, 1969).

Description of large scale oceanographic processes over the tropical Pacific Ocean have been reported by eminent researchers, i. e.: Bjerknes, 1961, 1966 (a), (b), 1969 (a), (b), Berlage, 1966, Wyrtki, 1966, Roden and Reid, 1961, Roden, 1962, 1965, Shell, 1965. These climatological and analytical studies were made in the last decade despite the shortage of basic oceanographic data over large areas of the Pacific Ocean. Research efforts conducted during the 1960 STEP-I Expedition (Wooster, 1961), the 1963-1965 Trade Wind Zone Oceanography Pilot Study (Seckel, 1970) and the 1967-1968 EASTROPAC cruises (U.S. Dept. of Commerce, 1970a) are relatively recent attempts to fill this serious data gap.

Bjerknes, 1969(a) described the relationship between increased monthly Canton Island rainfall and the local presence of warm sea surface temperatures and suggested that the strong interannual variability of sea surface temperatures and rainfall observed at Canton Island could be applied to the eastern tropical Pacific Ocean. On the other hand, Krueger and Gray (1969) analyzed 5 years of winter (December to February) sea surface temperatures (1962-1967) over the eastern tropical Pacific. They found decreased tropical cloudiness in the winter of 1966 using satellite data in the presence of anomalously warm sea surface temperatures. Widespread tropospheric subsidence was suggested as the cause for this suppressed cloudiness.

In order to gain a comprehensive insight into these complex air-sea interactions, we will examine long-term variations of satellite-derived tropical cloudiness, sea surface temperatures, tropical Pacific island rainfall and also the strength of the semi-permanent anticyclones in the northern and southern Pacific Ocean between latitudes 30°-40°N and S.

Ocean-Atmosphere Interaction Considerations

The ultimate source of energy that drives the atmosphere and the oceans is the differential heating of the earth's surface by the sun. The immense amount of heat capacity of the oceans, which constitute about 70% of the earth's surface, acts as a huge flywheel for this coupled system. In general, the movement of the major Pacific Ocean current systems, shown in Figure 1 (US Navy, 1966) are caused by the wind stress on the water, the downslope movement of low density water which is dynamically higher than high density water, the blockage of the currents by land masses and the earth's rotation (Svedrup, 1947, Malkus, 1962, U.S. Navy, 1962, Stewart, 1969). Since the large

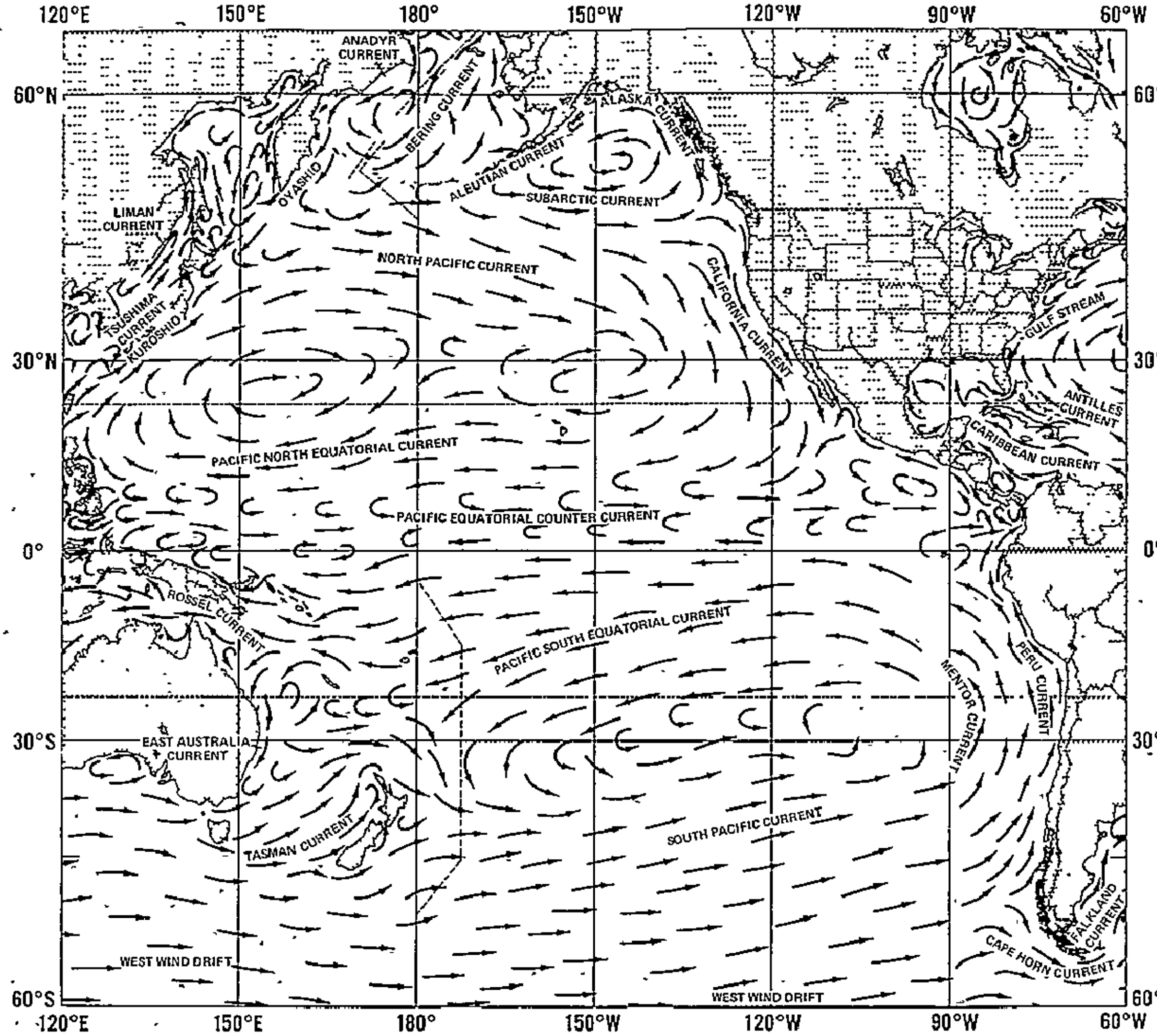

SURFACE CURRENTS OF THE PACIFIC OCEAN
JULY

Figure 1. Surface currents of the Pacific Ocean during July (US Navy, 1966).

North Pacific anticyclone is the major pressure source driving the surface currents in the northeastern temperate and tropical Pacific Ocean, the region 30°N-40°N, 180°-100°W was selected for analysis. This area encompases the range of movement of the anticyclones' central pressure during its yearly trek north and south in synchronization with the sun's seasonal migration.

Table 1 lists the monthly long-term mean central position of the North Pacific anticyclone (Crutcher and Meserve, 1970).

Roden and Reid (1961) had also noted the importance of the strength of the Aleutian Low in the winter months and its close relation to oceanic sea surface temperature anomalies. However, for this study, only the climatological variation of the North Pacific High will be examined.

Table 1

January	30°N	138°W
February	31°N	137°W
March	35°N	150°W
April	34°N	165°W
May	33°N	155°W
June	33°N	146°W
July	38°N	149°W
August	39°N	151°W
September	34°N	155°W
October	33°N	141°W
November	31°N	136°W
December	30°N	139°W

The sea level pressure and the 700 mb heights over the North Pacific High were collected for the period 1949-1971. The monthly surface pressure data from 5° latitude-longitude intersections, was obtained from microfilmed Northern Hemisphere surface maps provided by the National Climatic Center, NOAA, Asheville, N.C. The monthly 700 mb height anomalies, at the same intersections were obtained from the Monthly Weather Review (1949-1971). Figure 2 shows the close pattern similarity between these two levels using 12 month running means during the 20 year period ($r = +0.80$ with 0 lag). The letter r will be used in the paper to represent correlation coefficient.

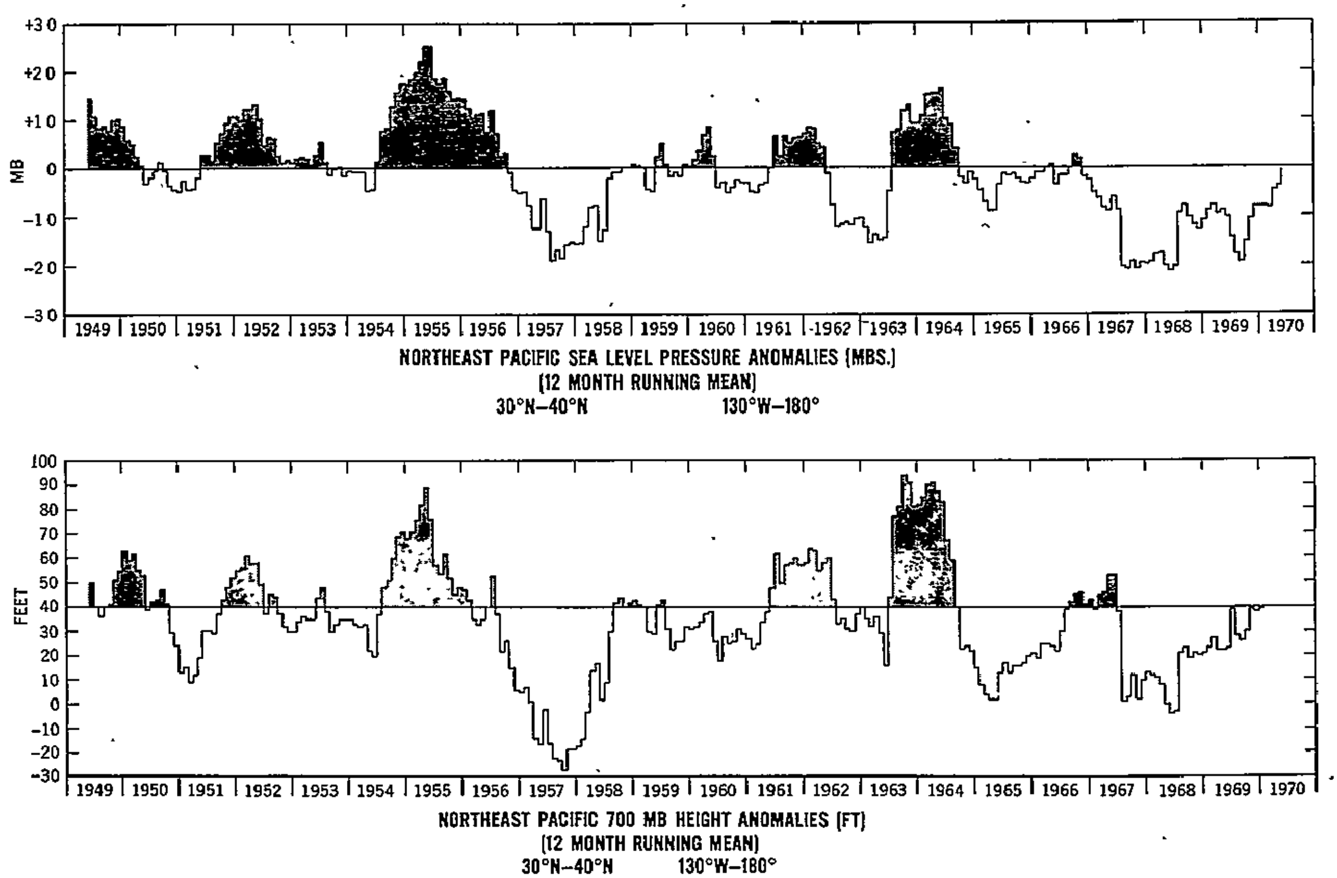

Figure 2. (a) Northeast Pacific (30°-40°N, 130°W-180°), sea level pressure anomalies, 12 month running mean. (b) Northeast Pacific (30°-40°N, 130°W-180°), 700 mb height anomalies, 12 month running mean.

Reid et al (1958), Reid and Roden (1961) had noted that the upwelling and cold water advection in the California Current (Fig. 1) was coupled with the northerly winds for the most part driven by

the North Pacific High. In addition, an areal coherence of monthly sea surface temperature (SST) anomalies of the same sign and approximate amplitude occur almost simultaneously from 40°N to 20°N in the California Current. In order to analyze a longer series of data, monthly sea surface temperature from the piers and recording sites along the west coast (Fig. 3) were collected from U.S. Coast and Geodetic Survey records from 1925 to 1970. Long-term means and monthly anomalies were assembled from this data. A single monthly average of all coastal sea surface temperature anomalies was then made and 12-monthly running means plotted in Figure 4(a). Both the monthly surface pressure and the 700 mb height anomalies only showed a r = - 0.68 with + 6 to 8 month lead time with these coastal sea surface temperatures. Figure 4(b) which is the 10°-20°N, 100°W-180° sea surface temperature anomalies over the extension of the California Current (Fig. 1), showed a close correlation as was expected with the U.S. west coast data (r = + 0.87 with -1 month lag). The source of the tropical ocean data will be described later in this article.

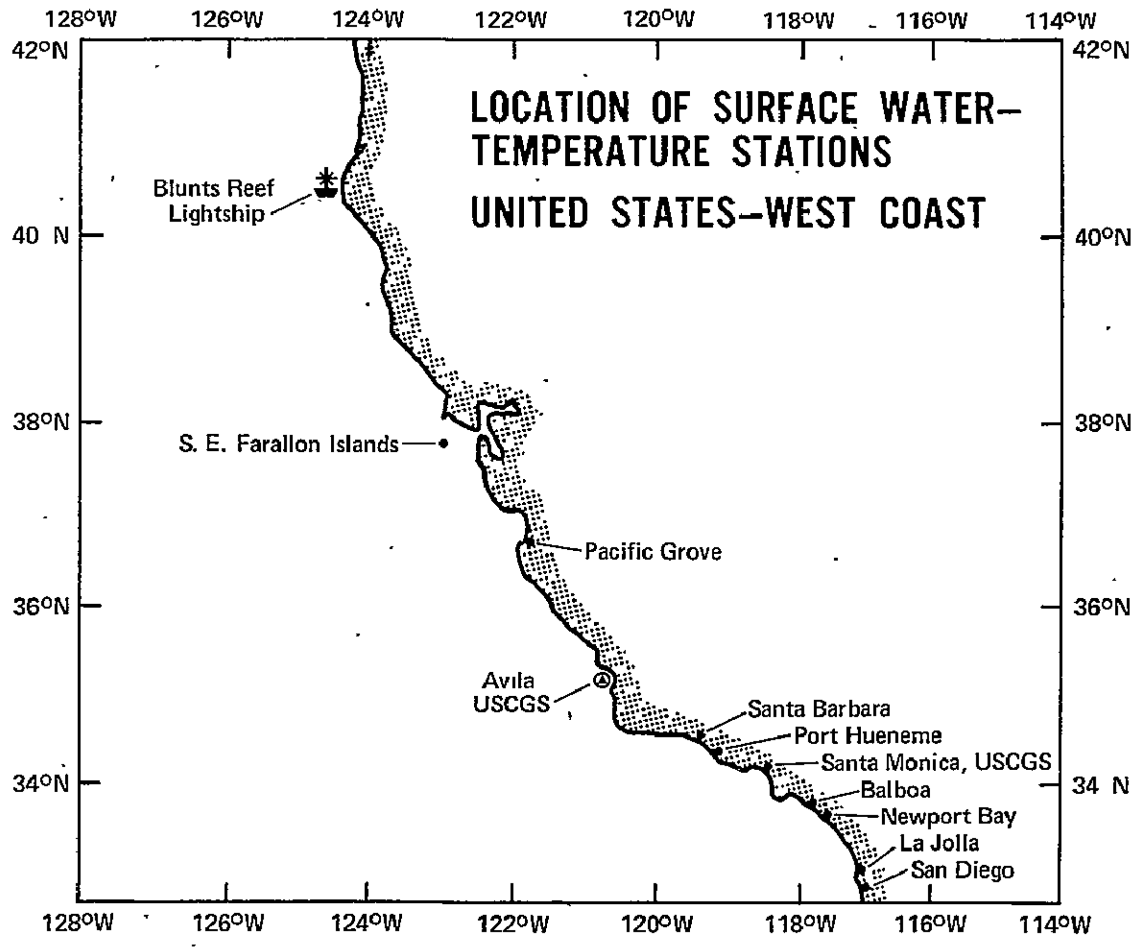

Figure 3. Location of surface water temperature stations along the U. S. west coast.

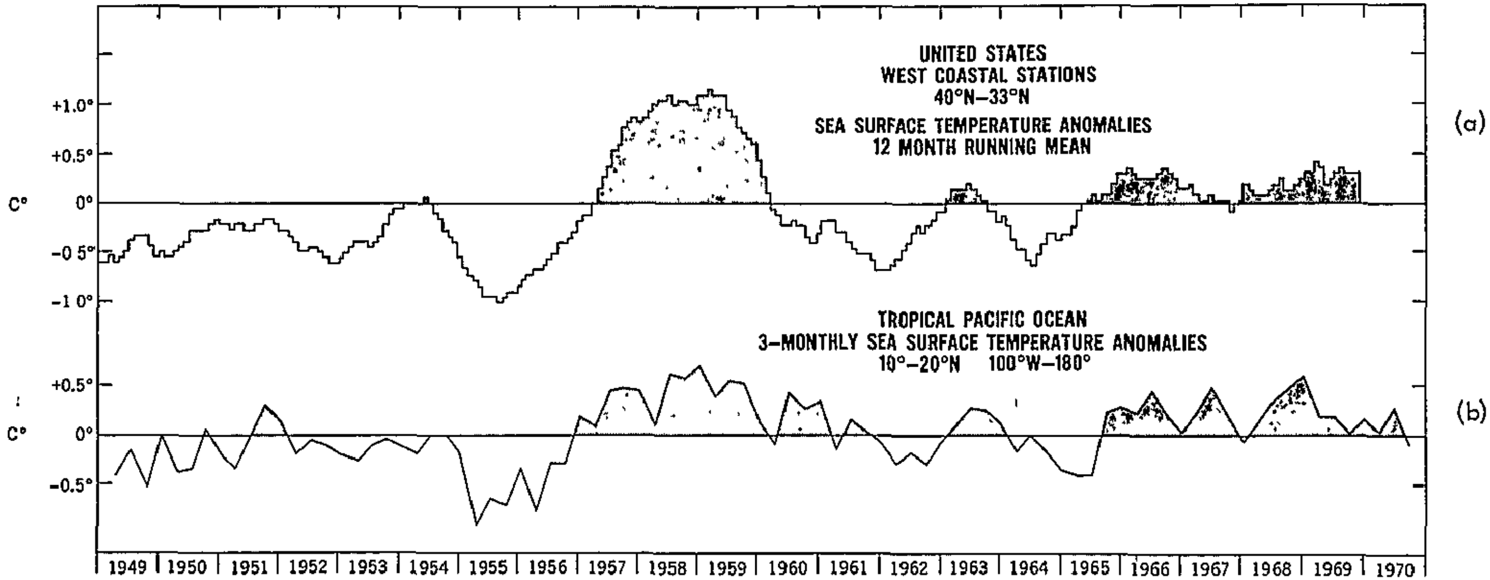

Figure 4. (a) U. S. coastal stations, (40°–33°N), sea surface temperature anomalies, 12 month running means.
(b) Tropical Pacific Ocean (10°–20°N, 100°W–180°) 3-monthly sea surface temperature anomalies.

A comparison of the Northeast Pacific 700 mb height anomalies was made with the sea surface temperature anomalies from 30°N to 10°S from 180° to the continental shorelines and surprisingly good relations (r = -0.70 to -0.74 with +5 to +9 months lead) were noted. Figure 5 shows this comparison with the 0-10°N sea surface temperature anomalies slipped 6 months in time. High pressure was related to cool sea surface temperatures and low pressure to warm sea surface temperature anomalies. Better correlations (r = +0.73 to 0.89) were noted with satellite-derived cloudiness from 30°N to 20°S. A more complete discussion of these statistical results will be made later in this article.

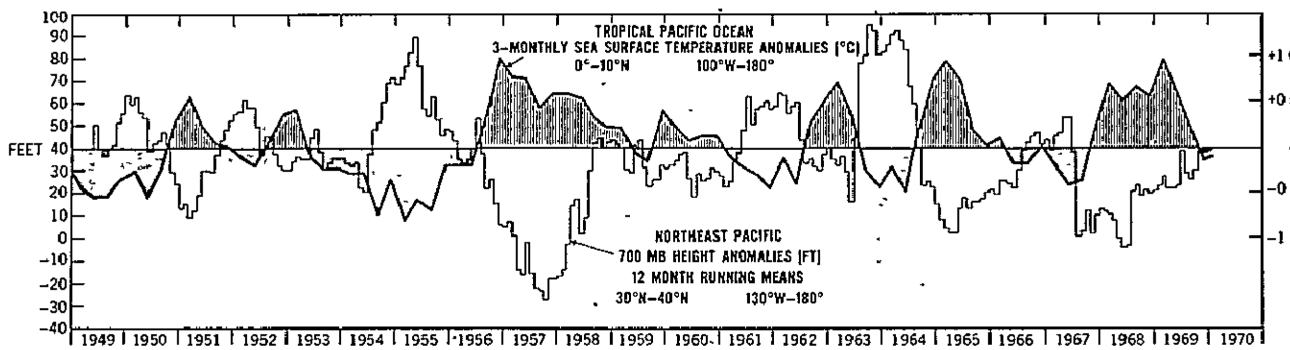

Figure 5. A comparison of Northeast Pacific (30°-40°N, 130°W-180°) 700 mb height anomalies and tropical Pacific Ocean (0°-10° N, 100° W-180°). 3-monthly sea surface temperature anomalies. The SST is lagged-6 months on this graph.

A similar analyses was made for the southern hemisphere in order to obtain the long-term variation of the Peru Current, a northward-flowing current along the west coast of South America (Fig. 1). Historical monthly sea surface temperature data was obtained from U.S. Coast and Geodetic Survey records from 1950 to 1967 for the South American west coastal stations shown in Figure 6. A monthly average of all station sea surface temperature anomalies was made and shown in Fig. 7 (a). Fig. 7(b) shows the 12-month running means of these anomalies and confirms the close coupling (r = +0.90 with +1 month lead) that should exist between the Peru Current (Fig. 1) and its extension from 0°-10°S, 80°W-180° (Wyrtki, 1965).

Due to the sparsity of South Pacific sea level pressure (SLP) and 700 mb data, the long period of SLP record of Juan Fernandez was utilized to relate to the South Pacific anticyclone.

Table 2 lists the monthly long-term mean central position of the South Pacific High (Taljaard et al, 1969).

Juan Fernandez Island (34°S, 80°W) is not completely representative of the South Pacific High during June to August, a period when it is influenced by disturbances in the extratropical westerlies (Bjerknes, 1966).

Figure 8 shows the agreement between the extension of the Peru Current 0°-10°S, 180°-100°W and the Juan Fernandez SLP data (r = -0.63 with -2 months lag). Note the drop off in Juan Fernandez surface pressure, which relates the abnormal weakening in trade wind circulation and the

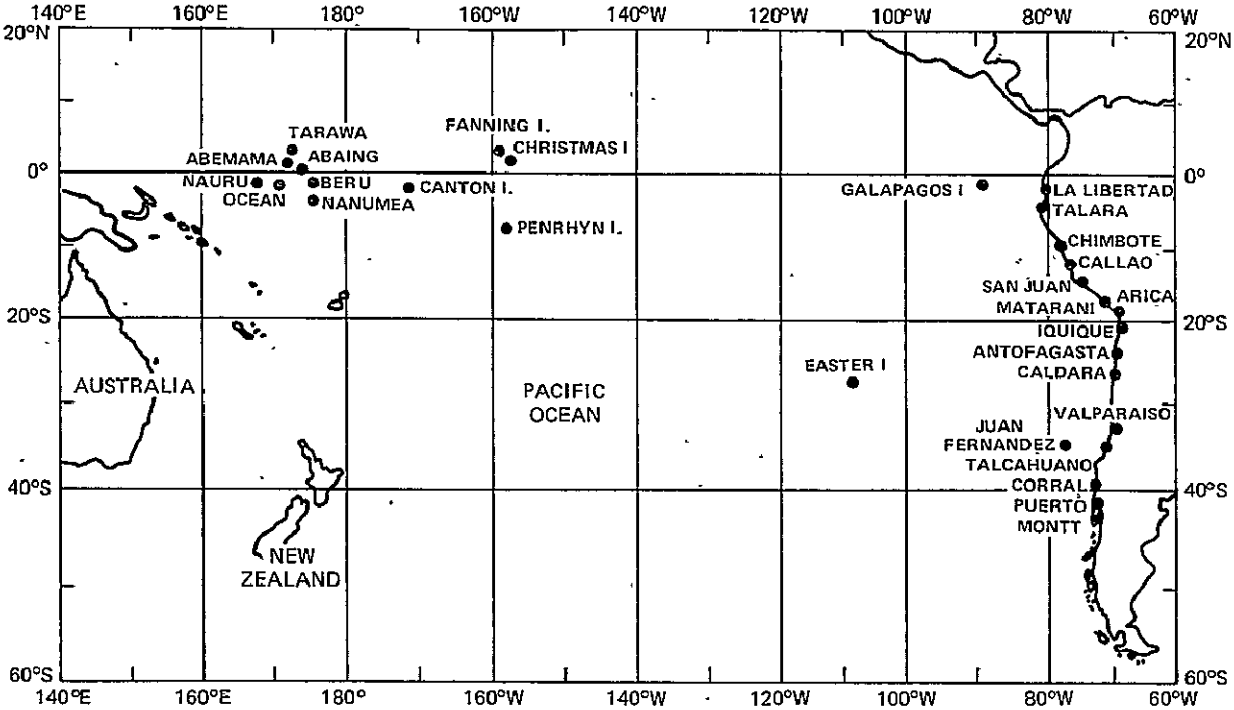

Figure 6. Location of South American west coastal sea surface temperature recording stations and tropical Pacific island rainfall recording network.

Table 2

January	31°S	89°W
February	31°S	90°W
March	30°S	90°W
April	30°S	88°W
May	27°S	85°W
June	25°S	90°W
July	26°S	90°W
August	27°S	88°W
September	28°S	89°W
October	29°S	88°W
November	30°S	89°W
December	30°S	89°W

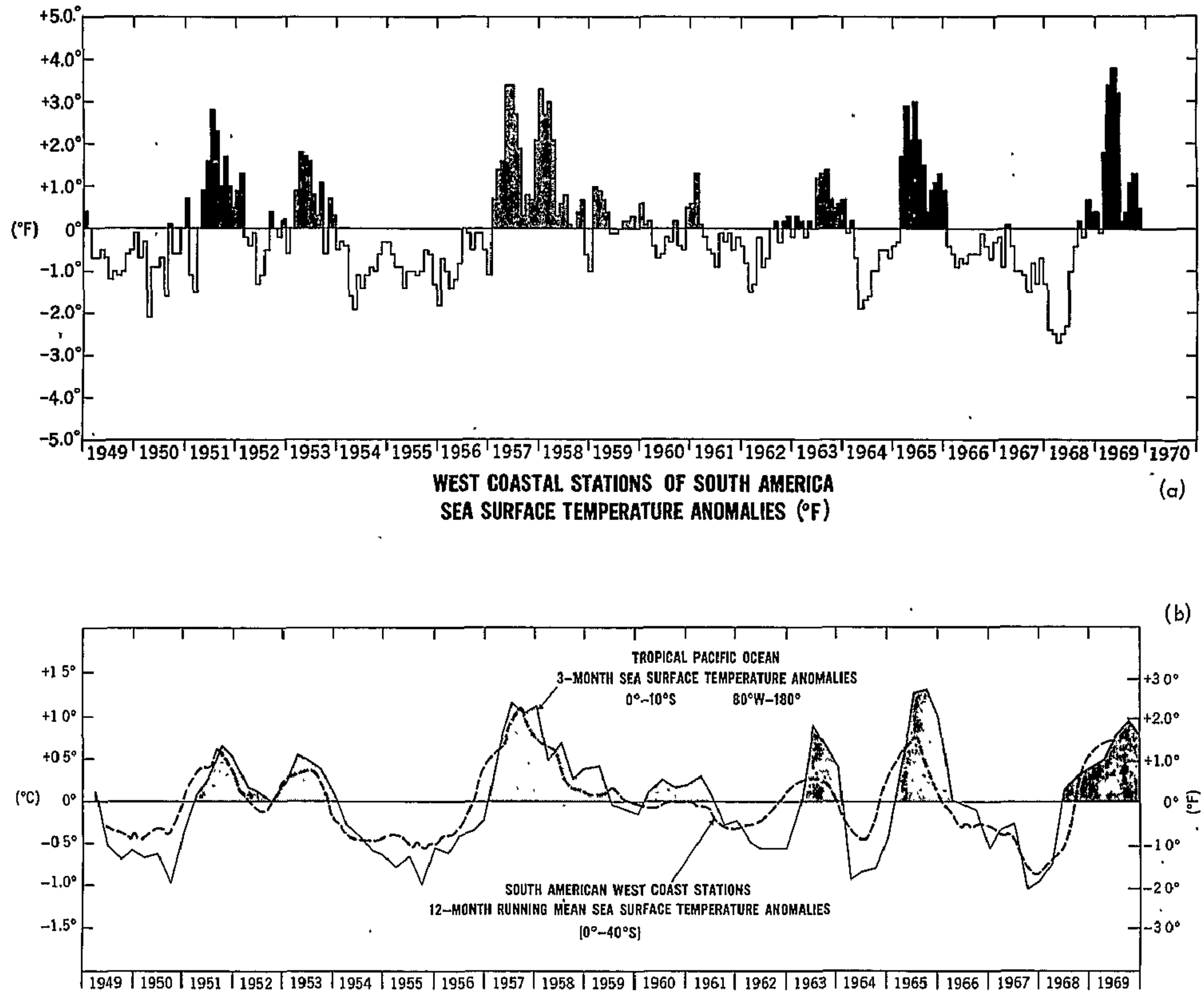

Figure 7. (a) South American west coast stations, (0°-40°S) sea surface temperature anomalies (monthly mean). (b) A comparison of South American west coast stations (0°-40°S) sea surface temperature anomalies (12 month running means) and tropical Pacific Ocean (0°-10°S, 80°W-180°), 3-monthly sea surface temperature anomalies.

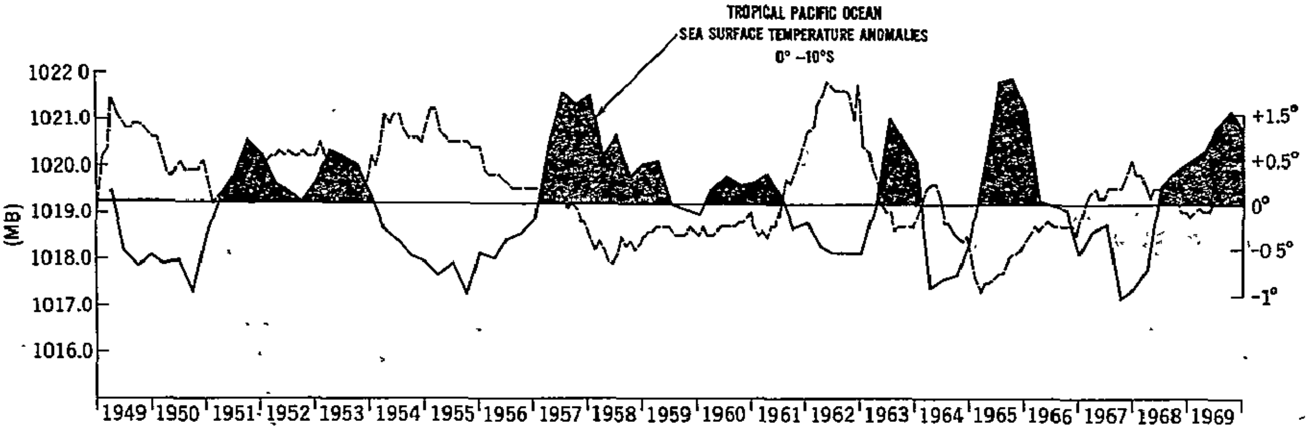

JUAN FERNANDEZ SEA LEVEL PRESSURE (MB)
(12 MONTH RUNNING MEAN)

Figure 8. A comparison of Tropical Pacific Ocean (0°-70°S, 80°W-180°), 3 monthly sea surface temperature anomalies and Juan Fernandez Island sea level pressure (12-month running mean).

resultant anomalous sea surface temperature warming during 1951, 1953, 1957-61, 1963, 1965, 1968-69. The work of Bjerknes, 1961 and Wooster 1961(a), tend to support this interpretation between the strength of the trade winds and equatorial upwelling in the central tropical Pacific Ocean. Berlage (1966), noted that SLP differences between Juan Fernandez and Santiago would better relate to Peru Current changes. This premise will be tested in a later study.

Satellite-Derived Cloudiness and Sea Surface Temperature Data

With the launching of the TIROS, ESSA, Nimbus, ITOS, and ATS meteorological satellites in the last decade, it is now possible to view tropical cloudiness on a day-to-day, weekly, monthly, seasonal and yearly basis over vast oceanic regions of the world (Atkinson and Sadler, 1970, Leese et al., 1970, Miller, 1970; U.S. Department of Commerce, 1970, Allison et al., 1969, Bjerknes et al, 1969(b), Sadler, 1968, Salomonson, 1969, Sherr et al, 1968, Taylor et al, 1968, Wallace, 1970, Anderson et al 1969, Kornfield and Hasler, 1971, Suomi and Vonder Haar, 1970).

Only recently has the time span of satellite data become extensive enough to satisfactorily view the longer term variations in cloud amounts over the tropical Pacific Ocean. Figure 9 shows the monthly variation in cloud cover (in percent of area covered by $\geq 6/10$ cloudiness) derived from satellite television analyses over the eastern tropical Pacific from 0°-30°N, 180°-100°W from August 1962-October 1970. Examples of monthly cloudiness minimum and maximum periods, April 1965 and 1969, respectively are shown in the lower half of this figure. These cloudiness amounts were derived from daily television nephanalyses which were produced by the Analyses Branch, National Environmental Satellite Service, NOAA, Washington, D.C. The daily charts were composited from 4 to 5 orbits of TIROS, ESSA and ITOS television data. Cloud amounts in tenths were weighted and hand plotted in 2° lattitude-longitude squares and averaged to produce monthly cloud values (Godshall, 1968, Godshall et al, 1969, 1971).

CLOUD COVER VARIATIONS FROM SATELLITES

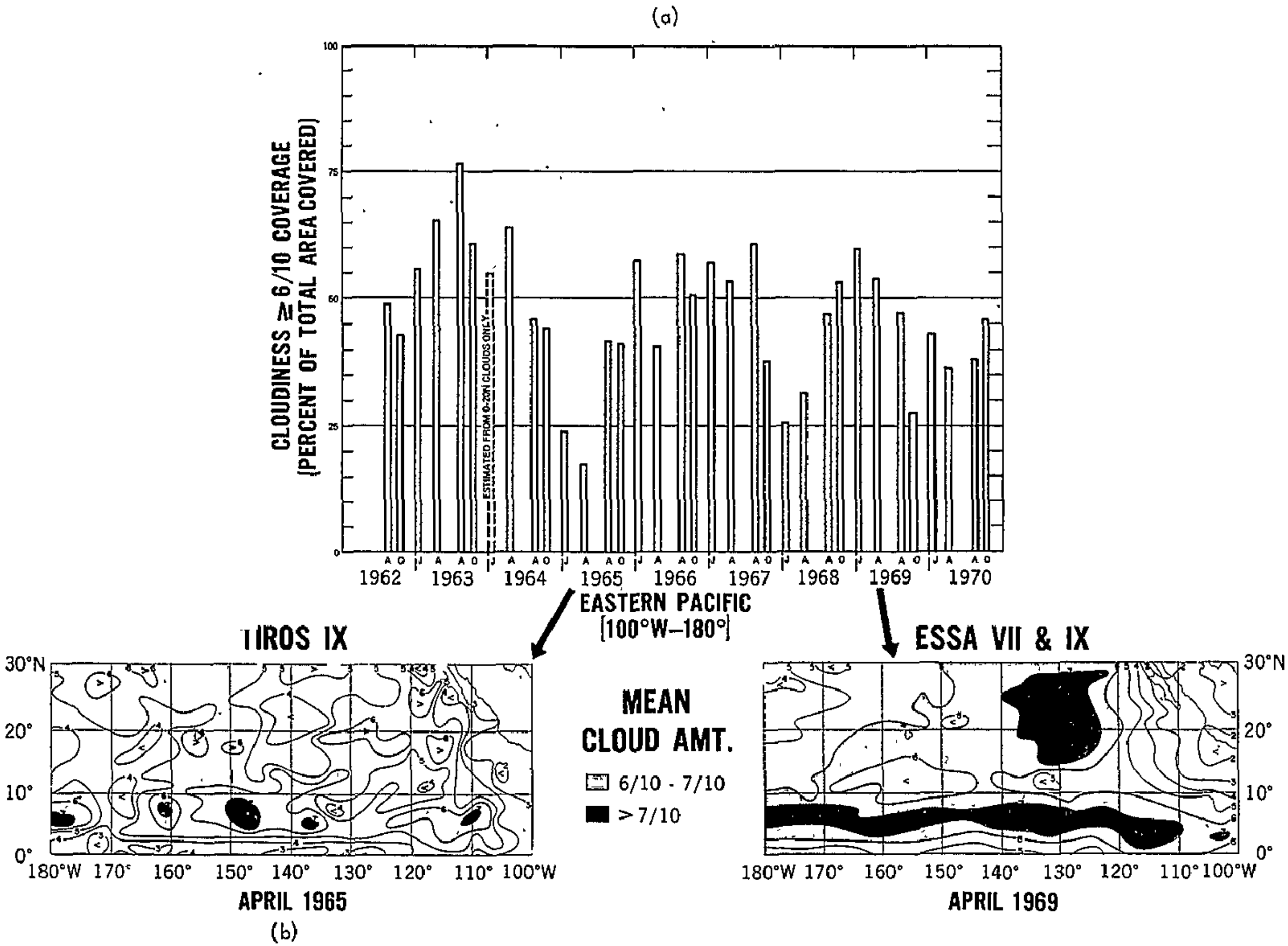

Figure 9. (a) A histogram of satellite derived cloudiness (precent of area covered by ≥ 6/10 cloudiness) from 0°-30°N, 100°W-180° from 1962 to 1970. (b) Mean cloud amount (in tenths) derived from TIROS IX neph-analysis: April 1965. (c) Mean cloud amount (in tenths) derived from ESSA VII and IX nephanalysis, April 1969.

In order to determine the relationship that could exist between tropical cloudiness and sea surface temperatures, it was decided to study the monthly SST data for the tropical Pacific Ocean, published by the National Marine Fisheries Services, NOAA (Renner, 1962-1970). Since ship SST data were sparse in the tropical ocean, 3-monthly means of the data were produced, using the technique described by Krueger and Gray (1969). Long-term means, obtained from the U.S. Naval Oceanographic Office, Special Publication 123, 1969 were used for the anomaly data base at the center of the 5° latitude-longitude squares from 20°N to 10°S, 180° to 80°W. Charts showing these 3-monthly sea surface temperature anomalies (°C) from 1962-1970 are shown in the Appendix A. The area covered by a positive sea surface temperature anomaly were planimetered and weighted by the mean sea surface temperature anomaly (°C) for each latitude band. Histograms of the monthly cloud cover and 3-monthly sea surface temperature variations are shown in Appendix B. A discussion of the correlations between these two sets of data will follow in the next section of this study.

In order to extend our SST data base back prior to 1962, an atlas of monthly sea surface temperatures (Eber et al, 1968) was processed by the technique described previously and reduced to 3-monthly sea surface temperature anomalies for the period 1949 to 1962. A complete atlas of these anomaly charts are shown in Appendix A.

Figures 10 and 11 which summarize the results of this atlas, show the seasonal sea surface temperature anomalies from 10°-20°N, 0°-10°N, 0°-10°S, 5°-15°N, 5°N-5°S from 1949 to 1970 using all available data. The 5°-15°N band covers the Intertropical Zone of Convergence, the Equatorial Counter Current and California Current extension while the 5°N-5°S band covers the Peru Current extension (Wyrtki, 1965).

Note the warm periods: 1951, 1953, 1957-59, 1960-61, 1963, 1965, 1968-69 for the 20°N-10°S region. Note the gross similarity with the yearly sea surface temperature anomaly for the 20°-30°N band across the entire Pacific Ocean (Namais, 1970).

Figures 12 and 13 show the percent of area covered by a positive anomaly for the 20°N-10°S regions. A good relationship was noted between these two types of sea surface temperature analyses (Figs. 10 to 13).

In previous studies, Bjerknes, 1966(a), 1968, 1969(a) had noted the importance of the Canton Island sea surface temperatures in that it should relate strongly to the eastern tropical Pacific Ocean circulation. Figure 14 confirms the fact that Canton Island sea surface temperature anomalies are in good agreement and very representative of the sea surface temperature features of the eastern half of the South Equatorial Current (5°N-5°S, 80°W-180°). In addition, the island rainfall and sea surface temperature relationship previously reported by Bjerknes (1969(a)), also show good qualitative agreement with the 5°N-5°S sea surface temperature anomalies (Fig. 15). Conventional monthly surface cloud amounts observed at Canton Island (Fig. 15) and satellite-derived monthly cloudiness (Fig. 16) over the tropical Pacific islands 165°E-155°W also show a fair relationship with the 5°N-5°S sea surface temperature anomalies.

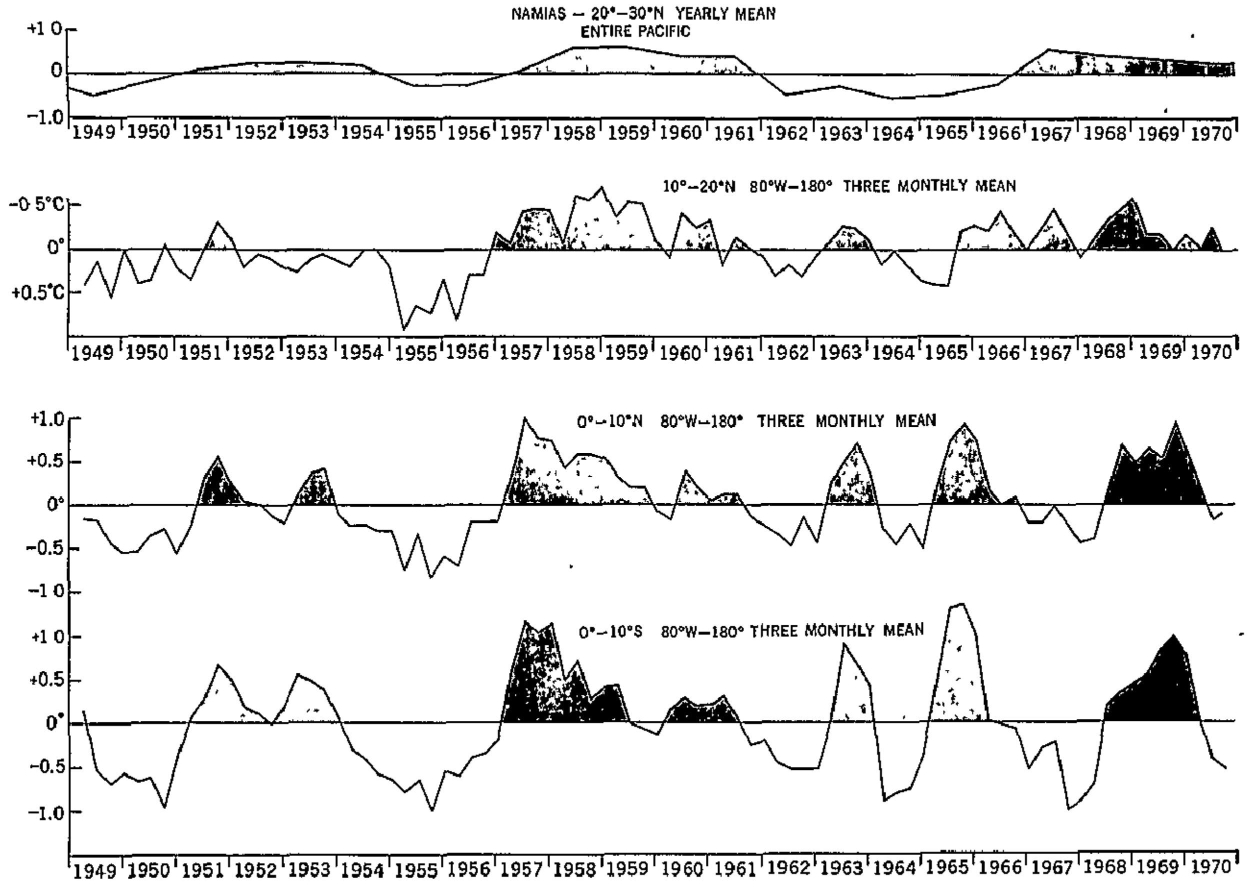

SEA SURFACE TEMPERATURE ANOMALIES

Figure 10. Sea surface temperature anomalies, 20-30°N, entire Pacific; yearly mean (Namais, 1970), 10-20°N, 0°-10°N, 0°-10°S, 80°W-180°, 3-monthly mean from 1949 to 1970.

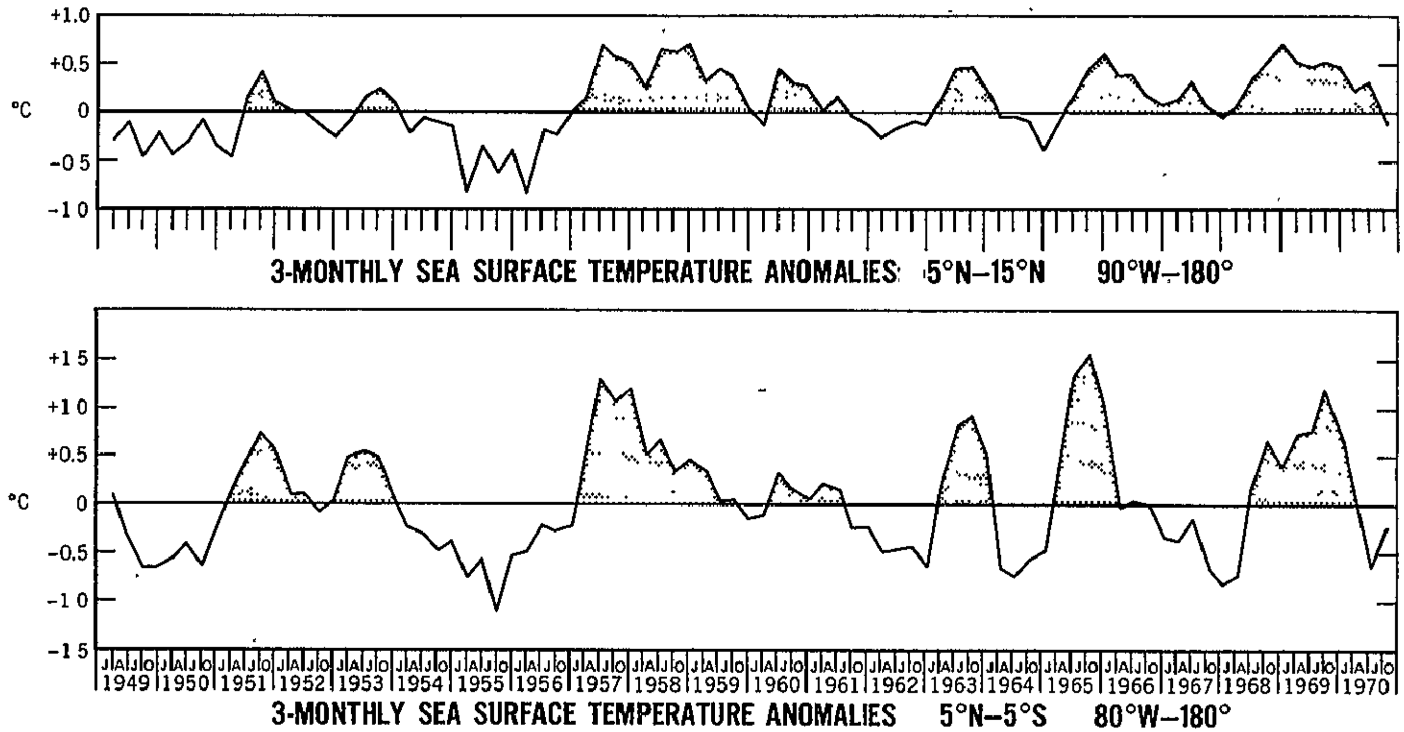

Figure 11. Sea surface temperature anomalies, 5°-15°N, 90°W-180°, 5°N-5°S, 80°W-180°, 3-monthly mean from 1949-1970.

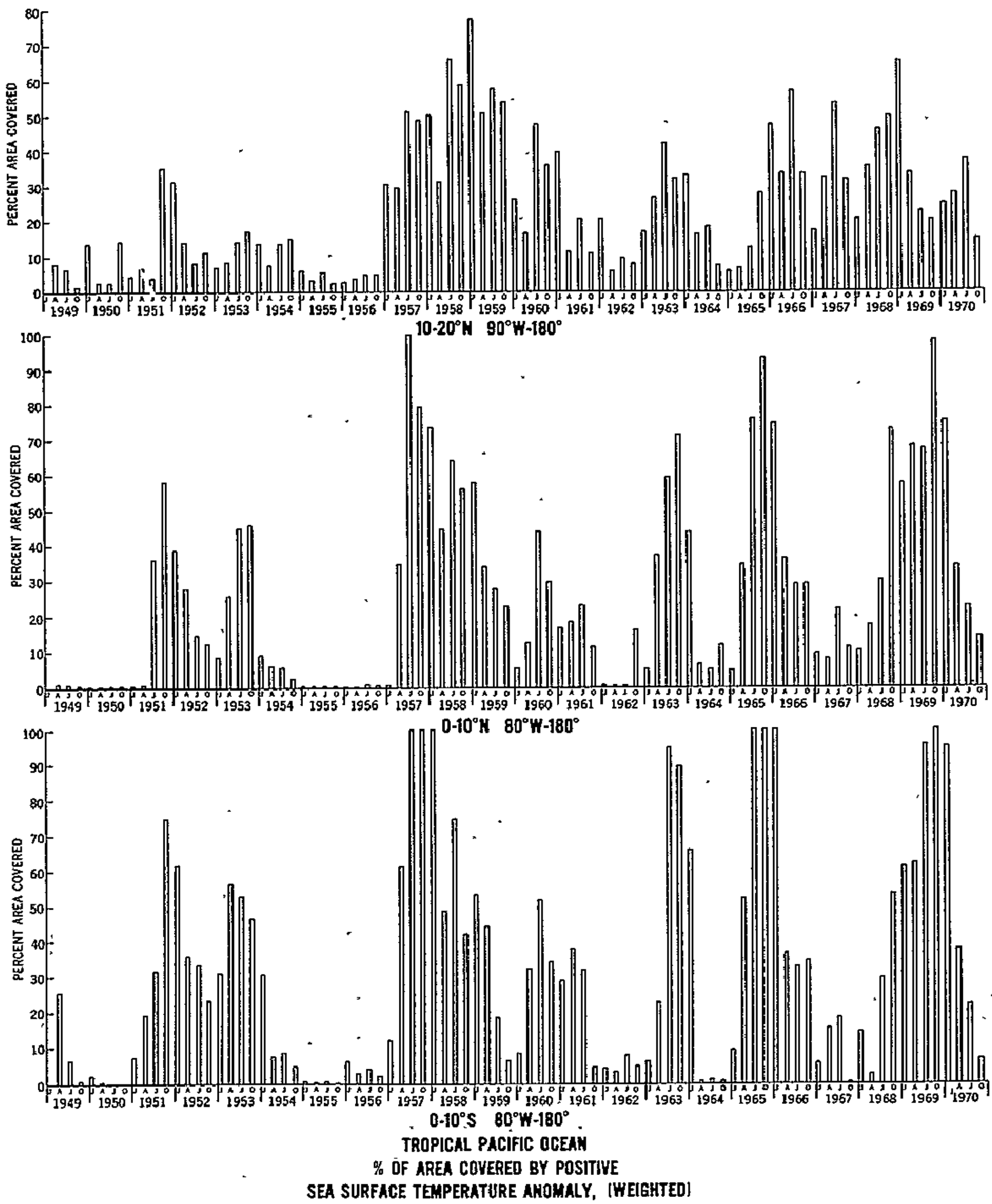

Figure 12. Tropical Pacific Ocean; percent of area covered by a positive sea surface temperature anomaly (weighted), 10-20°N, 90°W-180°, 0°-10°N, 80°W-180°, 0°-10°S, 80°W-180°.

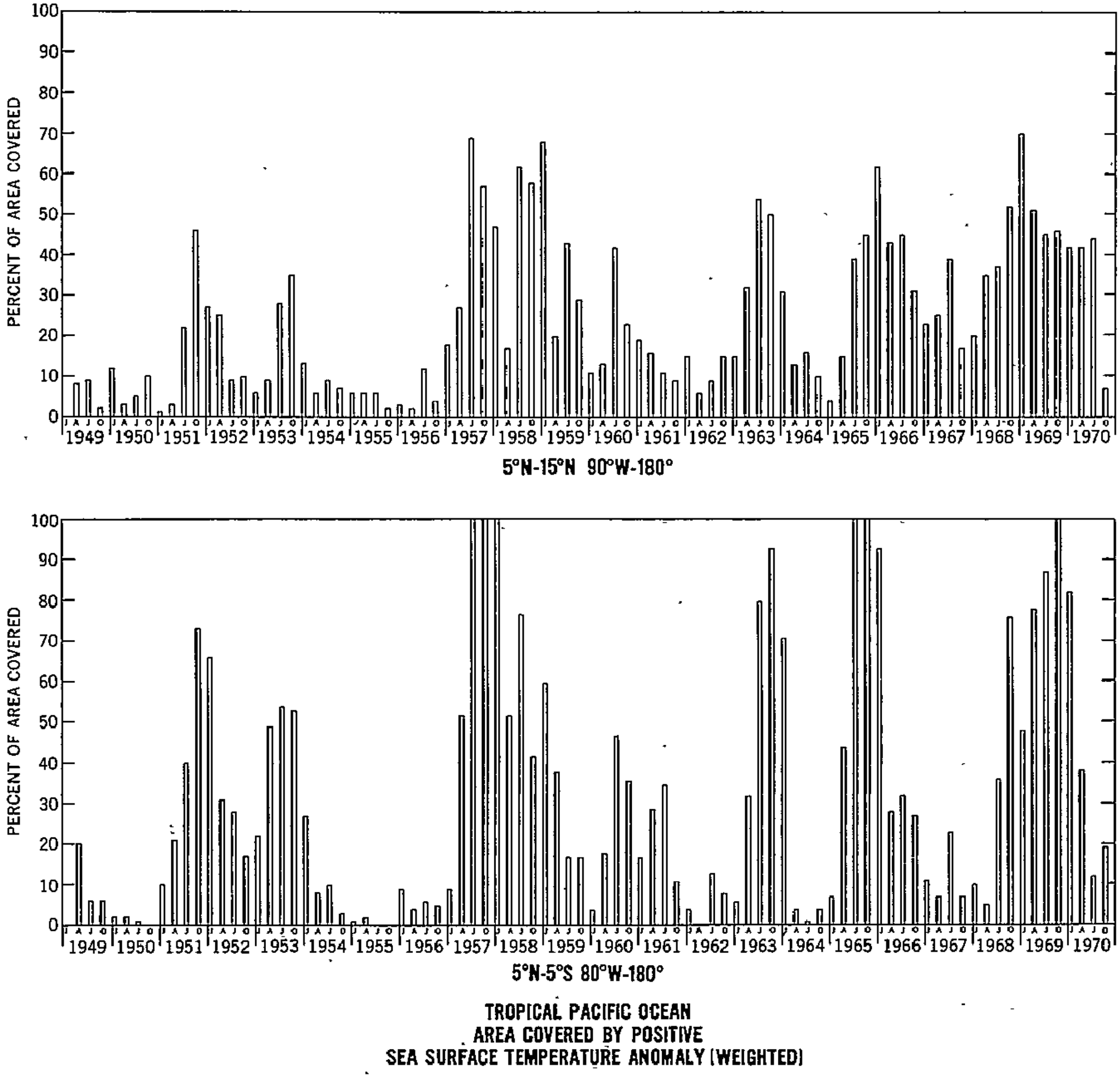

Figure 13. Tropical Pacific Ocean, percent of area covered by a positive sea surface temperature anomaly (weighted) 5°-15°N, 90°W-180°, 5°N-5°S, 80°W-180°.

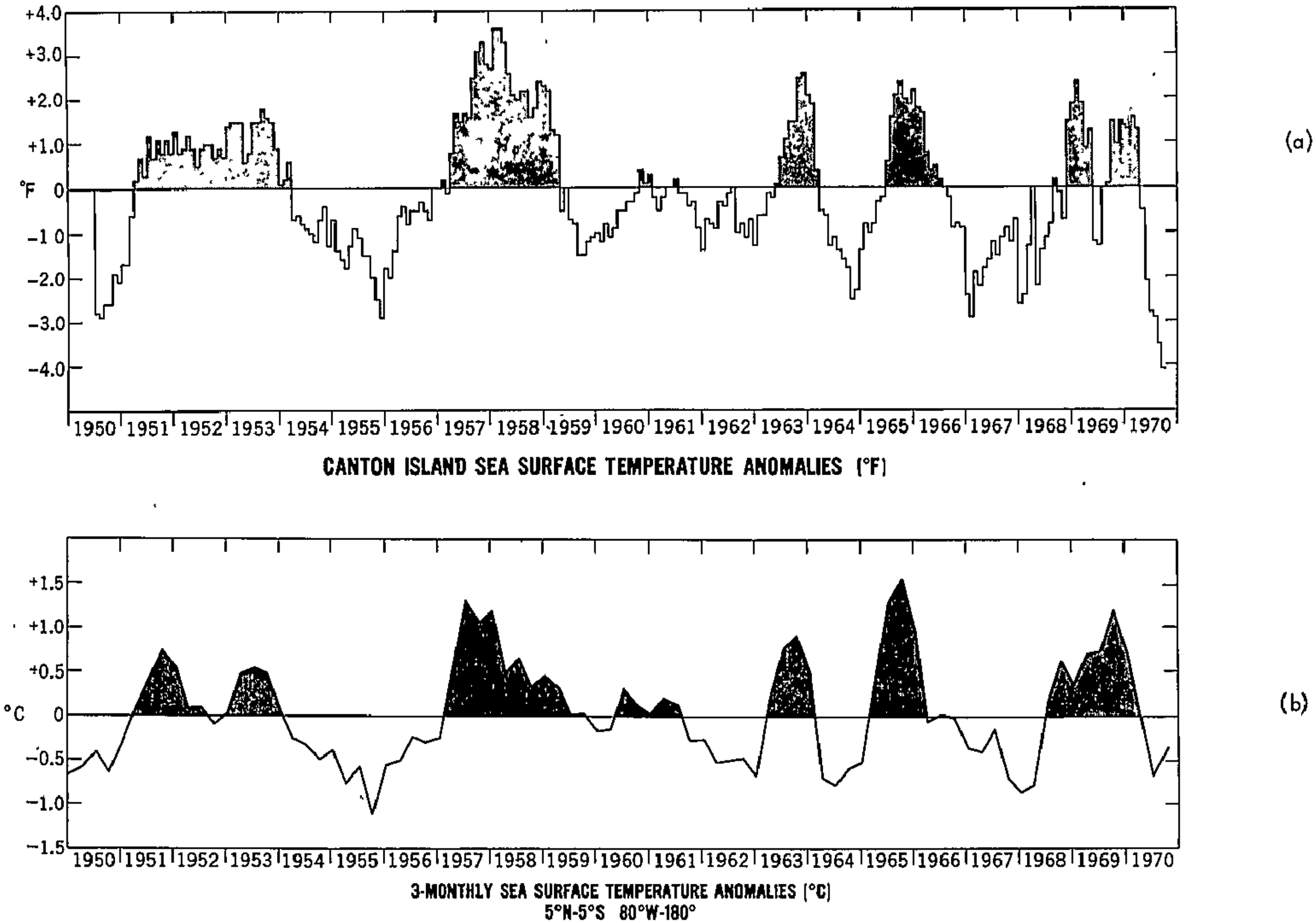

Figure 14. Sea surface temperature anomalies for Canton Island (monthly mean) from 1950–1967. Christmas Island data was inserted from 1967–1970. (b) Sea surface temperature anomalies, 5°N–5°S, 80°W–°80°, 3-monthly mean from 1950–1970.

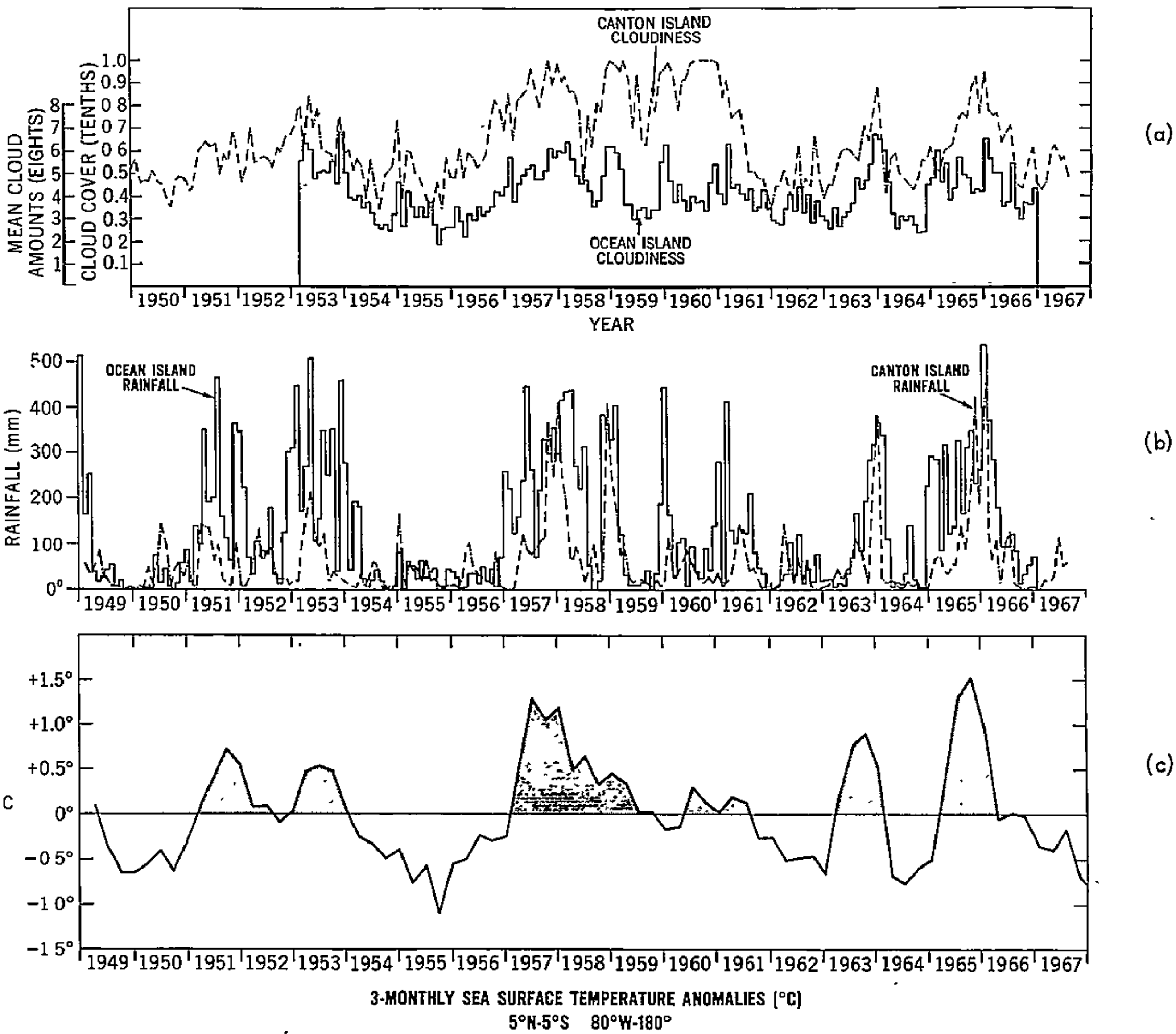

Figure 15. (a) Mean monthly cloudiness (surface observed) at Canton Island (in tenths) and Ocean Island (in eighths) from 1950 to 1967. (b) Mean monthly rainfall (mm) for Canton and Ocean Island from 1949 to 1967. (c) Sea surface temperature anomalies, 5°N–5°S, 80°W–180°, 3-monthly mean from 1949 to 1967.

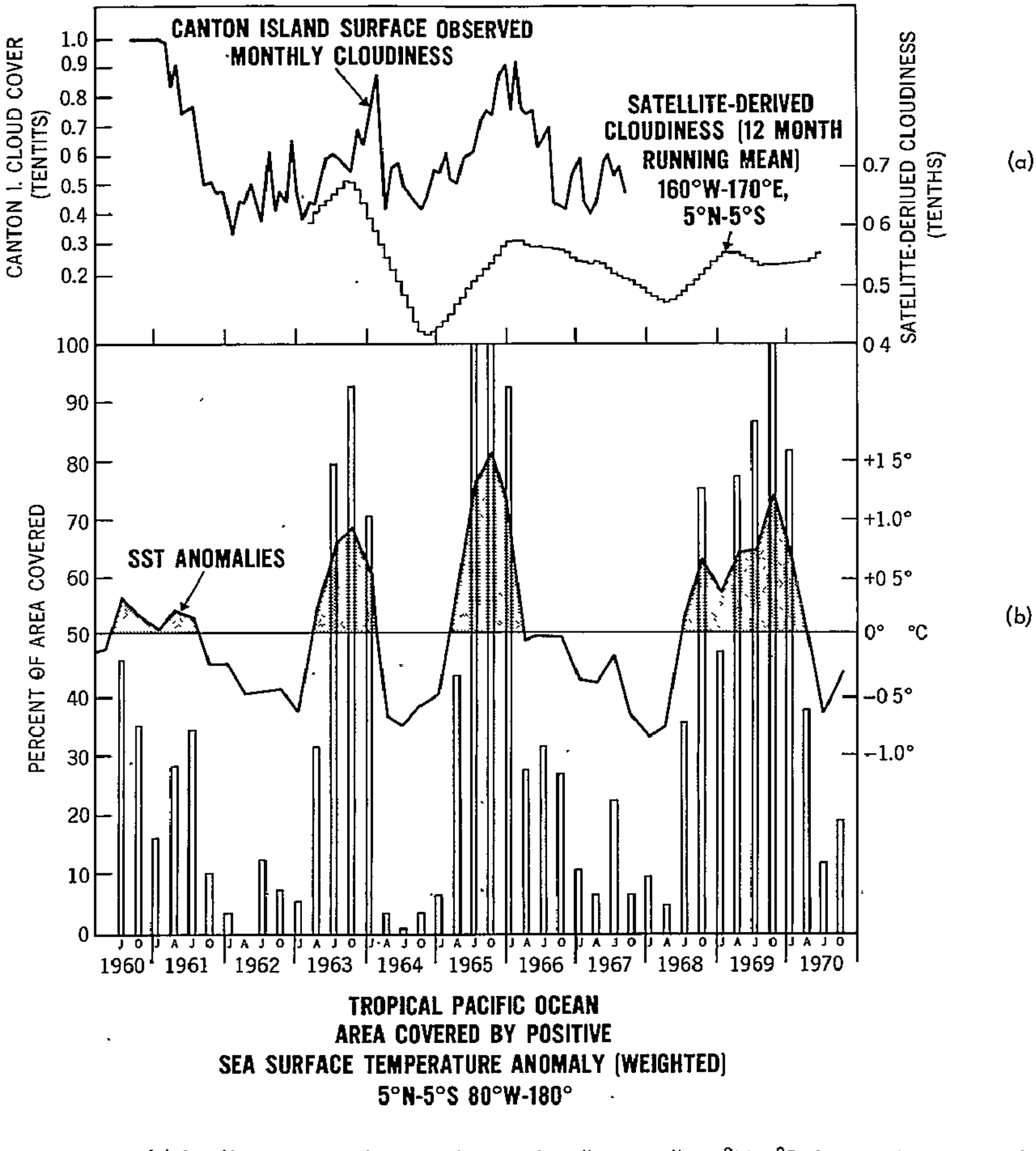

Figure 16. (a) Satellite-derived cloudiness (monthly) 160°W to 170°E, 5°N-5°S, from 1962 to 1969 and Canton Island surface observed cloudiness (monthly) from 1961 to 1967. (b) Sea surface temperature anomalies, 5°N-5°S, 80°W-180°, 3-monthly and percent are a covered by a positive sea surface temperature anomaly (weighted) from 1960 to 1970.

In order to study the apparent oscillations in the general atmospheric circulation shown by changes in cloud cover in periods prior to 1962, monthly rainfall data were analyzed for eleven Central Pacific islands (Quinn and Burt, 1970). This rainfall data, which was statistically studied by Dobritz (1958(a), (b)), for the islands located in Figure 6, had shown a definite coherence in their periodicity. Apparently, the rainfall over the tropical Pacific islands responded to the sea surface temperature pulsations in the South Equatorial Current during their long period of record. Twelve month running means were made from all coincident monthly averaged rainfall records from 1949 to 1970. A strong pattern similarity (Fig. 17) was noted between the tropical island rainfall and sea surface temperature anomalies for 5°N-5°S, 180°-80°W. The results of a statistical comparison of these two parameters for six oceanographic regions are shown in the following table.

Table 3

Sea Surface Temperature Anomalies	Correlation Coefficient	Month Lead/Lag
South American west coast stations	+0.75	-2
0°-10°S	+0.90	-1
5°N-5°S	+0.93	-1
0°-10°N	+0.92	-1
5°N-15°N	+0.78	+1
10°N-20°N	+0.62	+2

The high correlation coefficients $> +0.90$, would indicate that the variation in sea surface temperatures would be an excellent indication of tropical rainfall and cloudiness.

It was then a simple step to use linear regression techniques (Panosky and Brier, 1963) to derive sea surface temperature anomalies (Fig. 18) for 3 latitude bands, 0°-10°S, 0°-10°N and 10°-20°N back in time to 1905. The validity of this approach was checked by climatological records in two ways. Figure 18 shows that 5 out of 7 years of "El Nino" occurrences were indicated by anomalously warm periods in the derived sea surface temperature data (Quinn and Burt, 1970, Bjerknes, 1966(b), Berlage, 1966, Wooster, 1961). A second check involved the favorable comparison with U.S. west coast stations (Reid and Roden, 1961), and Puerto Chicama, Peru sea surface temperature anomalies which are affected by the coastal upwelling in the California Current and Peru Current (Wooster, 1961).

Statistical Techniques

Many geophysical records show a definite seasonal and/or annual variation which can be of such a magnitude as to obscure important long-term cycles, which may be of a smaller amplitude. The problem then becomes one of filtering out this annual cycle without losing useful information or introducing misleading statistical errors. Early in this project, the decision was made to use 12-month equally-weighted running means (EWRM). While this smoothing technique is widely used in climatological research, it does have however, one unfortunate property. As seen in Figure 19,

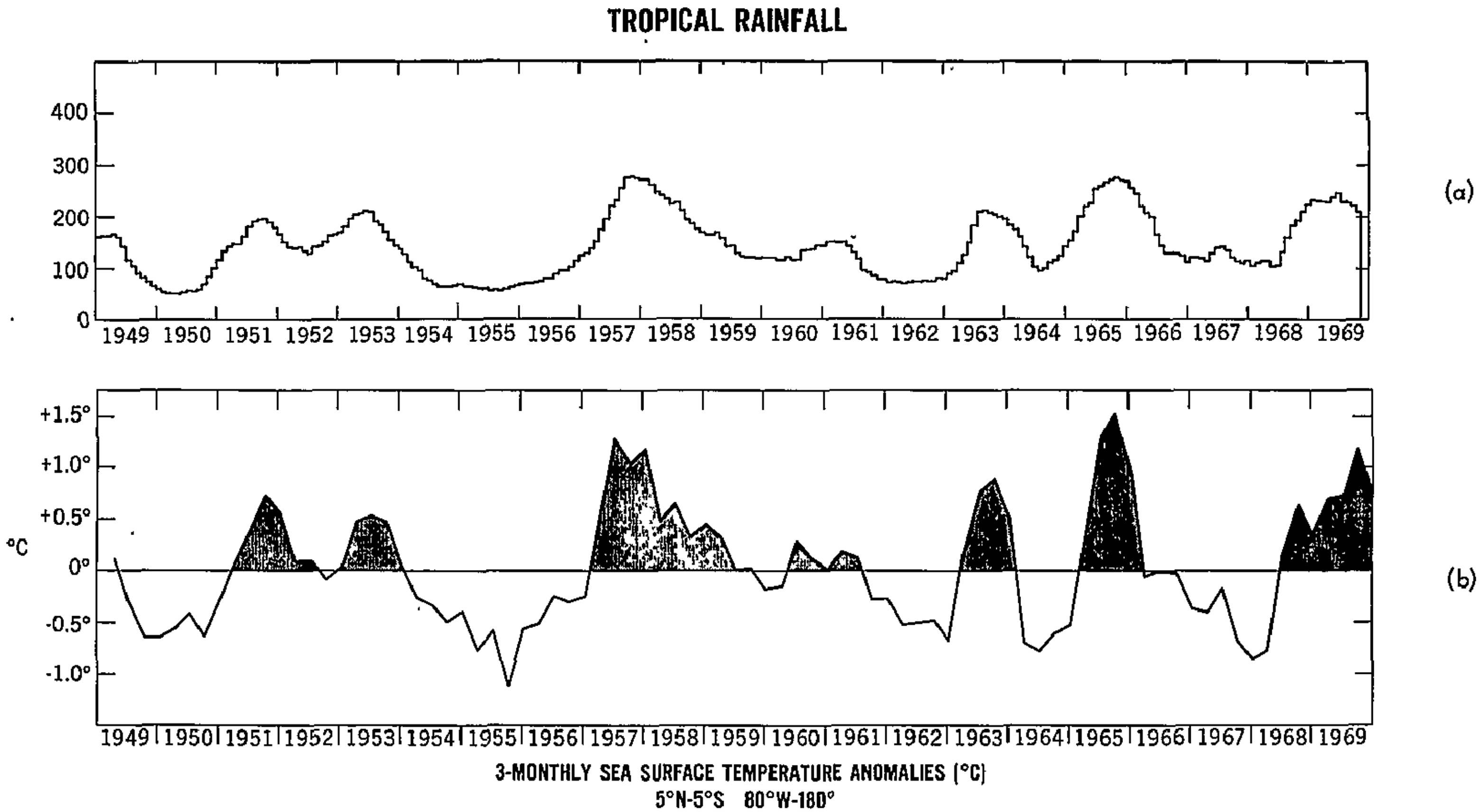

Figure 17. (a) Tropical Pacific Island rainfall (mm), 150°W-165°E, 5°S, (12 months running means) from 1949 to 1969. (b) Sea surface temperature anomalies, 5°N-5°S, 80°W-180°, 3-monthly means from 1949 to 1968.

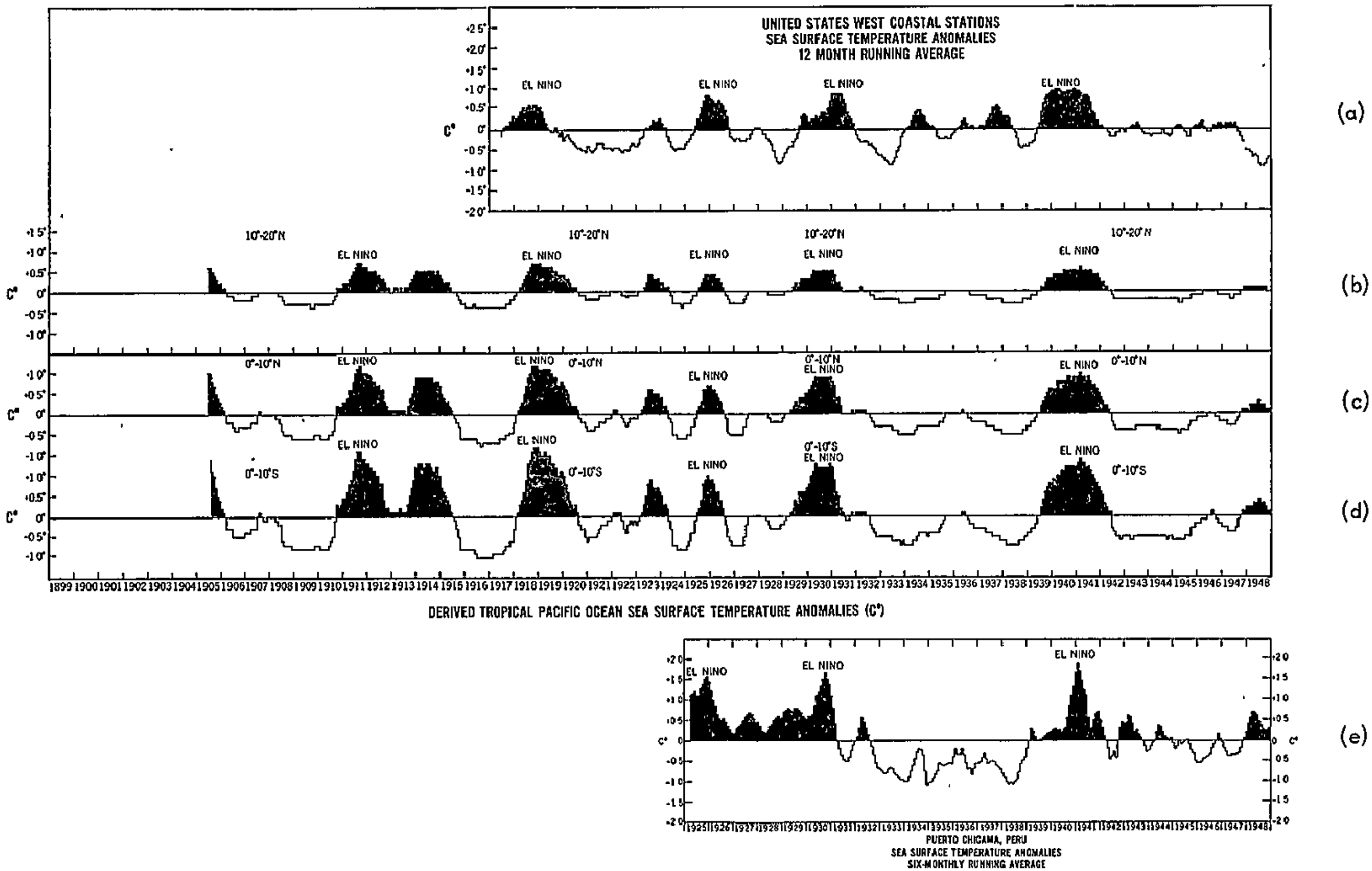

Figure 18. (a) U. S. west coast stations, 40°–33°N, sea surface temperature anomalies 12 month running means, from 1917 to 1948. (b) Derived sea surface temperature anomalies 10°–20°N, 180°–90°W from 1905 to 1948, 12 month running means. (c) Derived sea surface temperature anomalies 0°–10°N, 180°–80°W from 1905 to 1948, 12 month running means. (d) Derived sea surface temperature anomalies 0°–10°S, 180°–80°W from 1905 to 1948, 12 month running means. (e) Puerto Chicama sea surface temperature anomalies (6 months running means) from 1925 to 1948.

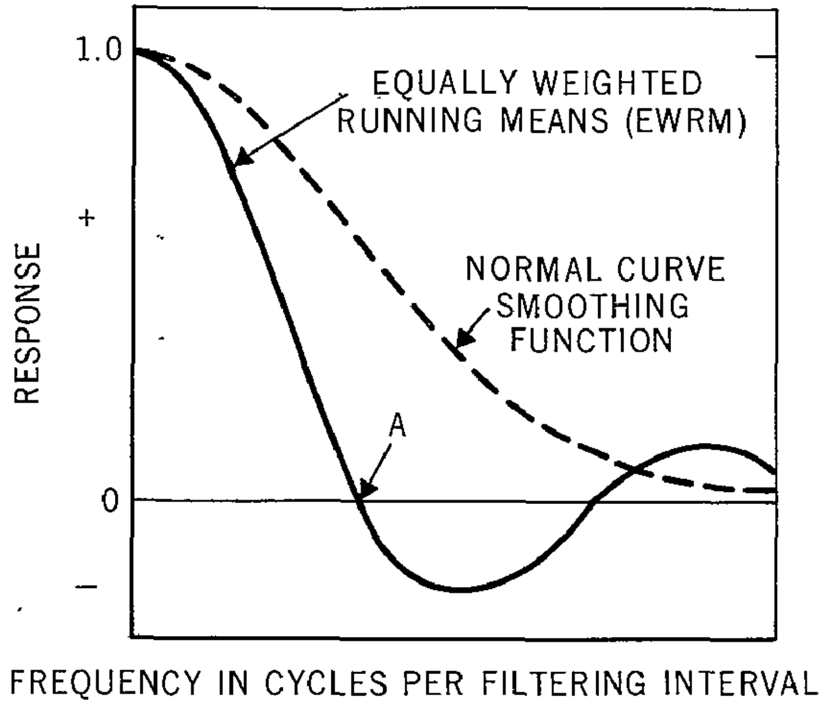

Figure 19. A comparison of the Equally Weighted Running Means(EWRM) and the Normal Curve Smoothing Techique. Polarity reversal is known at point "A".

there is a polarity reversal at point "A," which can produce erroneous frequencies in a spectral analyses. A solution to this problem would be to place all the data to be studied in an anomaly format using long-term means from the data itself. The monthly mean represents the annual cycle and its subtraction from the long-term mean should eliminate this regular cycle. A plot of the monthly anomaly data proved too noisy so the EWRM technique was utilized.

Another smoothing technique was tested to see if the polarity reversal effect was indeed damaging to the data analyses. Two parameters, Darwin monthly surface pressure and tropical island monthly rainfall for 30 years of record were put into anomaly form by using long term means from the data itself. Then a normal curve smoothing technique was applied. This technique does not introduce polarity reversals or phase shifts found with exponential techniques. It makes use of unequal weighting factors (f) which are computed by

$$f = \frac{N!}{m!\,(N-m)} \Big|\, 2^n$$

where N = 12 and m = 0, 1, 2, . . . 12.

After smoothing in this manner, the results proved highly comparable with the data processed by the EWRM technique (Table 4).

Table 4

A Comparison of Darwin Monthly Surface Pressure vs
Monthly Tropical Rainfall Anamolies

Technique	Correlation Coefficient (r)	Lag (months)
12-month equally weighted running means	+0.80	0
Normal curve smoothing of anomalies	+0.74	0

As can be seen, there is only a small reduction in the correlation values when the normal curve smoothing technique was used. Similarly the lag value for both cases was the same. Considering the long length of record used, it now appears that the polarity reversal was of such a minor nature as not to be of any significance. The EWRM technique was then accepted as valid for this research study. Figure 20 shows an example of the monthly, 3-monthly and the final format of EWRM for SST anomalies 0°-10°N which was used in the correlation program.

The main tool used in the statistical examination of the data was the Autocovariance and Power Spectral Analysis Program (APSA), the April 20, 1966 version which was published by the Health Sciences Computing Facility at the University of California, Los Angeles.

One of the useful features of the program was the calculation of the autocovariance of each data set from 0 to some stated number of lags, in both a positive and negative direction. Normally 10 percent of the total number of data points was used to establish the lag limit. Examination of the autocorrelation versus the lag curve then gave a good indication as to the success of efforts to remove regular trends such as the annual cycle. If everything appeared in order, the square root of the autocovariance at 0 lag was then taken to give the standard deviation for the individual series. A second feature of the program then crossed the designated base series (1) with another series (2) in both a positive and negative direction out to the number of lags used for the autocovariance calculations.

Crosscovariance values were then calculated at each lag point for the two series being crossed. Examination of plots of crosscovariance values versus lag values for any two series, then allowed selection of the most significant lag point. The final step was the hand calculation of the correlation coefficient. Throughout this paper, the correlation values shown in Tables 8 to 14 represent crosscovariance values for two series at a selected lag divided by the multiple of the standard deviation of both series.

The smoothing and extrapolation techniques that were used before the statistical analyses of the data raise some question as to the absolute validity of the correlation and lag values. One example that is readily apparent is that the beginning and end of trends can be easily smeared in a EWRM series. The lag values could thus be easily off one to two months in either direction. The correlation coefficients themselves also show a variation due to the EWRM smoothing used

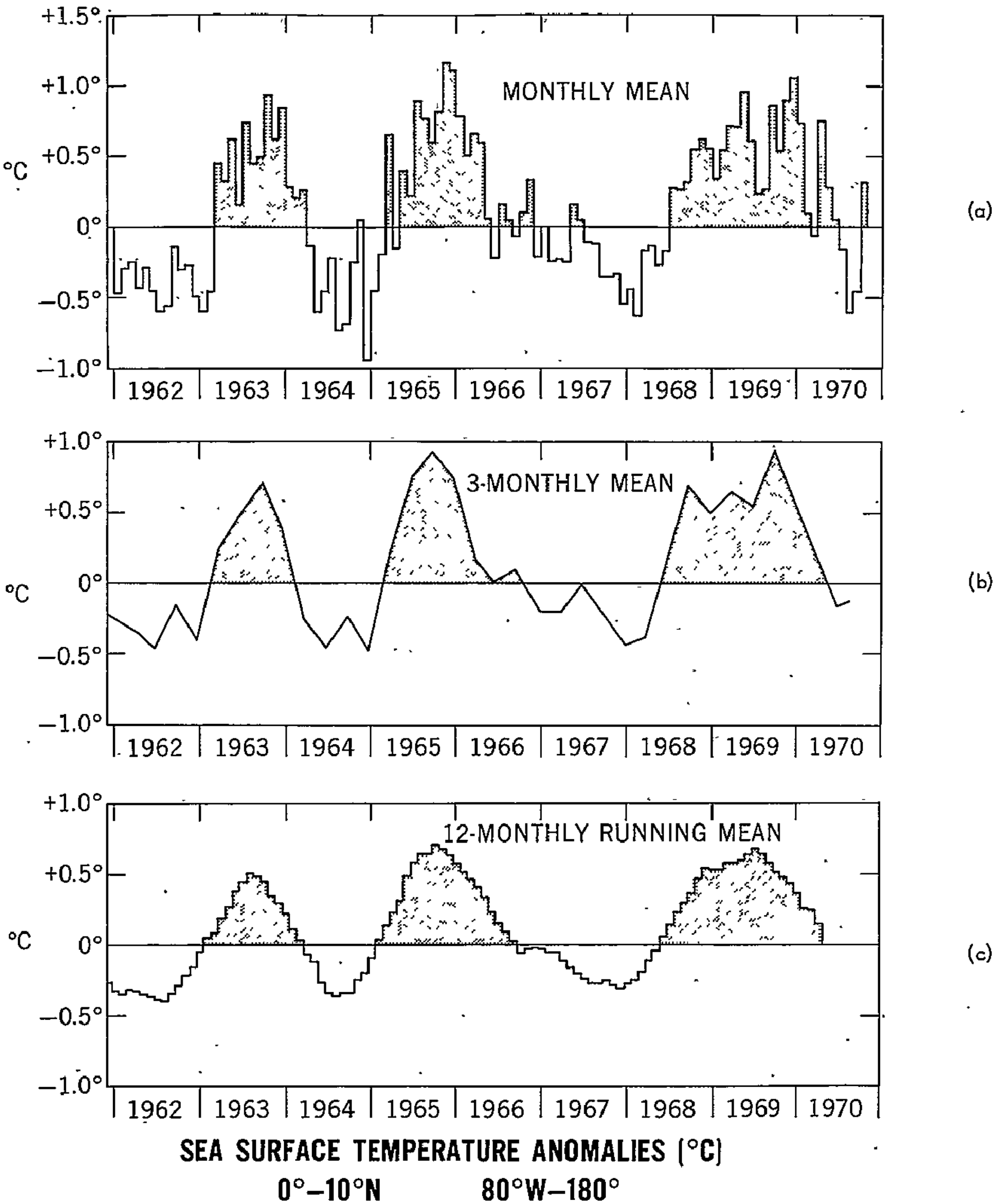

Figure 20. Comparison of: (a) the monthly mean, (b) 3-monthly mean and (c) 12-monthly running mean (EWRM) of tropical Pacific sea surface temperature anomalies (0°–10°N, 80°W–180°) from 1962 to 1970.

and should not be accepted as an absolute value. However, since this EWRM smoothing was used throughout this study, all correlation coefficients and lags can be intercompared in a relative sense.

The following tables show the monthly observations and linear interperable observations of the parameters used in the statistical analysis:

Table 5

Eastern Tropical Pacific Ocean

Satellite-Derived Cloudiness	Monthly Observations	Linear Interperable Observations
20°N-30°N	34	99
10°N-20°N	34	99
5°N-15°N	34	99
0°N-10°N	34	99
5°N-5°S	34	99
0°-10°S	34	99
10°S-20°S	34	99
20°S-25°S	34	99

Table 6

Sea Surface Temperature Anomalies	Monthly Observations	Linear Interperable Observations
U.S. West Coast Stations	624	624
20°-30°N	36 (3 mo. mean)	108
10°-20°N	60 "	240
5°N-15°N	60 "	240
0°-10°N	60 "	240
5°N-5°S	60 "	240
0°-10°S	60 "	240
South American west coast stations	240	240

Table 7

		Monthly Observations	Linear Interperable Observations
NE Pacific-SLP anomalies	30°-40°N	240	240
700 mb Height anomalies	180°-100°W	240	240
SE Pacific-Area covered by ≥ 1020 mb at sea level*	30°-40°S 180°-75°W	147	147
Juan Fernandez I sea level pressure		677	677
Darwin, Australia sea level pressure		677	677
Tropical Pacific island rainfall		677	677

* Obtained from Deutscher Wetterdienst, 1956-1970.

The first parameter to be correlated by the APSA program was satellite-derived cloudiness (≥.6/10), from 30°N to 25°S from 1962 to 1970 and the results are shown in Table 8.

Table 8

Correlation Coefficients (r)

Satellite-Derived Cloudiness (≥ 6/10)	Satellite-Derived Cloudiness (Percent of Area Covered by ≥ 6/10 Cloudiness) over the Eastern Tropical Pacific Ocean															
	20°-30°N	lag	10°-20°N	lag	5°-15°N	lag	0°-10°N	lag	5°N-5°S	lag	0°-10°S	lag	10°-20°S	lag	20°-25°S	lag
20°-30°N			+0.82	-1	+0.71	0	+0.93	-1	+0.76	-2	+0.68	-1	+0.87	-1	+0.63	-1
10°-20°N	+0.82	+1			+0.92	0	+0.85	+2	+0.66	+2	+0.66	+4	+0.69	+2	+0.63	-1
5°-15°N	+0.76	0	+0.92	0			+0.75	+1	+0.40	+1	+0.38	+3	+0.60	+2	+0.77	-1
0°-10°N	+0.93	+1	+0.85	-2	+0.75	-1			+0.80	-1	+0.67	+1	+0.83	+1	+0.63	-1
5°N-5°S	+0.76	+2	+0.66	-2	+0.40	-1	+0.80	+1			+0.96	+1	+0.63	+2	-0.40	-9
0°-10°S	+0.68	+1	+0.66	-4	+0.38	-3	+0.67	-1	+0.96	-1			+0.60	+1	-0.30	-9
10°-20°S	+0.87	+1	+0.69	-2	+0.60	-2	+0.83	-1	+0.63	-2	+0.60	-1			+0.75	-1
20°-25°S	+0.63	+1	+0.63	+1	+0.77	+1	+0.63	+1	-0.40	+9	-0.30	+9	+0.75	+1		

By way of clarification, a -4 under the lag column, means that the parameter at the top of the table lags the compared parameter at the side. A +4 implies that the "top" parameter leads the "side" parameter by 4 months.

The correlation coefficients which ≥ 0.70 were underlined in this table to indicate the more significant relationships. The first impression which one gets from Table 8 is that the NE and SE Pacific cloud bands appear to be positively interrelated. Over 65% of the correlation coefficients are ≥ 0.65, with a very short response time of ±1 to 2 months. The 20-30°N and 0°-10°N cloudiness are more closely related to southern hemisphere cloudiness than any other bands.

As a further check on this interesting relationship, 12 month running means of satellite cloudiness by quadrants over the entire tropical Pacific Ocean 130°E-100°W, 30°N-25°S were plotted (Figure 21, a, b). The equator and 180° meridian divided each quadrant analyzed. The high correlation coefficients (r = to .80 to +0.93) and short ±3 month lag which relate each quadrant's cloudiness are shown in Table 9.

Table 9
Correlation Coefficients (r)
Satellite-Derived Cloudiness (6/10)

	NE Pacific 0°-30°N	lag	SE Pacific 0°-25°S	lag	NW Pacific 0°-30°N	lag	SW Pacific 0°-25°S	lag
NE Pacific 0°-30°N			+0.84	0	+0.93	+3	+0.87	0
SE Pacific 0°-25°S	+0.84	0			+0.80	+2	+0.87	-1
NW Pacific 0°-30°N	+0.93	-3	+0.92	-3			+0.92	-3
SW Pacific 0°-25°S	+0.87	0	+0.87	+1	+0.92	+3		

A single (EWRM) curve of the entire tropical Pacific Ocean cloudiness is shown at the bottom of Figure 21 (c). A possible explanation for the apparent "in phase" relationship between the cloudiness variations in the four Pacific quadrants may lie in the effect of the Southern Oscillation, a large surface pressure pulsation common to the Pacific and Indian Ocean described by Troup 1965, Berlage, 1966 and Bjerknes, 1969 (a).

Next the sea surface temperature anomalies were correlated from the U. S. west coastal stations 33°-40°N through the tropical ocean bands to 0°-40°S along the South American west coast. Figure 22 shows the interesting similarity in the warm and cool patterns through each latitude band over this vast stretch of eastern Pacific Ocean. Table 10 confirms this areal coherence and positive relationship between these sectors. Approximately 60% of the correlation coefficients were ≥ 0.65 with a short response time of ±1 to 3 months. The 0° - 10°N and 5° - 15°N sea surface temperature bands are more closely related to southern hemisphere sea surface temperature bands than any other band.

The sea surface temperature anomalies were next correlated with the satellite-derived cloudiness from 30°N to 25°S in the eastern Pacific (Table 11). Two correlations shown up in this table which appear of importance.

Approximately 50% of the correlation coefficients are negative and ≥ 0.65. A simple description of this relationship would be: cool sea surface temperature follow heavy cloudiness by a -7 to -9 month lag. This effect occurs mainly over the 5° -15°N, 0°-10°N oceanic bands and along the U. S. west coast and related to cloudiness on both sides of the equator. Bjerknes (1969(a)) description of the localized Hadley cell circulation in the eastern Pacific could be the logical dynamical explanation for this negative cloud-SST correlation with slow feedback loop.

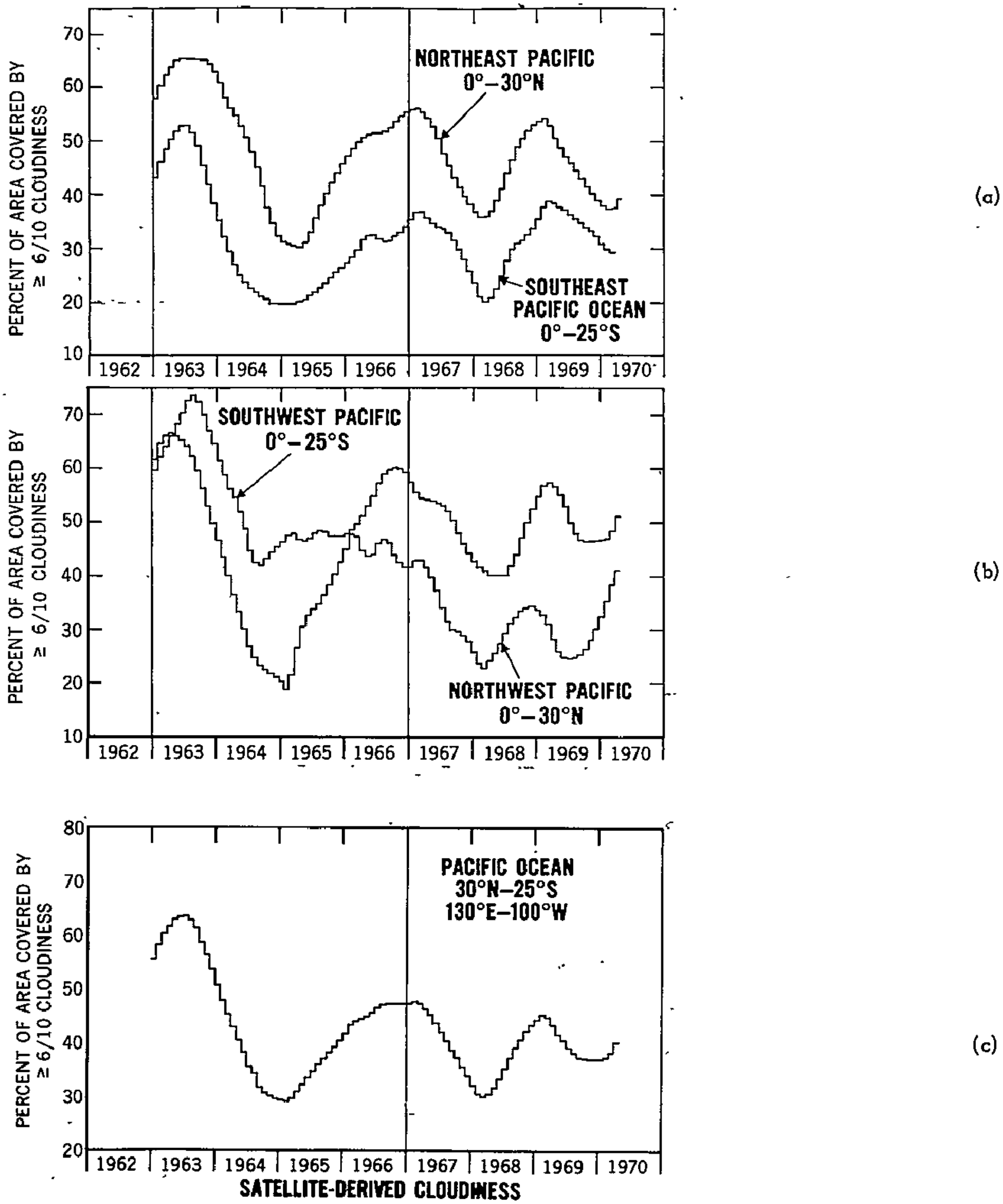

Figure 21. A comparison of satellite-derived cloudiness in percent of area covered by ≥ 6/10 clouds over the (a) northeast Pacific (0°–30°N), southeast Pacific (0°–25°S). (b) Northwest Pacific (0°–30°N), southwest Pacific (0°–25°S). The 180° merdian divided the east and west quadrants. (c) The entire tropical Pacific Ocean, 130°E–100°W, 30°N–25°S.

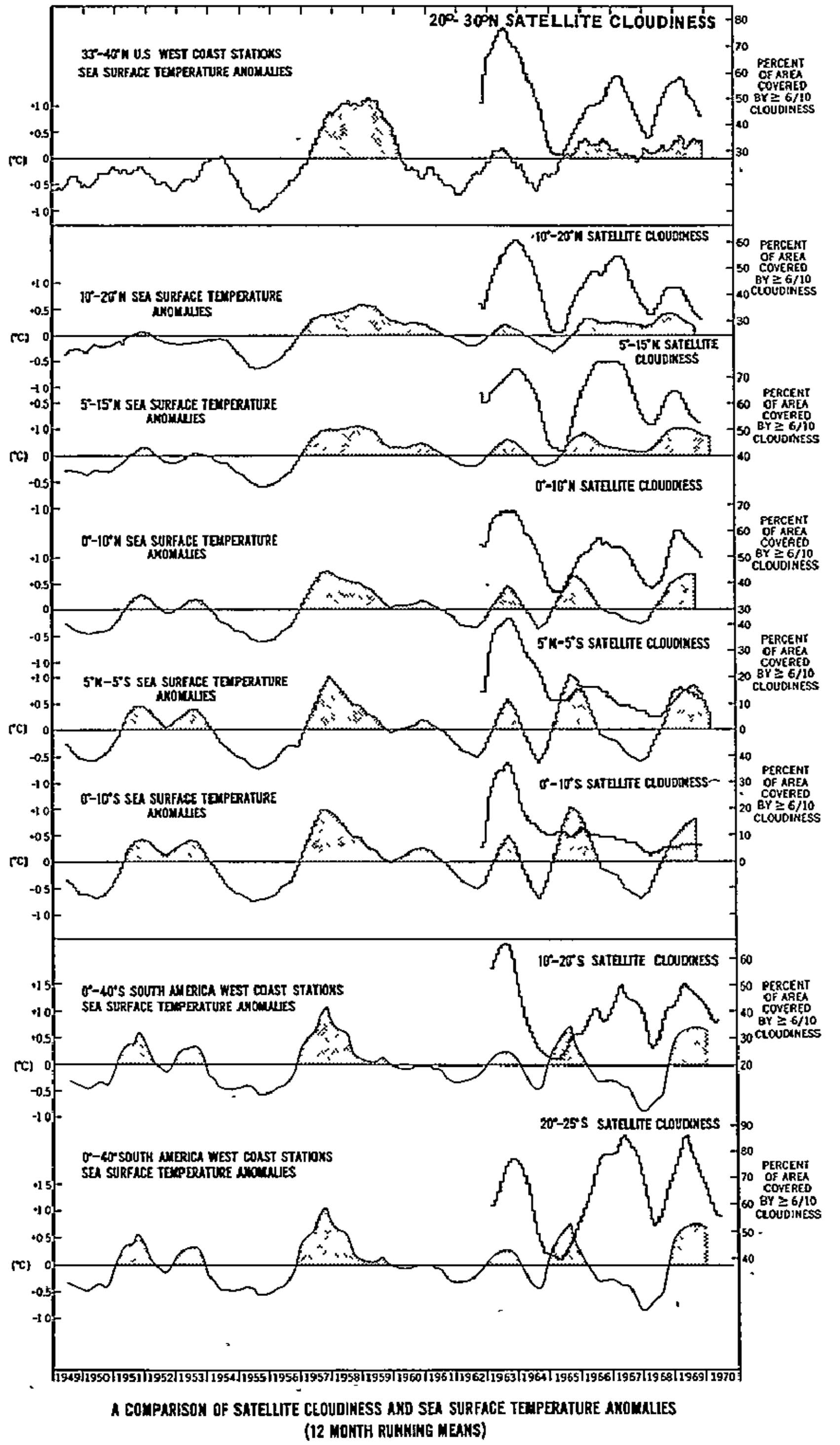

Figure 22. A comparison of 12-month running means of satellite-derived cloudiness, in percent of area covered by ≥ 6/10 clouds from 1962-1970 and sea-surface temperature anomalies from 1949-1970.

Table 10

Correlation Coefficients (r)

Sea Surface Temperature Anomalies

Sea Surface Temp. Anomalies	33°-40°N (U.S. West Coast)	lag	20°-30°N	lag	10°-20°N	lag	5°-15°N	lag	0°-10°N	lag	5°N-5°S	lag	0°-10°S	lag	0°-40°S (S.A. West Coast)	lag
33°-40°N (U.S. West Coast)			+0.65	-8	+0.87	-1	+0.84	0	+0.76	+2	+0.62	+3	+0.61	+4	+0.53	+6
20°-30°N	+0.65	+8			+0.77	+3	+0.35	0	-0.25	+8	-0.35	+8	-0.35	-5	-0.59	+7
10°-20°N	+0.87	+1	+0.77	-3			+0.95	0	+0.66	+4	+0.63	+3	+0.53	+5	+0.46	+5
5°-15°N	+0.84	0	+0.35	0	+0.95	0			+0.92	+1	+0.79	+1	+0.79	+1	+0.62	+3
0°-10°N	+0.76	-2	-0.25	-8	+0.66	-4	+0.92	-1			+0.96	0	+0.96	0	+0.85	+1
5°N-5°S	+0.62	-3	-0.35	-8	+0.63	-3	+0.79	-1	+0.96	0			+0.98	0	+0.89	+1
0°-10°S	+0.61	-4	-0.35	+5	+0.53	-5	+0.79	-1	+0.96	0	+0.98	0			+0.90	+1
0°-40°S (S.A. West Coast)	+0.53	-6	-0.59	-7	+0.46	-5	+0.62	-3	+0.85	-1	+0.89	-1	+0.90	-1		

Table 11

Correlation Coefficients (r)

Sea Surface Temperature Anomalies vs. Satellite-Derived Cloudiness

Satellite-Derived Cloudiness (≥ 6/10)	33°-40°N (U.S. West Coast)	lag	20°-30°N	lag	10°-20°N	lag	5°-15°N	lag	0°-10°N	lag	5°N-5°S	lag	0°-10°S	lag	0°-40°S (S A. West Coast)	lag
20°-30°N	-0.66	-8	+0.23	0	+0.45 -0.41	+3 -8	-0.52	-8	-0.49	-8	-0.50	-8	-0.55	-8	-0.29	-8
10°-20°N	-0.76	-9	-0.31	+9	+0.47 -0.48	+2 -8	-0.84	-9	+0.42 -0.87	+8 -8	-0.82	-8	+0.47 -0.88	+8 -8	-0.60	-8
5°-15°N	+0.69	-7	+0.35	+3	+0.66	+3	-0.70	-9	-0.87	-8	-0.85	-8	-0.92	-8	-0.69	-8
0°-10°N	-0.74	-9	+0.02 -0.13	+1 -9	+0.42 -0.49	+3 -8	-0.73	-9	+0.50 -0.65	+6 -8	-0.61	-9	+0.50 -0.66	+7 -8	-0.39	-8
5°N-5°S	-0.89	-9	-0.50 -0.36	-9 +5	-0.69	-8	-0.71	-9	-0.39	-8	-0.35	-9	-0.33	-8	+0.45	+6
0°-10°S	-0.81	-9	-0.49	+6	-0.53	-8	-0.59	-9	+0.13 -0.33	0 -8	-0.37	-9	-0.30	-8	-0.41	+5
10°-20°S	+0.52	+4	+0.36	-4	-0.50	-1	+0.44	+1	-0.50	-8	-0.56	-9	-0.61	-8	-0.54	-8
20°-25°S	+0.87	+6	+0.63	-2	-0.89	+3	+0.71	+4	-0.72	-8	-0.75	-9	-0.84	-8	-0.80	-8

A smaller group of positive correlations (approximately 20% of total) varying from +0.45 to +0.87 with generally +3 to +3 months lead, was also found in the data. This would relate increased cloudiness with warmer sea surface temperatures and vice versa; however, this effect was not dominant in the region of the Pacific. Figure 22 graphically illustrates these two air-sea interaction effects. Note the depressed cloudiness in the presence of warm sea surface temperature from 5°N-10°S during the winter of 1966 which was reported by Krueger and Gray (1969) and the increased cloudiness at 10°-25°S in the presence of cool sea surface temperature anomalies of the Peru current. The presence of dense stratiform clouds in this region has been noted in daily ATS III and ESSA-ITOS cloud photography (U. S. Dept. of Commerce, 1970(b)), (Goddard Space Flight Center, 1969*).

Figures 23 and 24 present the printout of the ASPA program and illustrates how the correlation coefficients and lags are determined for satellite-derived cloudiness and sea surface temperature anomalies in Table 11 from the relationship:

$$r_{1,2} = \frac{\text{cross-covariance}}{S_1 \, S_2}$$

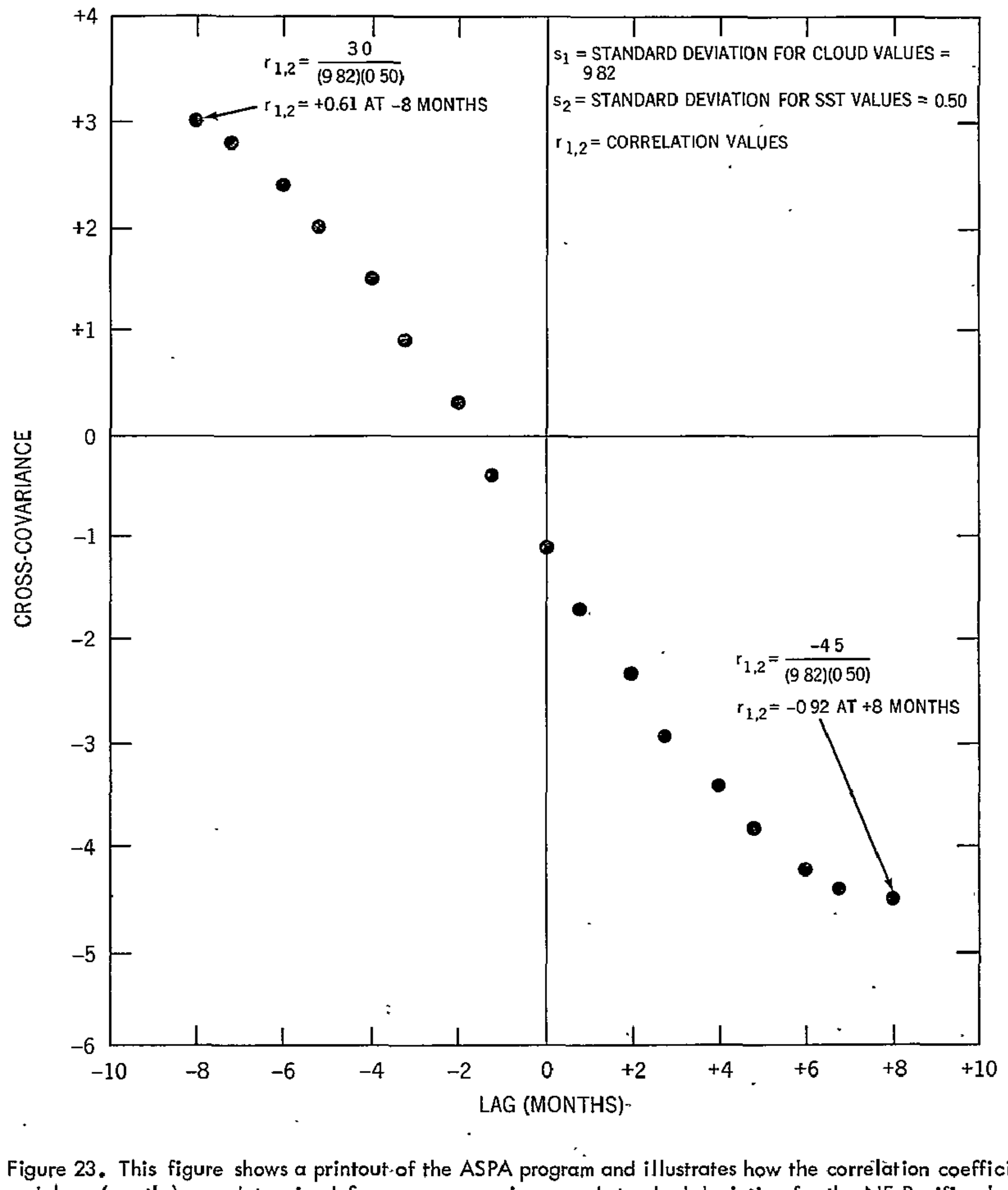

Figure 23. This figure shows a printout of the ASPA program and illustrates how the correlation coefficients (r) and lags (months) are determined from cross-covariance and standard deviation for the NE Pacific cloudiness (5°-15°N, 100°W-180°) and the SE Pacific sea surface temperature anomalies (0°-10°S, 80°W-180°) from 1962 to 1970.

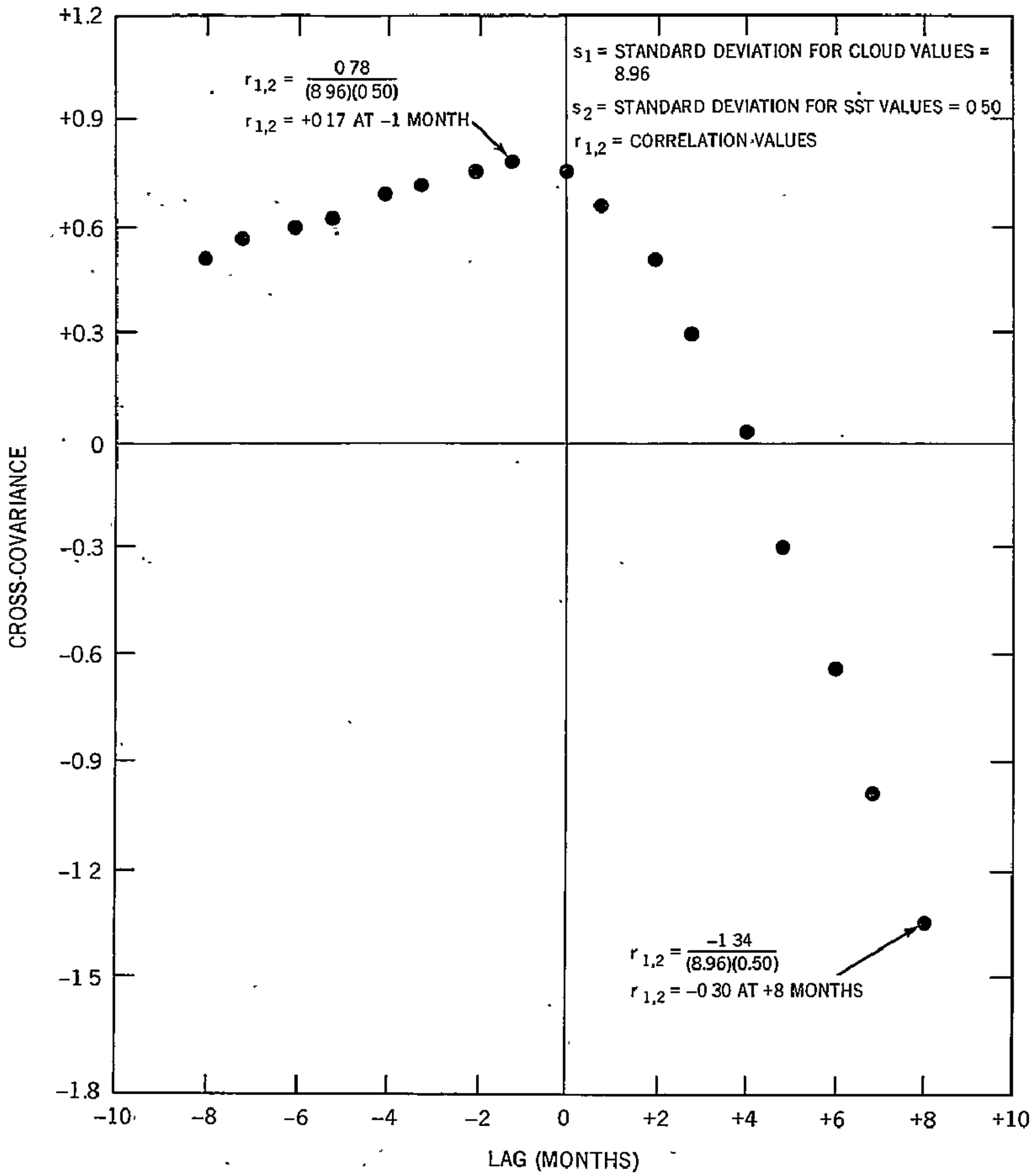

Figure 24. This figure shows a printout of the ASPA printout and illustrates how the correlation coefficients (r) and lags (months) are determined from cross-covariance and standard deviation for the SE. Pacific cloudiness (0°-10°S, 100°-180°) and the SE Pacific sea surface temperature anomalies (0°-10°S, 80°W-180°) from 1962 to 1970.

where

$r_{1,2}$ = the correlation coefficient for the two series
S_1 = standard deviation for series 1
S_2 = standard deviation for series 2.

The next three tables correlate the northeast Pacific anticyclone surface pressure anomalies, 700 mb ht anomalies the percent of area covered by ≥ 1020 mb in the region 30°-40°S, 180°-100°W (S.P. anticyclone) Juan Fernandez and Darwin surface pressure, tropical Pacific island rainfall against satellite-derived cloudiness (Table 12), sea surface anomalies (Table 13), and each other (Table 14).

Three interesting features shown in Table 12 are the cross-equatorial relationship between the NE Pacific 700 mb ht anomalies (see Figure 5), the Darwin and tropical island rainfall, surface

Table 12

Correlation Coefficients (r)

Sea Surface Temp. Anomalies	30°-40°N (NE Pacific) Surface Pressure	lag	30°-40°N (NE Pacific) 100 mb Ht	lag	30°-40°S (SE Pacific) Surface Pressure	lag	Juan Fernandez Surface Pressure	lag	Darwin Surface Pressure	lag	Tropical Pacific I. Rainfall	lag
33°-40°N (U.S. West Coast)	-0.68	+6	-0.68	+8	-0.41	+5	-0.43	+3	+0.59	0	+0.53	0
20°-30°N	-0.69	+8	-0.41	+8	-0.55	-8	+0.64	-5	-0.60	+8	-0.40	-8
10°-20°N	-0.72	+7	-0.73	+9	-0.34 -0.69	+10 +30	-0.61	+5	+0.56	+2	+0.62	+2
5°-15°N	-0.74	+7	-0.74	+8	-0.56	+5	-0.66	+3	+0.73	0	+0.78	+1
0°-10°N	-0.67	+6	-0.74	+6	-0.67	+4	-0.69	+2	+0.80	-1	+0.92	-1
5°N - 5°S	-0.56	+6	-0.72	+6	-0.71	+3	-0.64	+2	+0.83	-1	+0.93	-1
0°-10°S	-0.51	+5	-0.70	+5	-0.66	+3	-0.63	+2	+0.82	-2	+0.90	-1
0°-40°S (S.A. West Coast)	-0.36	+4	-0.56	+4	-0.51	+1	-0.52	0	+0.71	-3	+0.75	-2

Table 13

Correlation Coefficients (r)

Satellite-Derived Cloudiness (≥ 6/10)	30°-40°N (NE Pacific) Surface Pressure	lag	30°-40°N (NE Pacific) 700 mb HT.	lag	30°-40°S (SE Pacific) Surface Pressure	lag	Juan Fernandez Surface Pressure	lag	Darwin Surface Pressure	lag	Tropical Pacific I. Rainfall	lag
20°-30°N	+0.39	-8	+0.76	-4	+0.65	-8	+0.54	+3	-0.55	-8	-0.41	-8
10°-20°N	+0.53	-1	+0.78	-2	+0.67	-4	+0.37	-4	-0.84	-8	-0.73	-9
5°-15°N	+0.36	0	+0.62	-2	+0.79	-5	+0.48	-4	-0.78	-9	-0.79	-9
0°-10°N	+0.48	-5	+0.82	-5	+0.60	-4	+0.33	+3	-0.59	-8	-0.55	-9
5°N-5°S	+0.86	-7	+0.89	-6	+0.26	+3	+0.27	+8	-0.33	-9	-0.25	-9
0°-10°S	+0.88	-7	+0.89	-7	+0.27	+4	+0.29	+8	+0.22	-1	-0.20	-9
10°-20°S	-0.52	+9	+0.73	-7	+0.65	-6	+0.51	-7	-0.67	-9	-0.44	-8
20°-25°S	-0.55	+9	-0.60	+9	-0.80	-5	+0.68	-7	-0.83	-9	-0.74	-8

Table 14
Correlation Coefficients (r)

	30°-40°N (NE Pacific) Surface Pressure	lag	30°-40°N (NE Pacific) 700 mb HT.	lag	30°-40°S (SE Pacific) Surface Pressure	lag	Juan Fernandez Surface Pressure	lag	Darwin Surface Pressure	lag	Trppical Pacific I Rainfall	lag
30°-40°N (NE Pacific) Surface Pressure			+0.80	0	+0.30	-5	+0.39	-4	-0.52	-6	-0.55	-7
30°-40°N (NE Pacific) 700 mb HT	+0.80	0			+0.53	0	+0.46	-4	-0.54	-6	-0.65	-6
30°-40°S (SE Pacific) Surface Pressure	+0.30	+5	+0.53	0			+0.76	-1	-0.67	-3	-0.81	-4
Juan Fernandez Surface Pressure	+0.39	+4	+0.46	+4	+0.76	+1			-0.50	-3	-0.58	0
Darwin Surface Pressure	-0.52	+6	-0.54	+6	-0.67	+3	-0.50	+3			+0.80	0
Tropical Pacific I. Rainfall	-0.55	+7	-0.65	+6	-0.81	+4	-0.58	0	+0.80	0		

pressure, and the SST anomalies. Since this data is based upon 20 years of record, we feel that these positive and negative correlations are highly significant and useful for meteorological and oceanographic prediction. It was noted also that the NE Pacific surface pressure lead the 5°-20°N sea surface temperatures by a 7 months while the SE Pacific surface pressure had a shorter 3 months lead time in its effective region. The faster wind stress coupling time could be explained by the greater seasonal stability and size of the South Pacific anticyclone when compared with the North Pacific anticyclone.

Table 13 indicates the good correlations shown by the NE Pacific 700 mb height anomalies and cross-equatorial satellite derived cloudiness but since the period of record is only 9 years our confidence level is lower than shown for Table 12. Note the consistent negative correlations (-0.73 to -0.84) between Darwin surface pressure, tropical rainfall and 5° to 20°N cloudiness.

Table 14 indicates the good positive correlation (+0.80) between the NE Pacific surface pressure and 700 mb height anomalies (see Figure 2). This maritime relationship had been previously noted by Klein, 1967. In addition, tropical Pacific island rainfall related positively (r = +0.80) with Darwin surface pressure (Figures 25 and 26 a, b). This useful meteorological relationship implies a cross-equatorial coupling that has not been completely described dynamically in the literature (Quinn and Burt, 1970).

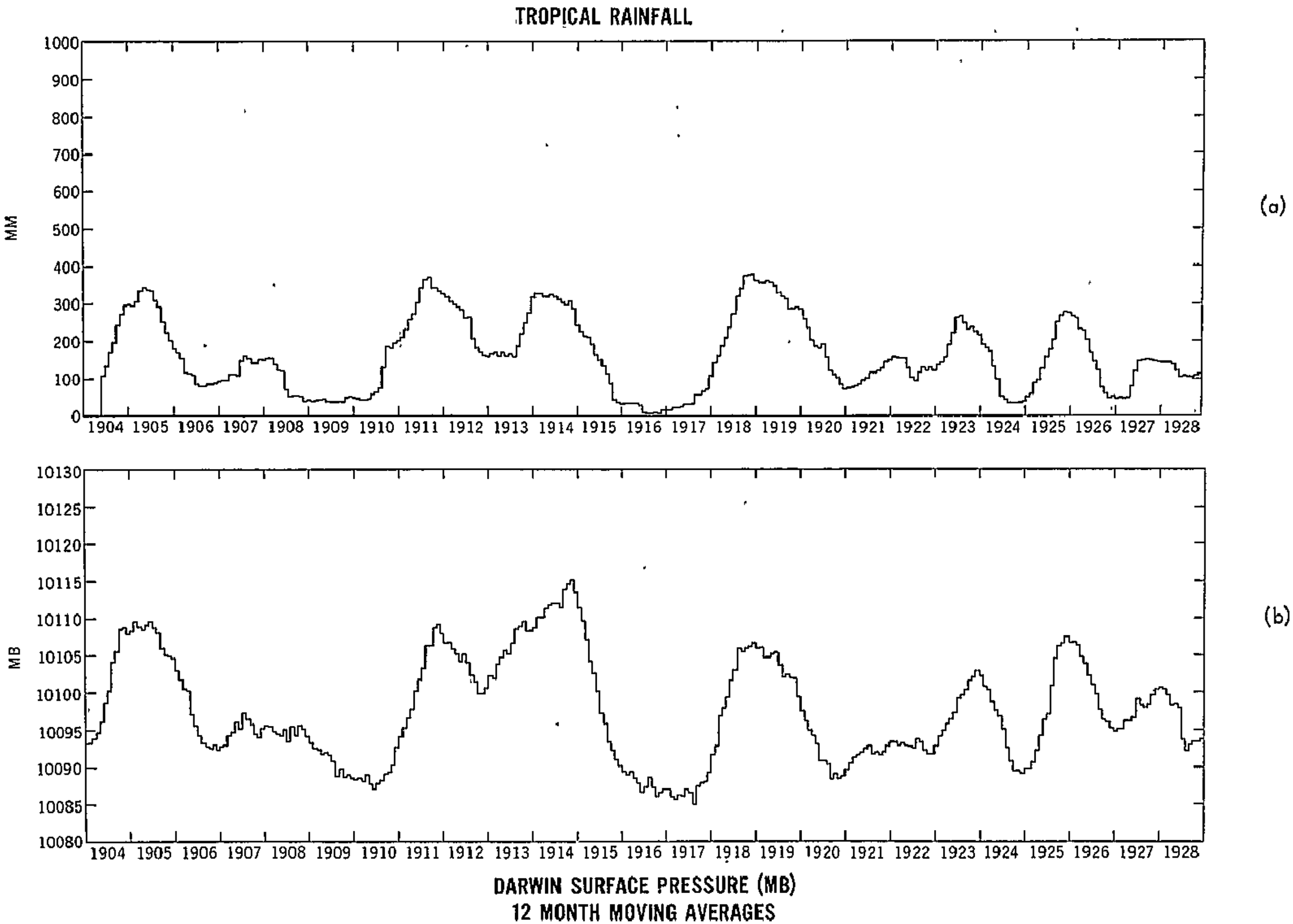

Figure 25. A comparison of 12-month running means of (a) tropical Pacific island rainfall (See Fig. 6). (b) Darwin, Australia surface pressure from 1904 to 1928.

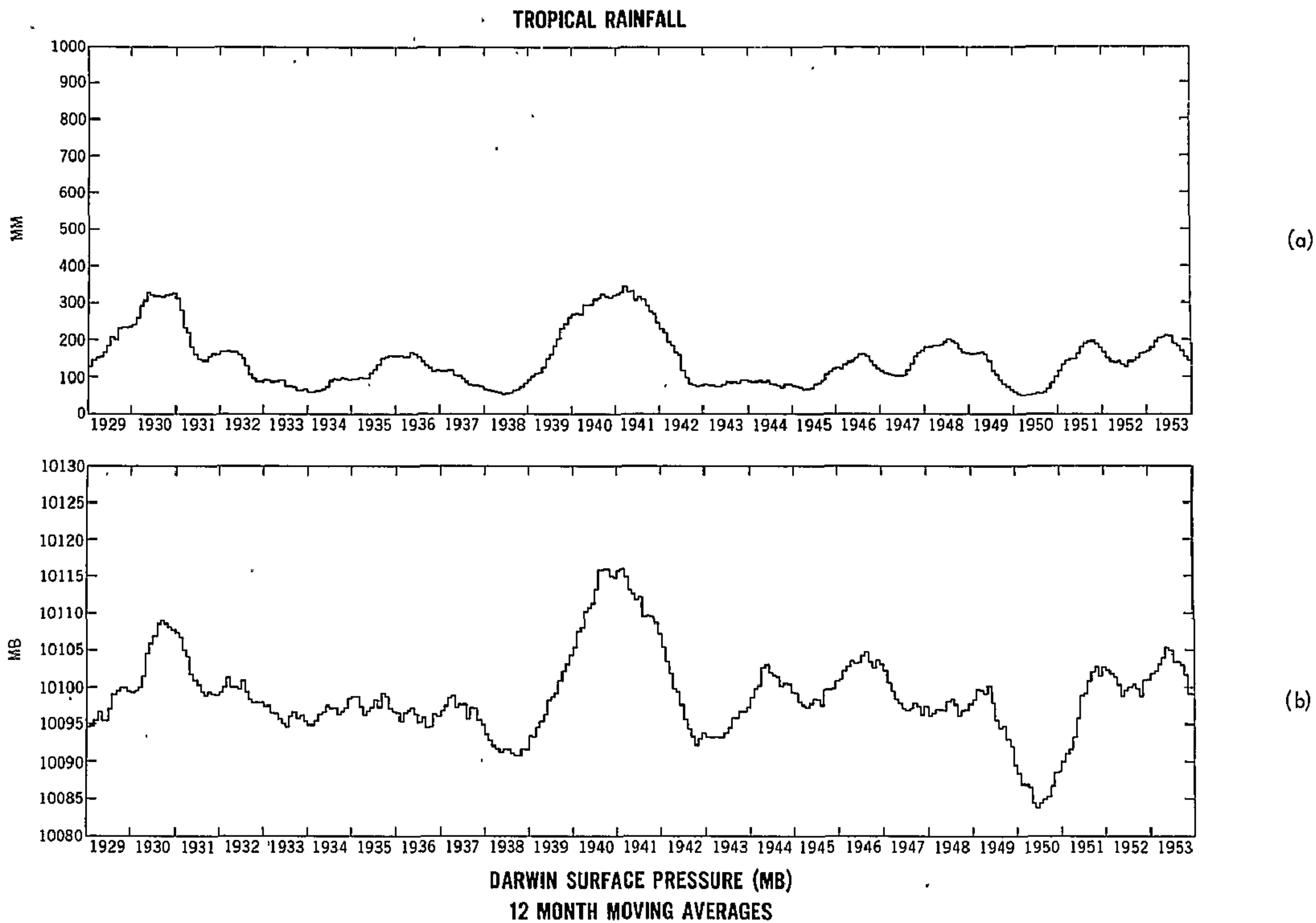

Figure 26. A comparison of 12-month running means of (a) tropical Pacific island rainfall (See Fig. 6). (b) Darwin, Australia surface pressure from 1929 to 1953.

CONCLUSIONS

Sea surface temperature variations in the California and Peru Currents from 1949 to 1970 have been traced from the west coasts of North and South America respectively, to the central tropical Pacific Ocean by means of a newly produced atlas of sea surface temperature anomalies (Appendix A). These sea surface temperature anomalies did indeed show a strong relation to Canton Island sea surface temperature data, as was hypothesized by Bjerknes in 1966.

Tropical Pacific island rainfall was found to be strongly correlated with tropical sea surface temperatures ($r = +0.93$) anomalies and by use of this direct relationship, it was possible to derive tropical SST anomalies back to 1905, a period of sparse oceanographic data.

The northeast Pacific 700 mb height field (30°-40°N) was found to be positively correlated ($r = +0.73$ to $+0.89$) to satellite derived cloudiness from 30°N to 20°S and negatively correlated ($r = -0.70$ to -0.74) with sea surface temperature anomalies from 20°N to 10°S.

The tropical sea surface temperatures were negatively correlated and lagged the satellite-derived cloudiness from 20°N to 10°S implying the presence of a localized Hadley circulation, previously suggested by Bjerknes 1969(a). The eastern Pacific sea surface temperature bands and coastal waters showed an close areal coherance in pattern from 40°N to 40°S while the satellite-derived cloudiness over the entire Pacific appeared to be pulsating in resonance. Possible relationship with the Southern Oscillation was suggested.

The South Pacific anticyclone appeared to couple faster (3 months lead) through wind stress to the sea surface than the North Pacific anticyclone (7 month lead time).

Tropical Pacific island rainfall was well correlated with Darwin surface pressure ($r = +0.80$) and implied a local atmospheric coupling which has not been completely documented in the literature.

This study has shown the various time frames of direct local and cross-equatorial air-sea relationships which exist over the tropical Pacific Ocean. With further analytical refinement several of these geophysical parameters could become useful for seasonal meteorological and oceanographic prediction.

ACKNOWLEDGEMENTS

The authors wish to thank Dr. Jacob Bjerknes, Professor Emeritus, University of California, Los Angeles, Dr. Alan Longhurst, Scripps Institution of Oceanography, Dr. Thomas Austin, NOAA and Dr. William Quinn, Oregon State University for their continued interest and encouragement during the course of this study and to Dr. Raymond Wexler, GSFC for his suggestions and helpful editorial comments on the manuscript.

REFERENCES

Anderson, R. K., J. P. Ashman, F. Bittner, G. R. Farr, E. W. Ferguson, V. Oliver, and A. H. Smith, 1969: "Application of Meteorological Satellite Data in Analysis and Forecasting," Tech. Report 212, Air Weather Service (MAC), U.S. Air Force.

Atkinson, G. D. and J. C. Sadler, 1970: "Mean Cloudiness and Gradient-Level-Wind Charts Over the Tropics. Vol. 1 and 2, Technical Report 215, Air Weather Service, U.S. Air Force.

Berlage, H. P., 1966: The Southern Oscillation and World Weather, Mededeel. Verhandel, Kon. Ned. Meteor. Inst., No. 88, 152 pp.

Bjerknes, J., 1961: El Nino Study Based on Analyses of Ocean Surface Temperatures, 1935-1957, Bull. Inter-American Tropical Tuna Comm., 5(3): pp. 217-303.

Bjerknes, J., 1966(a), "Survey of El Nino (1957-58) in its Relation to Tropical Pacific Meteorology," Vol. 12, No. 2, Inter-American Tropical Tuna Commission, La Jolla, California, pp. 45.

Bjerknes, J., 1966(b): "A Possible Response of the Hadley Circulation to Variations of the Heat Supply from the Equatorial Pacific," Tellus, XVIII, pp. 820-829.

Bjerknes, J., 1969(a), "Atmospheric Teleconnections from the Equatorial Pacific, Monthly Weather Review, Vol. 97, No. 3, pp. 163-172.

Bjerknes, J., with L. J. Allison, E. R. Kreins, F. A. Godshall, 1969(b), "Satellite Mapping of the Tropical Pacific Cloudiness," Bulletin of the American Meteorological Society, Vol. 50, No. 5, pp. 313-322.

Crutcher, H. L. and J. M. Meserve, 1970: "Selected Level Heights, Temperatures and Dew Points for the Northern Hemisphere," NAVAIR 50-1C-52, U.S. Naval Weather Service Command, Washington, D.C.

Deutscher Wetterdienst, 1956-1970: "Seawetteramt, Die Witterung in Ubersee," Hamburg, Germany.

Doberitz, R., 1968(a): "Koharenzanalyse von Mederschlag und Wassertemperatur im tropischen Pazifischen Ozean," Berichte Deutschen Wetterdienstes, NR 112, (Band 15) Selbstverlag des Deutschen Wetterdienstes.

Doberitz, R., 1968(b): "Cross Spectrum Analysis of Rainfall and Sea Temperature at the Equatorial Pacific Ocean," Meteorologisches Institute Der Universitat, Bonn, Bonner Meteorologische Abhandlungen, Heft 8 (1968), pp. 61.

Goddard Space Flight Center, 1969: Meteorological Data Catalog for the Applications Technology Satellites, Vol. III and IV, Greenbelt, Md.

Godshall, F., 1968: "Intertropical Convergence Zone and Mean Cloud Amount in the Tropical Pacific Ocean," Monthly Weather Review 96(3): 172-175.

Godshall, F., L. J. Allison, E. R. Kreins, G. Warnecke, 1969: "Examples of the Usefulness of Satellite Data in General atmospheric Circulation Research, Part II — An Atlas of Average Cloud Cover over the Tropical Pacific Ocean, NASA Tech Note. D-5631, pp. 41.

Godshall, F., L. J. Allison, J. Steranka, 1971: "Monthly Satellite-Derived Cloudiness Over the Tropical Pacific Ocean," NASA Tech. Note (in preparation).

Kornfield, J. and A. Hasler, 1971: "Photographic Cloud Averages," Weather Motions from Space, University of Wisconsin Press, Madison, Wisconsin.

Krueger, A. F. and T. I. Gray, Jr., 1969: "Long-Term Variations in Equatorial Circulation and Rainfall," Monthly Weather Review, Vol. 97, No. 10, pp. 700-711.

Leese, J. A., A. L. Booth and F. A. Godshall, 1970: Archivingand Climatological Applications of Meteorological Satellite Data," ESSA Technical Report NESC 53, U.S. Dept. of Commerce, Washington, D.C.

Malkus, J. S., 1962: "Large-Scale Interactions," The Sea - M. H. Hull, Ed., Interscience Publishers, New York, N.Y., Vol. 1, pp. 88-294.

Miller, D. B., 1971: "Automated Production of Global Cloud Climatology Based on Satellite Data," Proceedings of 1970 Meteorological Technical Exchange Conference, Annapolis, Md., September 1970, USAWS Tech. Report 242, Air Weather Service, U.S. Air Force, Scott Air Force Base, Illinois.

Monthly Weather Review, 1949-1971: "Weather and Circulation," U.S. Weather Bureau, Washington, D.C.

Namaris, J., 1970: Macroscale Variations in Sea-Surface Temperatures in the North Pacific, Journal of Geophysical Research, Vol. 75, No. 3, pp. 565-582.

Panofsky, H. A., and G. W. Brier, 1963: Some Applications of Statistics to Meteorology, Pennsylvanis State University, Pa., pp. 226.

Quinn, W. and W. V. Burt, 1970: Prediction of Abnormally Heavy Precipitation over the Equatorial Pacific Dry Zone, Journal of Applied Meteorology, Vol. 9, No. 1, pp. 20-28.

Rasool, S. I. and J. S. Hogan, 1969: "Ocean Circulation and Climatic Changes," Bulletin of the American Meteorological Society, Vol. 50, No. 3, pp. 130-134.

Reid, J. L., G. I. Roden, and J. G. Wyllie, 1958: "Studies of the California Current System" State of California Marine Research Committee, California Cooperative Ocean – Fisheries Investigative Progress Report; 1 July 1956 - 1 Jan 1958, Sacramento State Printer, pp. 27-56.

Renner, J. A., 1962-1970: "Sea Surface Temperature Charts, Eastern Pacific Ocean," California Fishery Market News Monthly ~~Summary,~~ ~~Part~~ II, Fishing Information, U.S. Dept. of Interior, Bureau of Commerical Fisheries, Biological Laboratory, San Diego, California.

Roden, G. I. and J. L. Reid, Jr., 1961: Sea Surface Temperature Radiation and Wind Anomalies in the North Pacific Ocean. Records of Oceanographic Works in Japan, Vol. 6, No. 1, pp. 36-52.

Roden, G. I., 1962: Oceanographical Aspects of the Eastern Equatorial Pacific, Geophysica International, Contribution 1527, Vol. 2, No. 4, pp. 601-615.

Roden, G. I., 1965: On Atmospheric Pressure Oscillations Along the Pacific Coast of North America, 1873-1963, Journal of Atmospheric Sciences, Vol. 22, No. 3, pp. 280-295.

Sadler, J. C., 1968: "Average Cloudiness in the Tropics from Satellite Observations," International Indian Ocean Expedition Meteorological Monograph No. 2, East-West Press, Honolulu, Hawaii.

Seckel, G. R., 1970: "Trade Wind Zone Oceanography Pilot Study," Part VIII, Special Sci. Rep.-Fisheries No. 612, U.S. Fish and Wildlife Service, Washington, D.C., 129 pp.

Shell, I. I., 1965: The Origin and Possible Prediction of the Fluctuations in the Peru Current and Upwelling, Journal of Geophysical Research, Vol. 70, No. 22, pp. 5529-5540.

Stewart, R. W., 1969: "The Atmosphere and the Ocean," Scientific American, Vol. 221, No. 3, p. 76-106.

Suomi, V. E. and T. H. VonderHaar, 1970: "Geosynchronous Meteorological Satellites," Measurements from Satellite Platforms, University of Wisconsin, Madison, Wisconsin, pp. 1-7.

Svedrup, H. U., 1947: Proceedings, Natl. Acad. Sci., USA, 33, 318-326.

Taljaard, J. J., H. vanLoon, H. L. Crutcher and R. L. Jenne, 1969: "Climate of the Upper Air Part I – Southern Hemisphere, Vol. 1, NAVAIR 50-1C-55, U.S. Naval Weather Service Command, Washington, D.C.

Troup, A. J.; 1965: "The Southern Oscillation," Quarterly Journal of the Royal Meteorological Society, Vol. 91, No. 390, pp. 490-506.

U.S. Committee for the GARP, 1969: "Plan for U.S. Participation in the Global Atmospheric Research Program," National Academy of Sciences, Washington, D.C., pp. 79.

U.S. Department of Commerce, 1970(a): "Eastropac Atlas," C. M. Love, Ed., Circular 330, Vol. 4, NOAA, Washington, D.C.

U.S. Department of Commerce, 1970(b): Catalog of Meteorological Satellite Data, No. 5.320-5.321, ESSA, Silver Spring, Md.

U.S. Navy, 1962: "Oceanography," Hydrographic Office Publication No. 9, Part 6, pp. 691-762.

U.S. Navy, 1966: Handbook of Oceanographic Tables, U.S. Navy Oceanographic Office, SP-68, Washington, D.C., pp. 425.

U.S. Naval Oceanographic Office, 1969: "Monthly Charts of Mean, Minimum and Maximum Sea Surface Temperature of the North Pacific Ocean," Special Publication 123, pp. 56.

Wallace, J. M. 1970: "Time-Longitude Sections of Tropical Cloudiness," ESSA Technical Report NESC 56, U.S. Dept. of Commerce, Washington, D.C., pp. 37.

Wooster, W. S., 1961(a): "Yearly Changes in the Peru Current," Limnology and Oceanography, Vol. 6, No. 2, pp. 222-226.

Wooster, W.S., 1961(b), Data Report, STEP-I Expedition 15 Sept – 14 Dec. 1960, Preliminary Report Ref. 61-9, Part I, Physical and Chemical Data, Scripps Institution of Oceanography, University of California, LaJolla, Calif.

Wyrtki, K., 1965: "Surface Currents of the Eastern Tropical Pacific Ocean," Vol. IX, No. 5, Inter-American Tropical Tuna Commission, La Jolla, California, 11. 304.

Wyrtki, K., 1966: "Oceanography of the Eastern Equatorial Pacific Ocean," Oceanogr. Mar. Biol. Ann. Rev. 4, Harold Barnes, Ed., published by G. Allen and Unwin Ltd, London, pp. 33-68.

Zipser, E. J., 1969: "Survey of Progress and Plans in Tropical Meteorology Experiments," Air Weather Service Technical Report 217, AWS(MAC), U.S. Air Force, pp. 178-188.

APPENDIX A

SEA SURFACE TEMPERATURE ANOMALIES OVER THE EASTERN TROPICAL PACIFIC OCEAN (1949-1970)

An atlas of 3-monthly sea surface temperature anomalies over the eastern tropical Pacific Ocean for the following months.

A-1 March-May 1949, and June-August 1949

A-2 September-November 1949 and December 1949 - February 1950

A-3 March-May 1950 and June-August 1950

A-4 September-November 1950 and December 1950-February 1951

A-5 March-May 1951 and June-August 1951

A-6 September-November 1951 and December 1951-February 1952

A-7 March-May 1952 and June-August 1952

A-8 September-November 1952 and December 1952-February 1953

A-9 March-May 1953 and June-August 1953

A-10 September-November 1953 and December 1953-February 1954

A-11 March-May 1954 and June-August 1954

A-12 September-November 1954 and December 1954-February 1955

A-13 March-May 1955 and June-August 1955

A-14 September-November 1955 and December 1955-February 1956

A-15 March-May 1956 and June-August 1956

A-16 September-November 1956 and December 1956-February 1957

A-17 March-May 1957 and June-August 1957

A-18 September-November 1957 and December 1957-February 1958

A-19 March-May 1958 and June-August 1958

A-20 September-November 1958 and December 1958-February 1959

A-21 March-May 1959 and June-August 1959

A-22 September-November 1959 and December 1959-February 1960

A-23 March-May 1960 and June-August 1960

A-24 September-November 1960 and December 1960-February 1961

A-25 March-May 1961 and June-August 1961

A-26 September-November 1961 and December 1961-February 1962

A-27 March-May 1962

A-28 June-August 1962 and September-November 1962

A-29 December 1962 - February 1963 and March-May 1963

A-30 June-August 1963 and September-November 1963

A-31 December 1963-February 1964 and March-May 1964

A-32 June-August 1964 and September-November 1964

A-33 December 1964-February 1965 and March-May 1965

A-34 June-August 1965 and September-November 1965

A-35 December 1965-February 1966 and March-May 1966

A-36 June-August 1966 and September-November 1966

A-37 December 1966-February 1967 and March-May 1967

A-38 June-August 1967 and September-November 1967

A-39 December 1967-February 1968 and March-May 1968

A-40 June-August 1968 and September-November 1968

A-41 December 1968-February 1969 and March-May 1969

A-42 June-August 1969 and September-November 1969

A-43 December 1969-February 1970 and March-May 1970

A-44 June-August 1970 and September-November 1970

A-45 Long-term mean sea surface temperature, for 5° lat-long. squares, for December-February and March-May. The numbers in descending order, to the left of the dot follow the monthly order. The 3-monthly long-term mean is at the bottom of the number column (U.S. Naval Oceanographic Office, 1969).

A-46 Long-term mean sea surface temperatures for 5° lat-long. squares, for June-August and September-November. The numbers, in descending order to the left of the dot follow the monthly order. The 3-monthly long term mean is at the bottom of the number column (U.S. Naval Oceanographic Office, 1969).

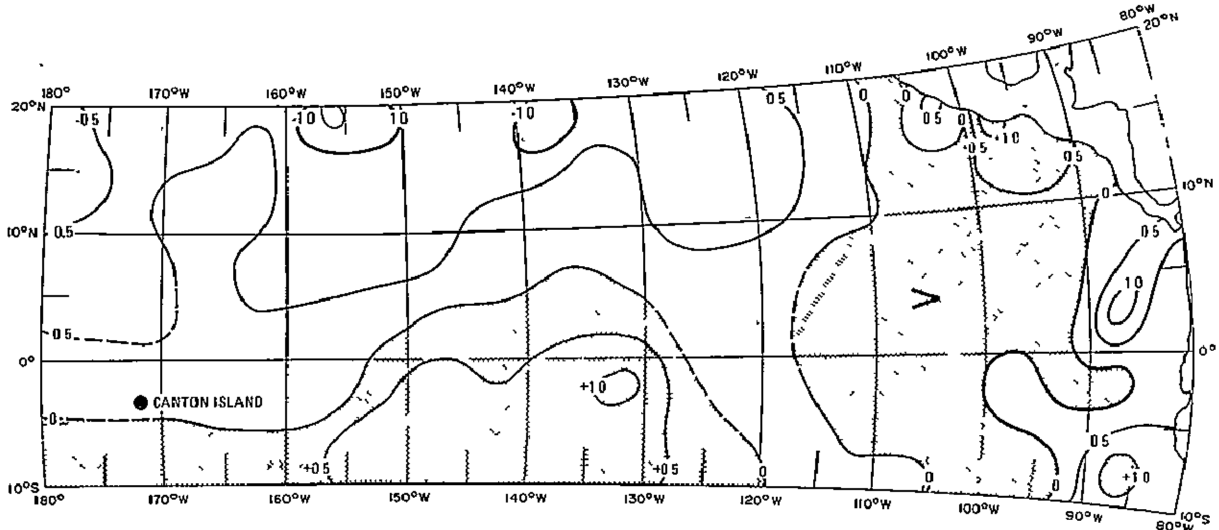

MARCH, APRIL, MAY, 1949

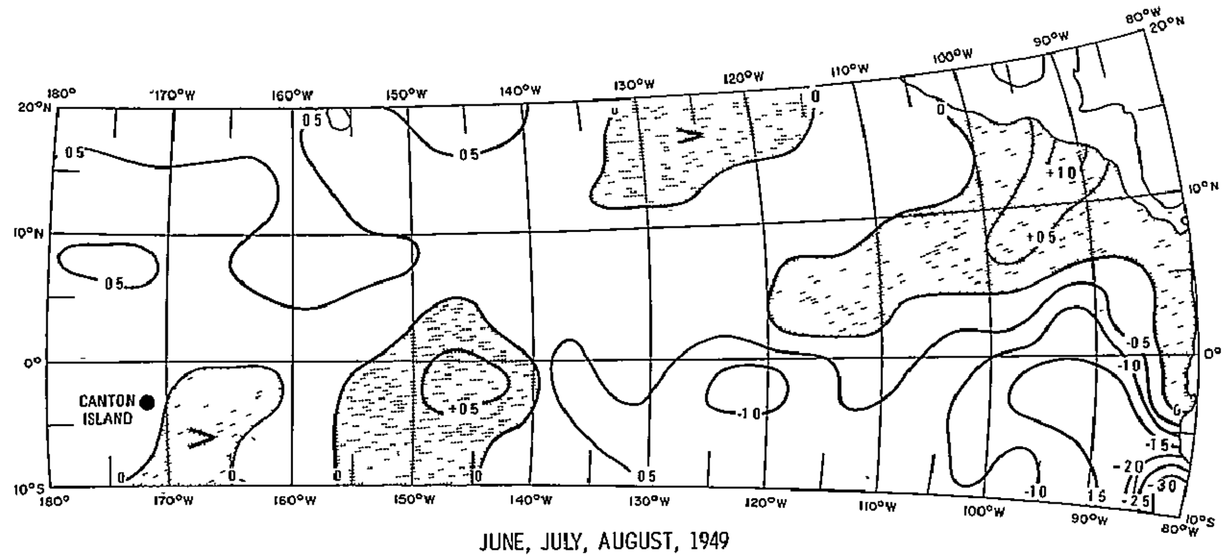

JUNE, JULY, AUGUST, 1949

Figure A-1

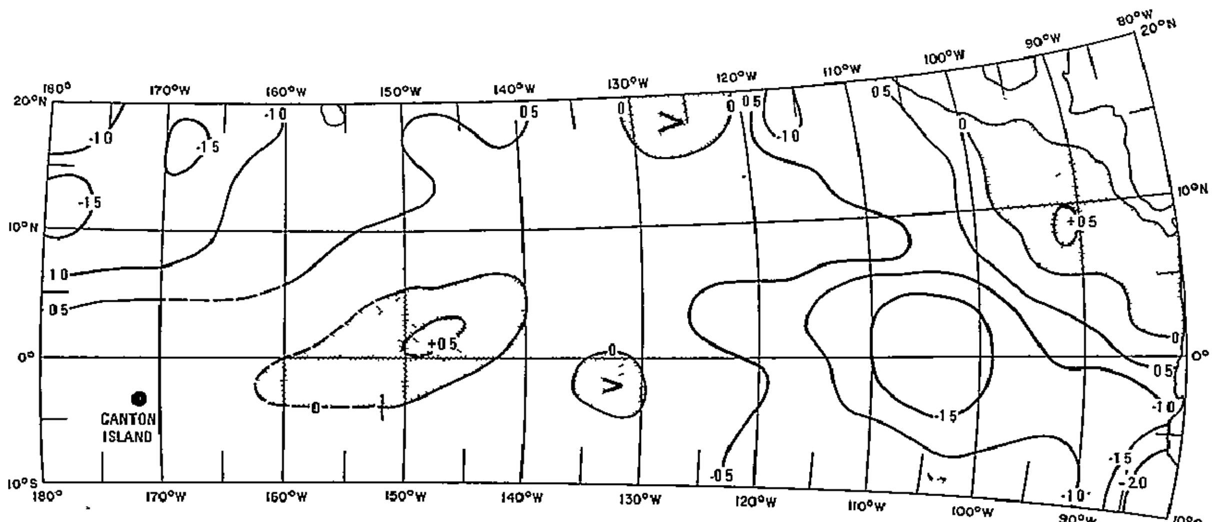

SEPTEMBER, OCTOBER, NOVEMBER, 1949

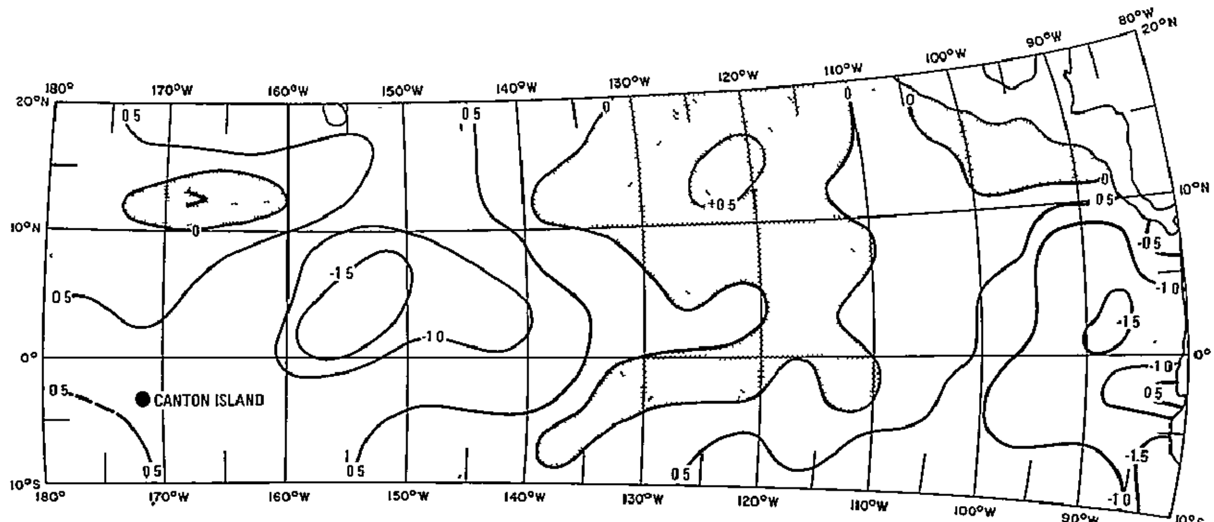

DECEMBER, 1949, JANUARY, FEBRUARY, 1950

Figure A-2

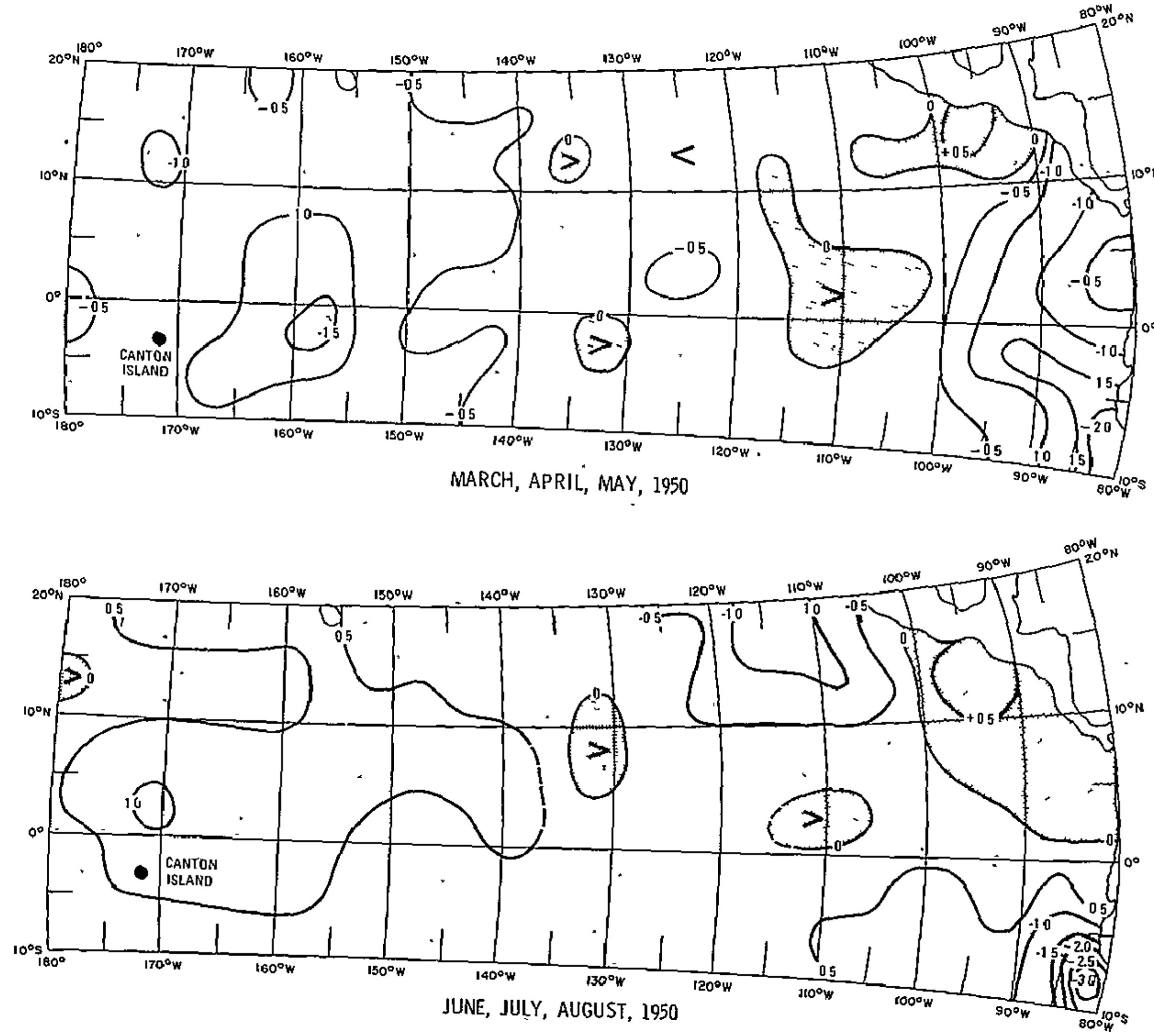

MARCH, APRIL, MAY, 1950
CANTON ISLAND
JUNE, JULY, AUGUST, 1950
CANTON ISLAND

Figure A-3

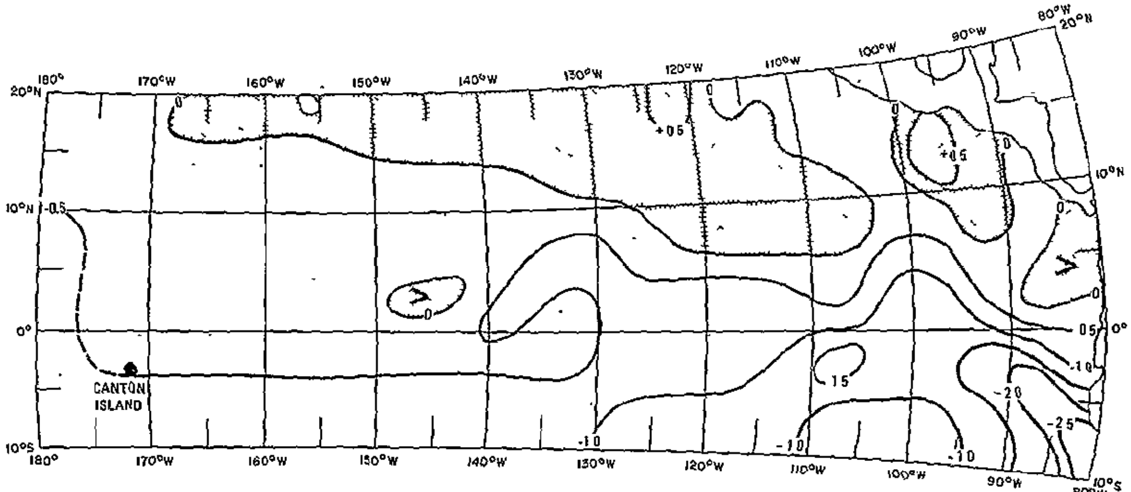

SEPTEMBER, OCTOBER, NOVEMBER, 1950

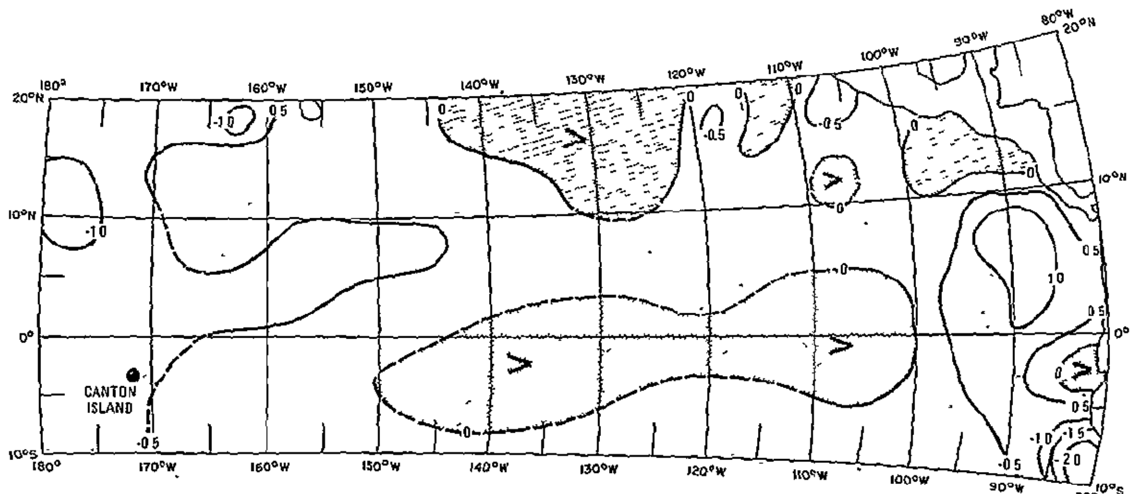

DECEMBER, 1950, JANUARY, FEBRUARY, 1951

Figure A-4

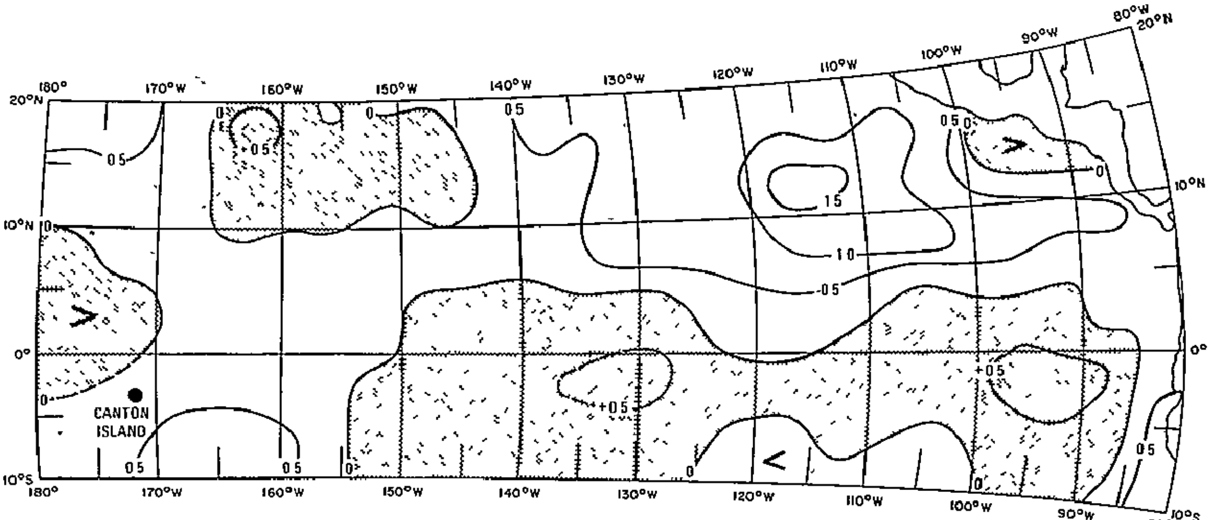

MARCH, APRIL, MAY, 1951

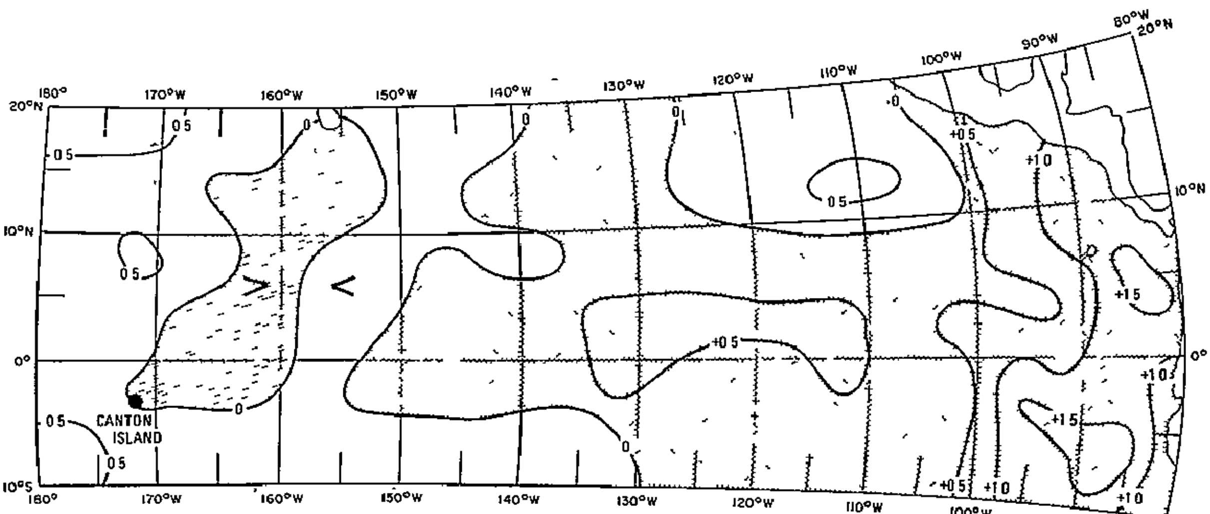

JUNE, JULY, AUGUST, 1951

Figure A-5

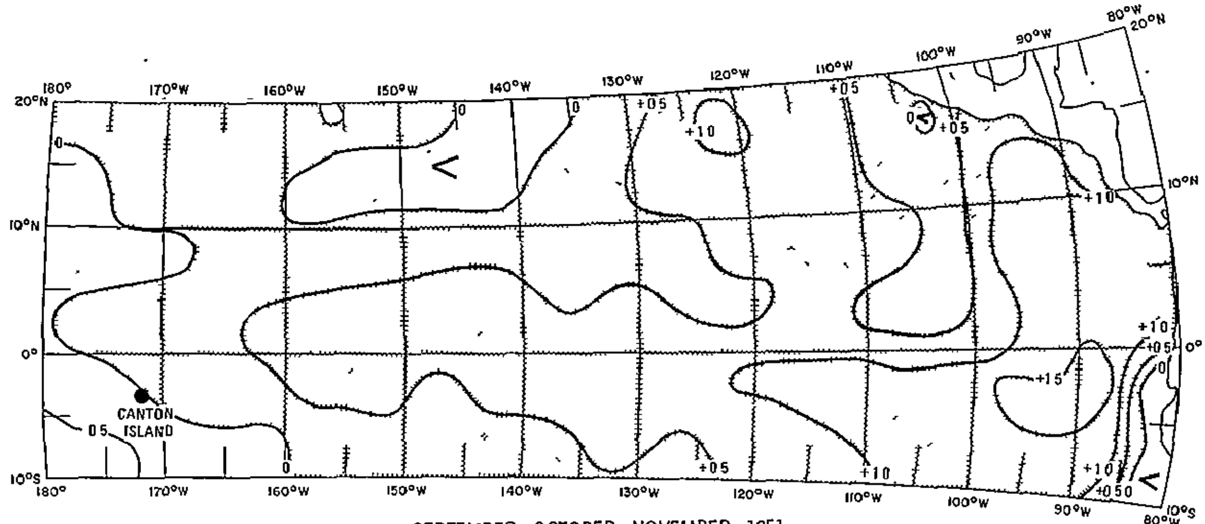

SEPTEMBER, OCTOBER, NOVEMBER, 1951

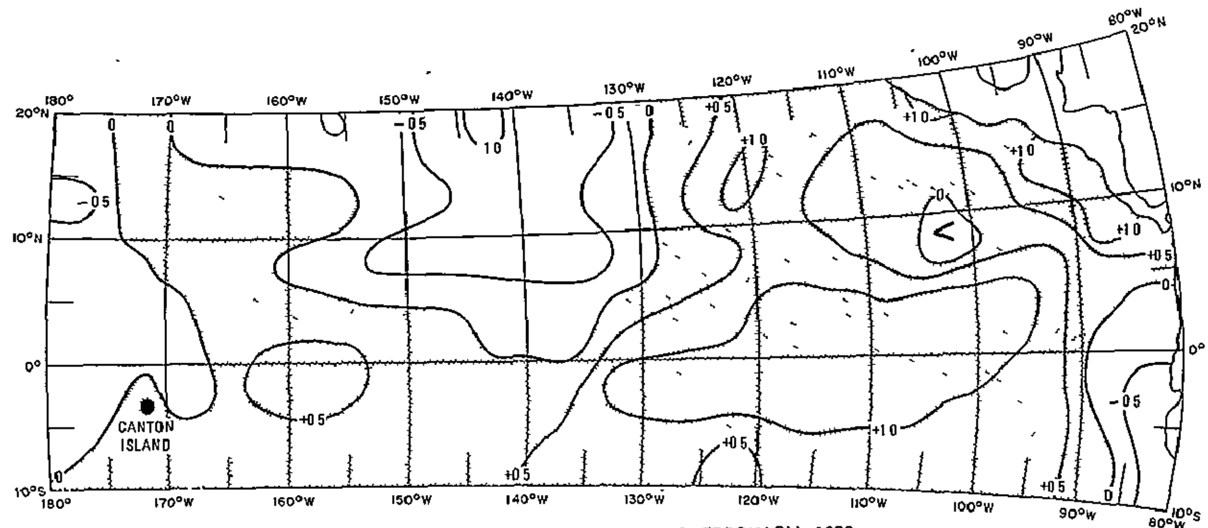

DECEMBER, 1951, JANUARY, 1952, FEBRUARY, 1952

Figure A-6

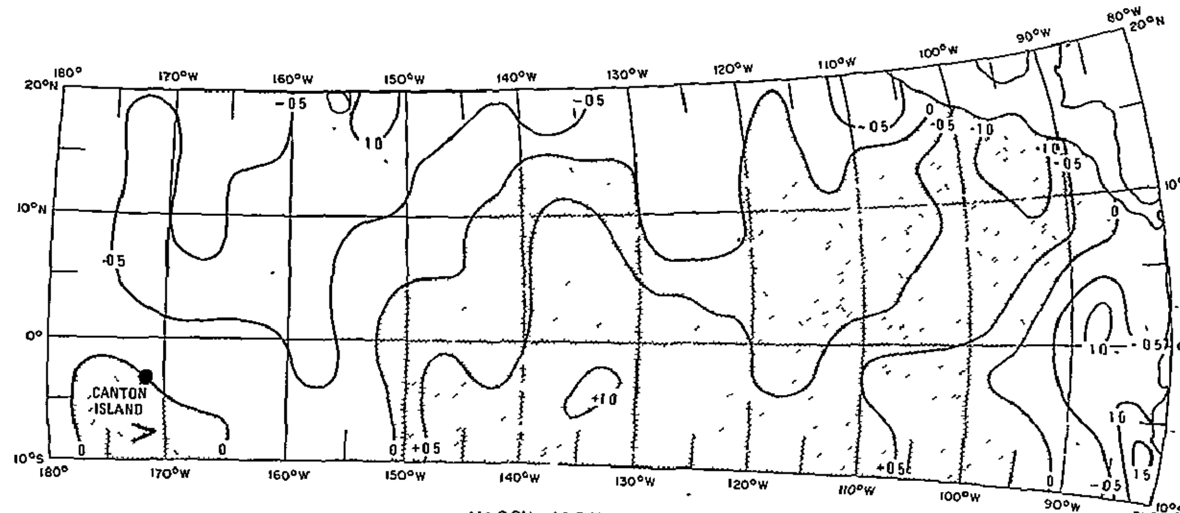

MARCH, APRIL, MAY, 1952

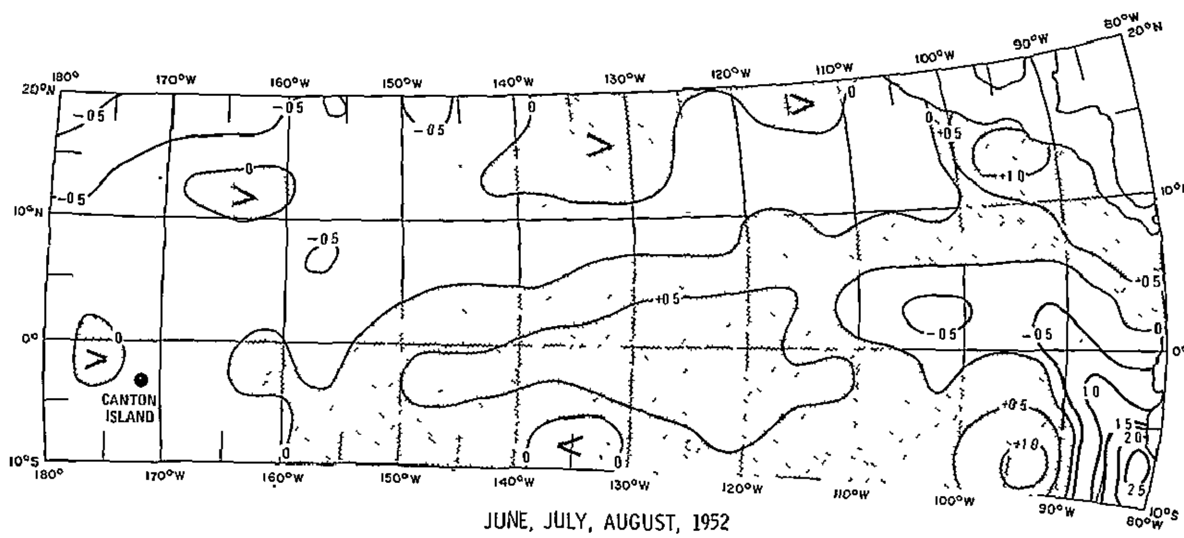

JUNE, JULY, AUGUST, 1952

Figure A-7

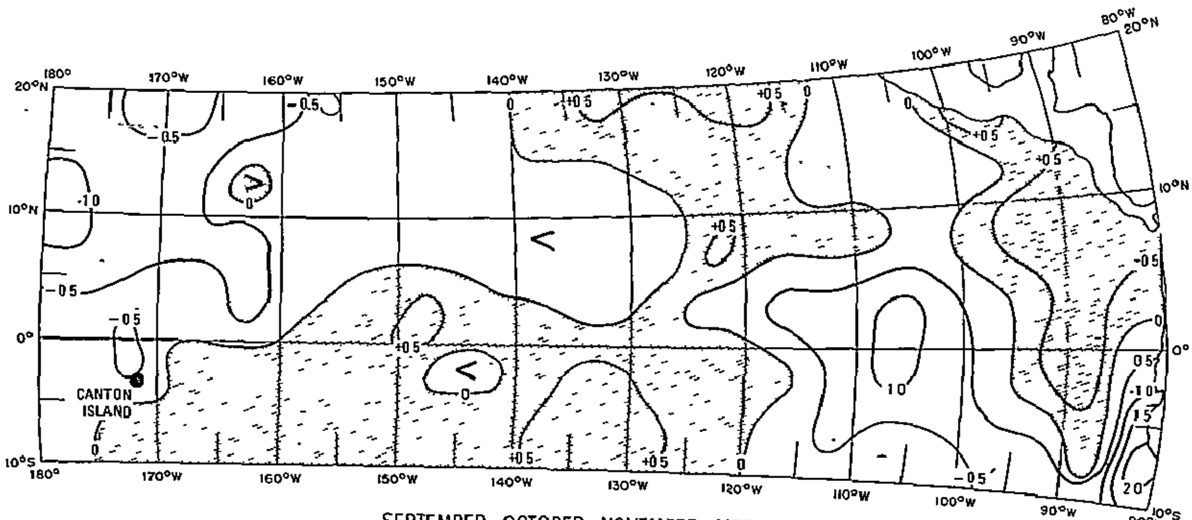

SEPTEMBER, OCTOBER, NOVEMBER, 1952

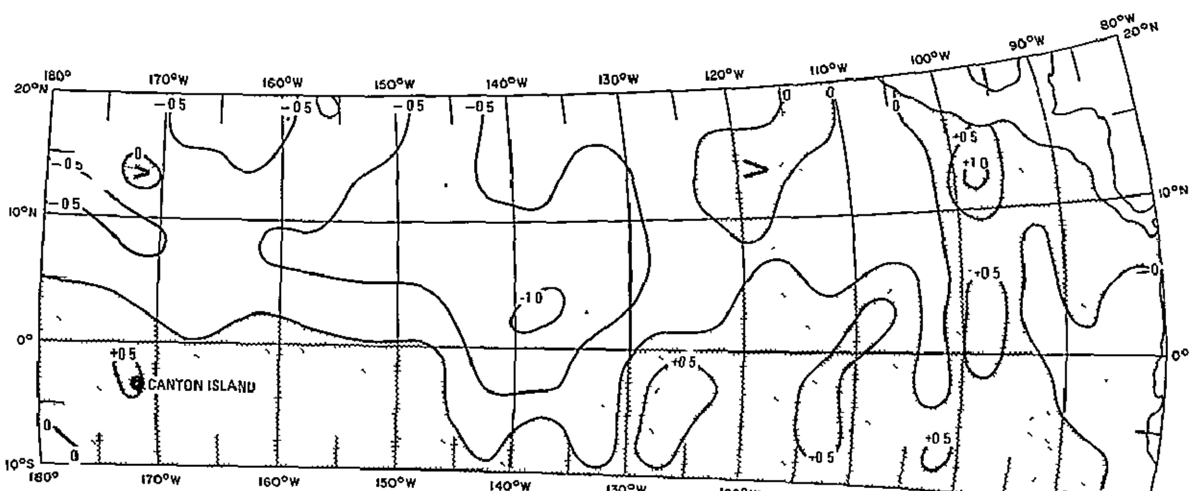

DECEMBER, 1952, JANUARY, FEBRUARY, 1953

Figure A-8

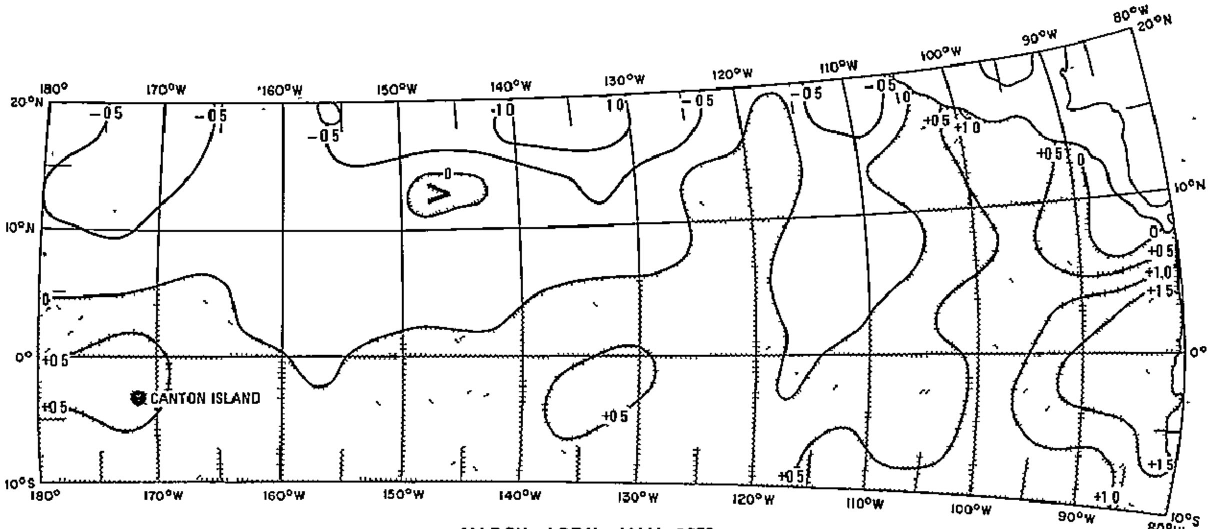

MARCH, APRIL, MAY, 1953

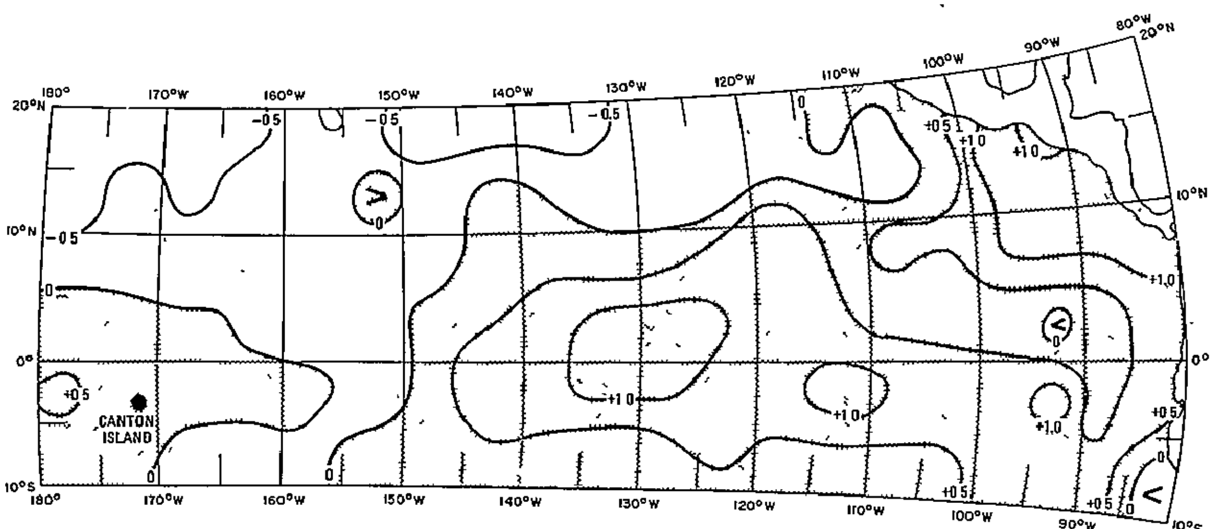

JUNE, JULY, AUGUST, 1953

Figure A-9

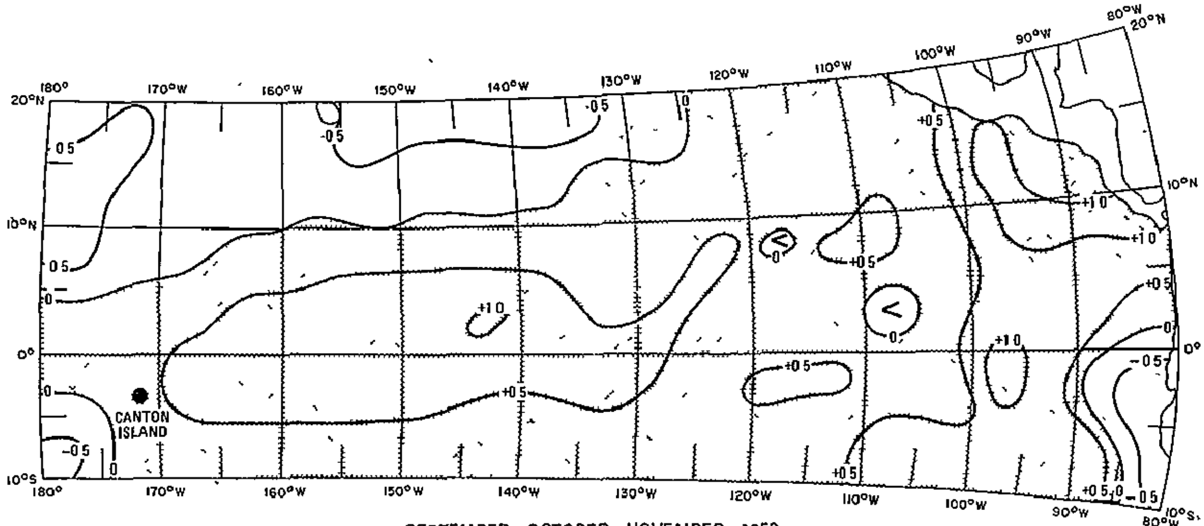

SEPTEMBER, OCTOBER, NOVEMBER, 1953

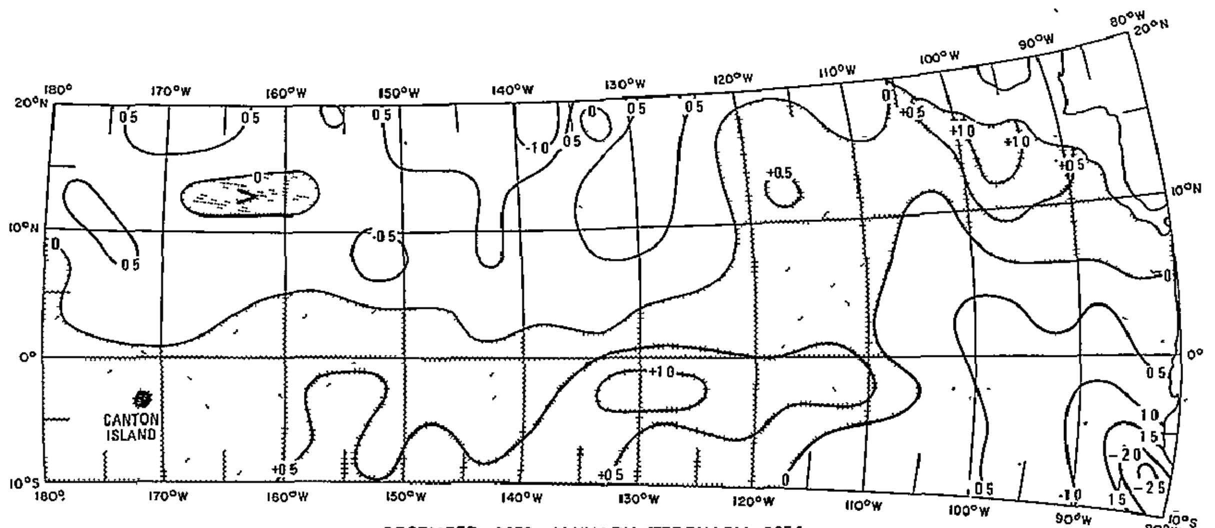

DECEMBER, 1953, JANUARY, FEBRUARY, 1954

Figure A-10

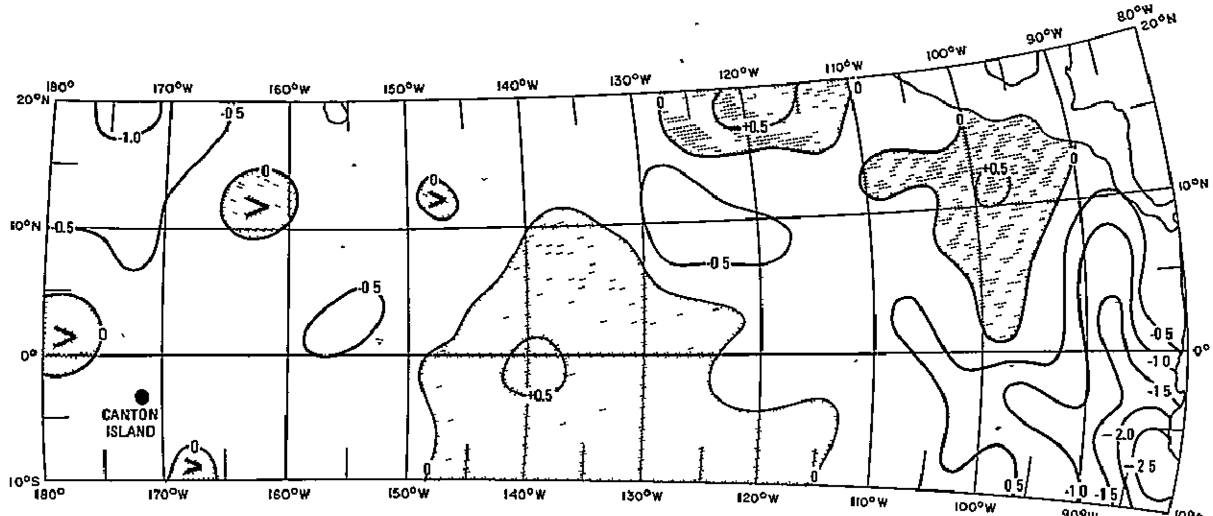

MARCH, APRIL, MAY, 1954

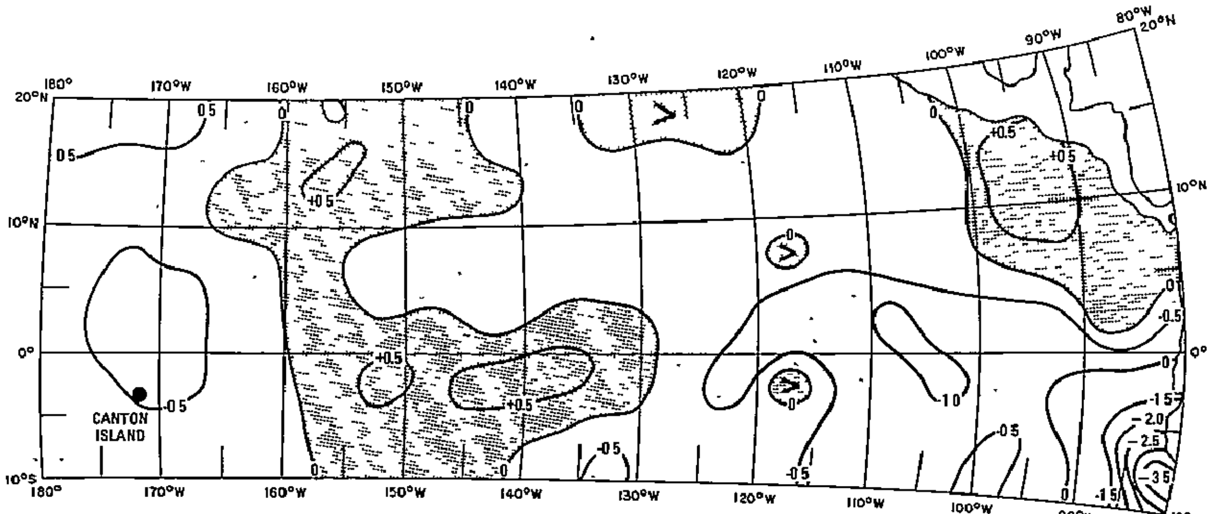

JUNE, JULY, AUGUST, 1954

Figure A-11

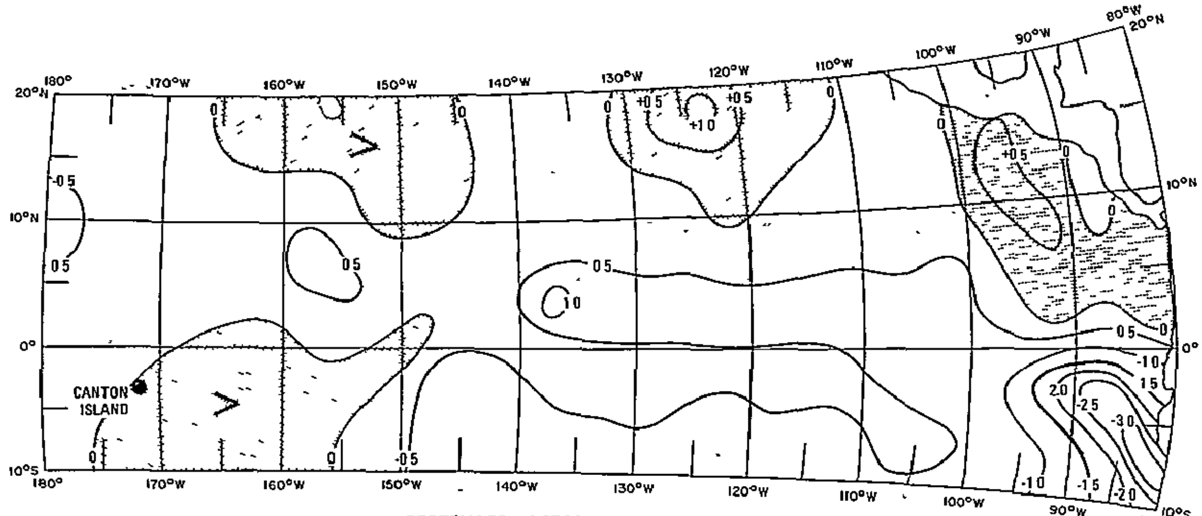

SEPTEMBER, OCTOBER, NOVEMBER, 1954

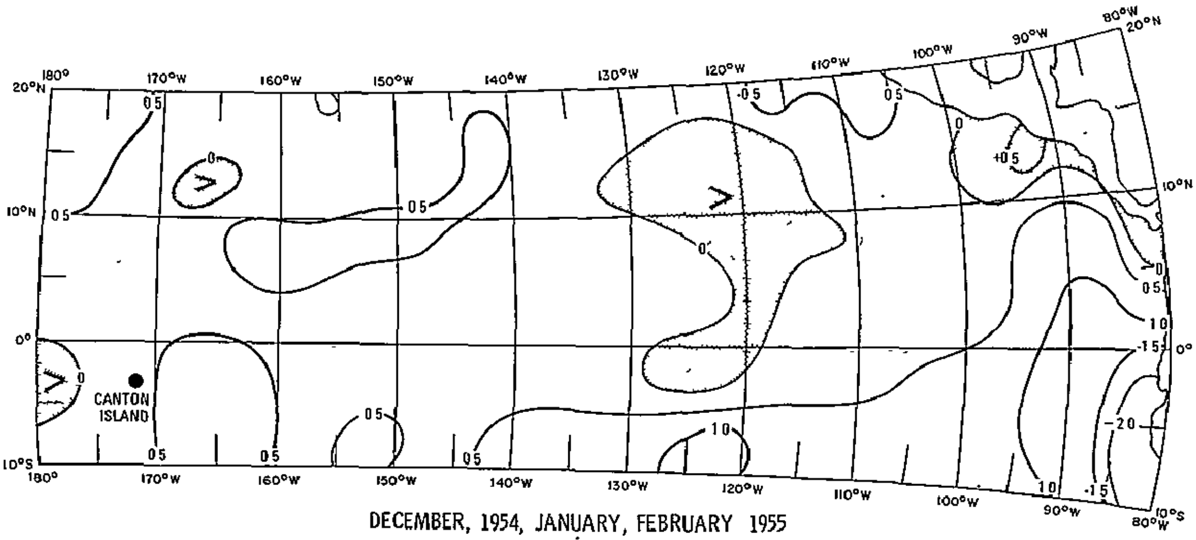

DECEMBER, 1954, JANUARY, FEBRUARY 1955

Figure A-12

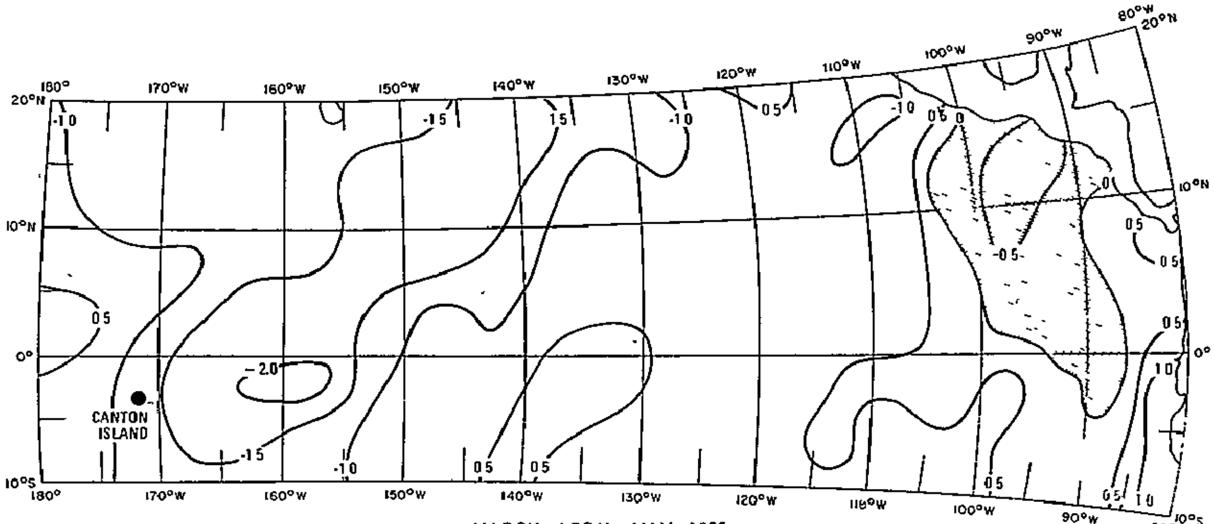

MARCH, APRIL, MAY, 1955

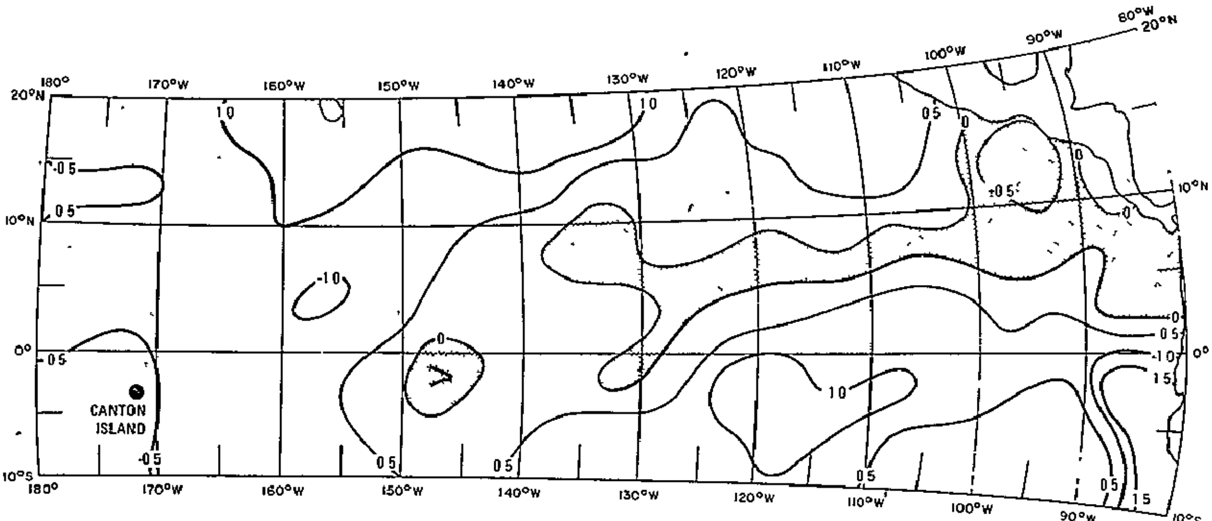

JUNE, JULY, AUGUST 1955

Figure A-13

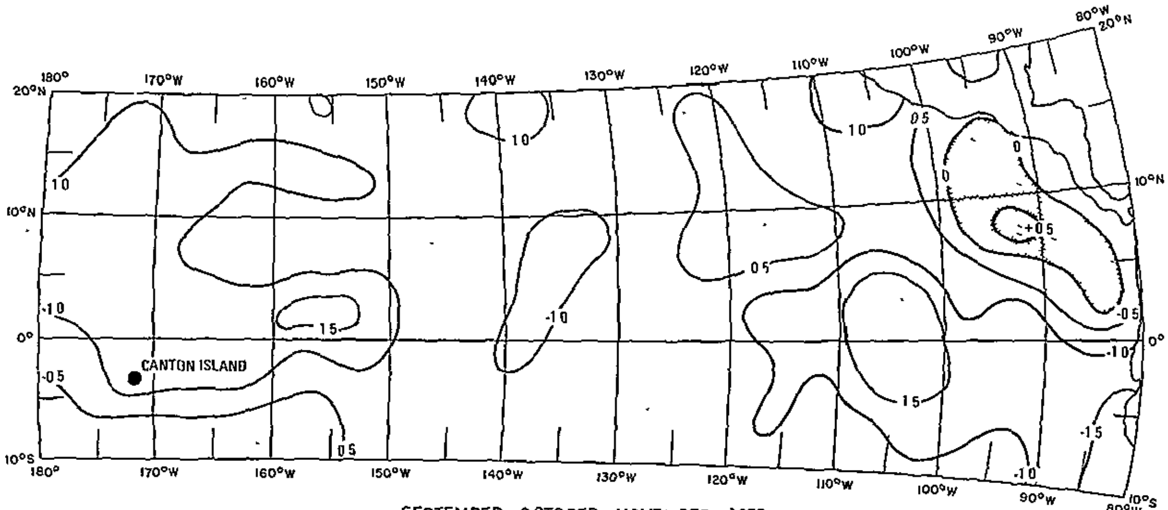

SEPTEMBER, OCTOBER, NOVEMBER, 1955

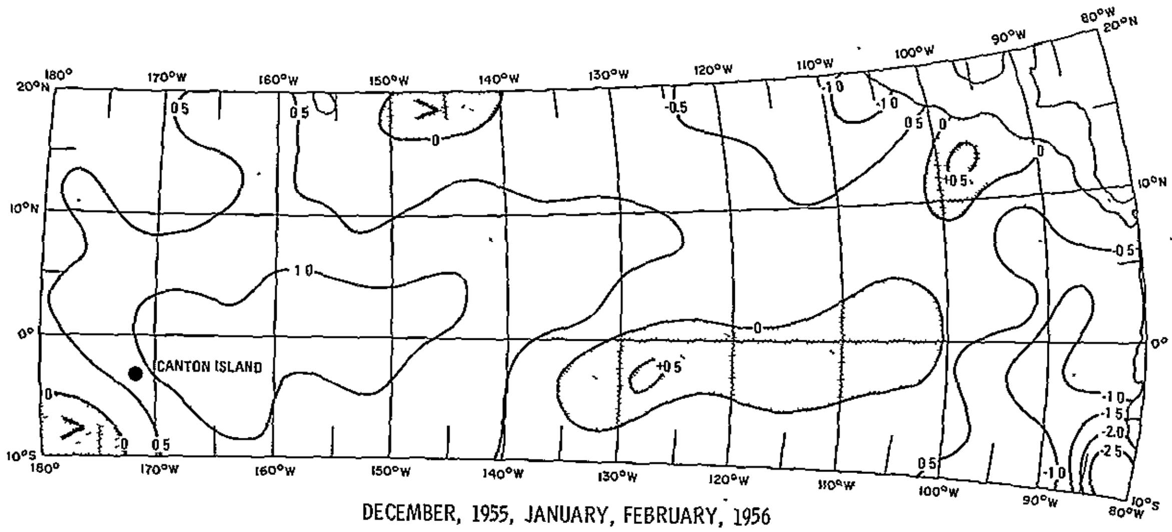

DECEMBER, 1955, JANUARY, FEBRUARY, 1956

Figure A-14

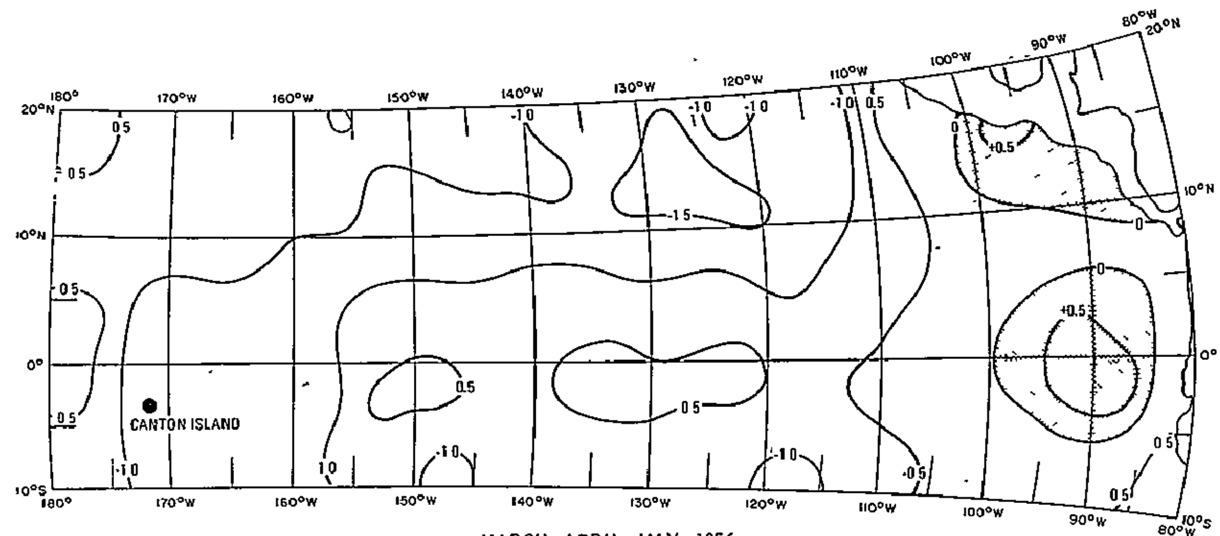

MARCH, APRIL, MAY, 1956

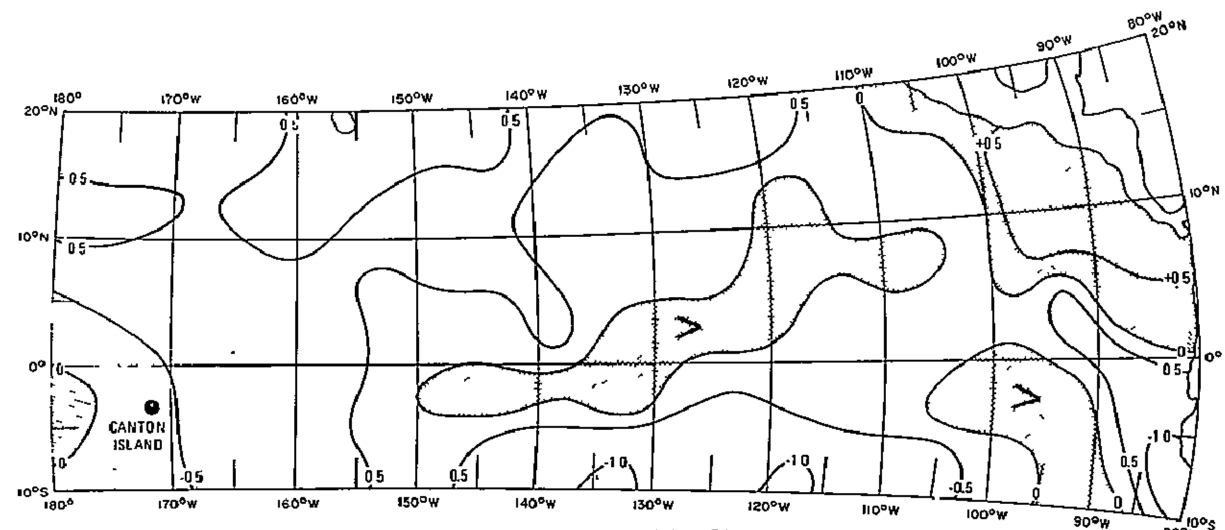

JUNE, JULY, AUGUST, 1956

Figure A-15

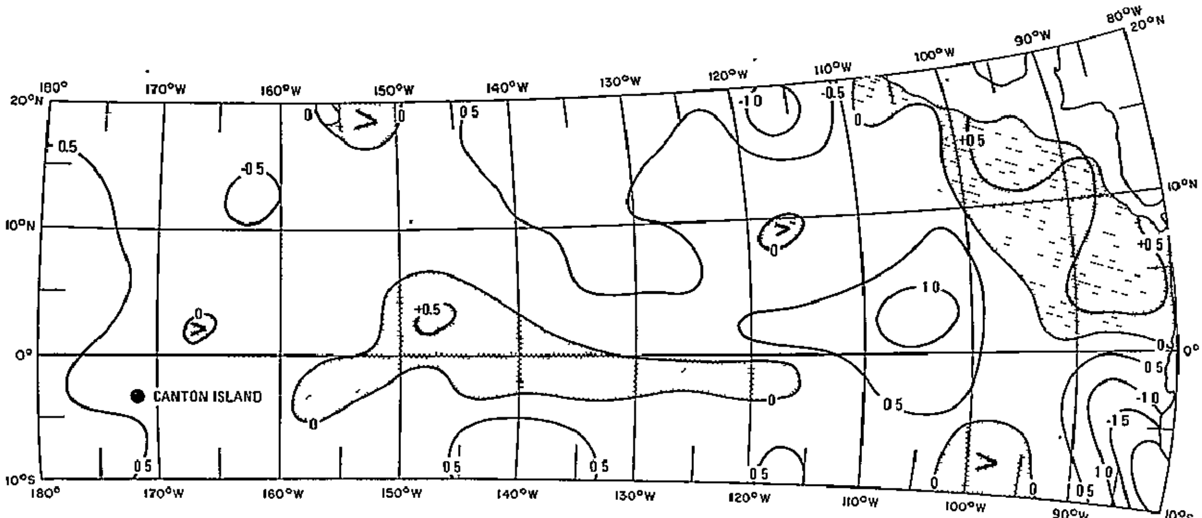

SEPTEMBER, OCTOBER, NOVEMBER, 1956

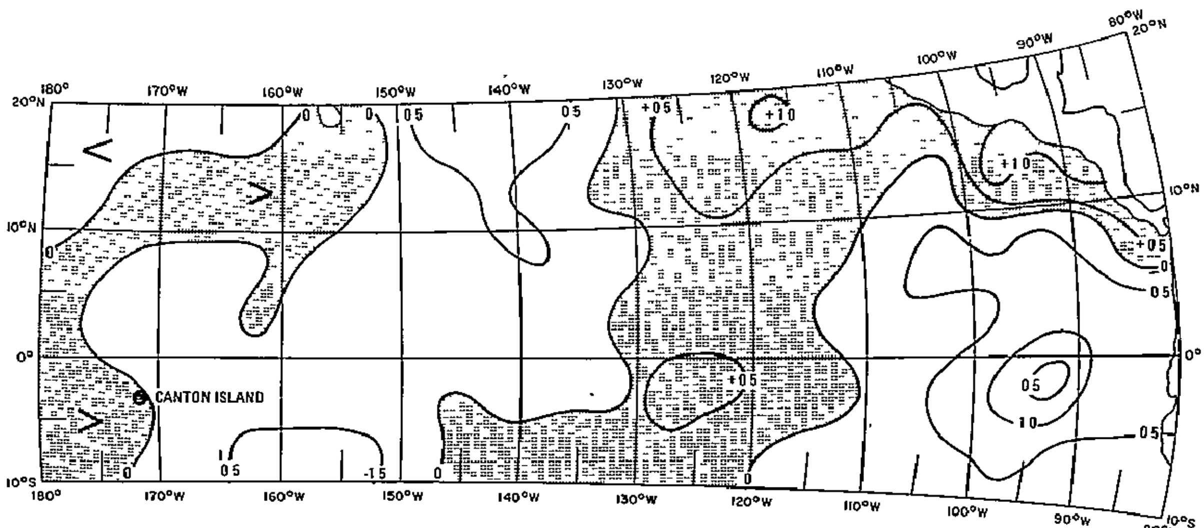

DECEMBER, 1956, JANUARY, FEBRUARY, 1957

Figure A-16

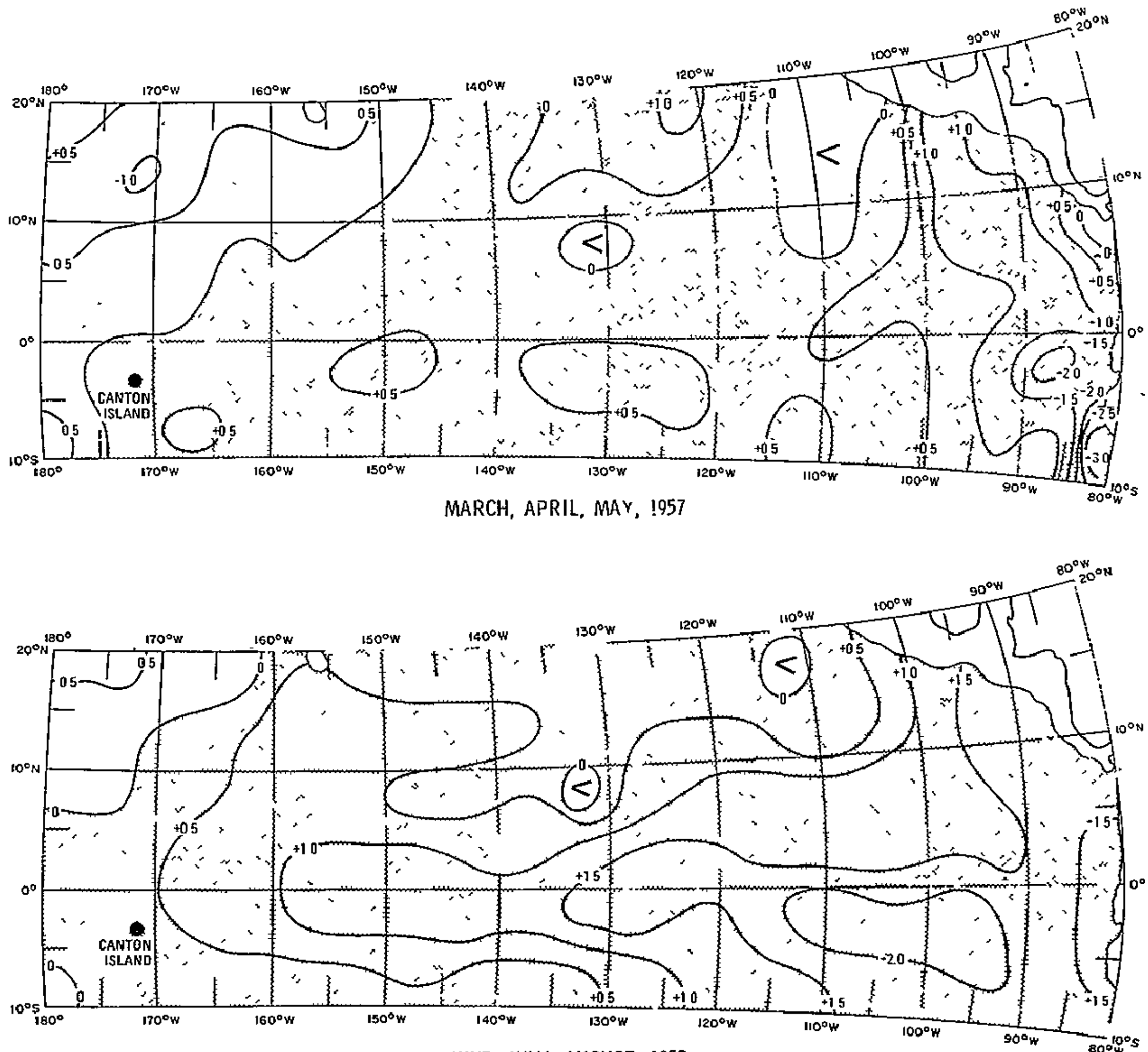

MARCH, APRIL, MAY, 1957

JUNE, JULY, AUGUST, 1957

Figure A-17

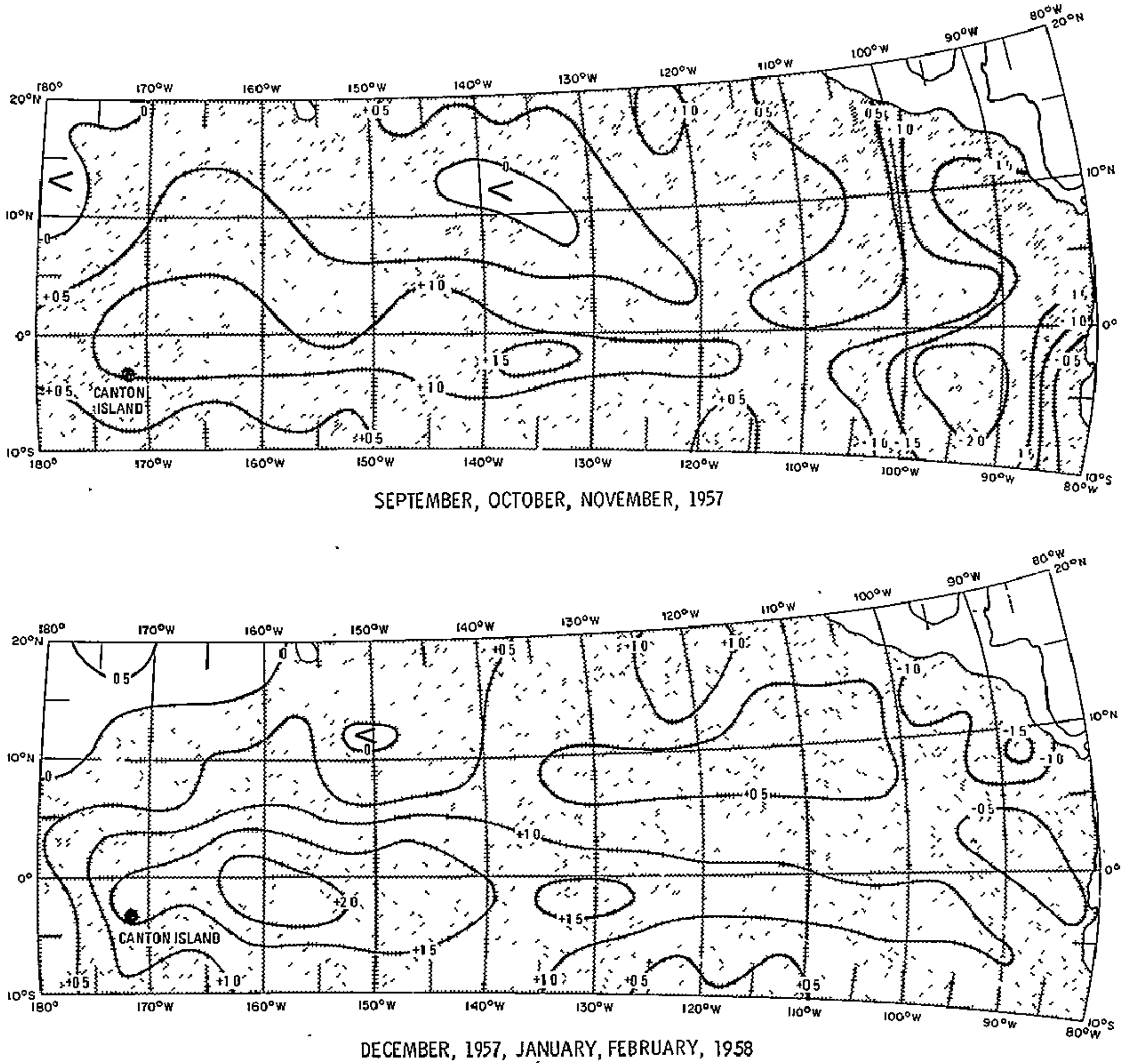

SEPTEMBER, OCTOBER, NOVEMBER, 1957

DECEMBER, 1957, JANUARY, FEBRUARY, 1958

Figure A-18

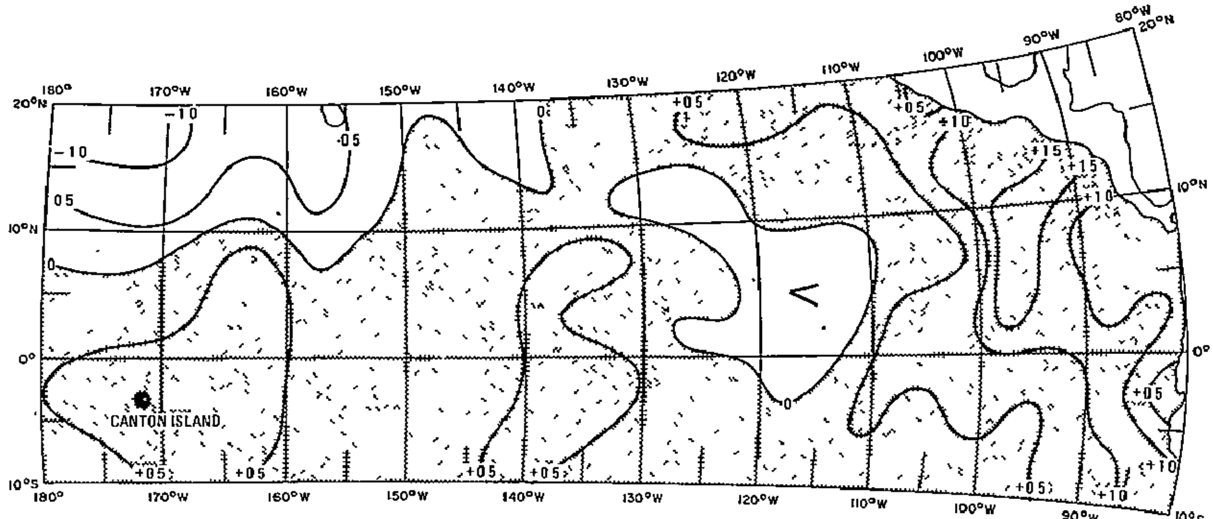
CANTON ISLAND
MARCH, APRIL, MAY, 1958

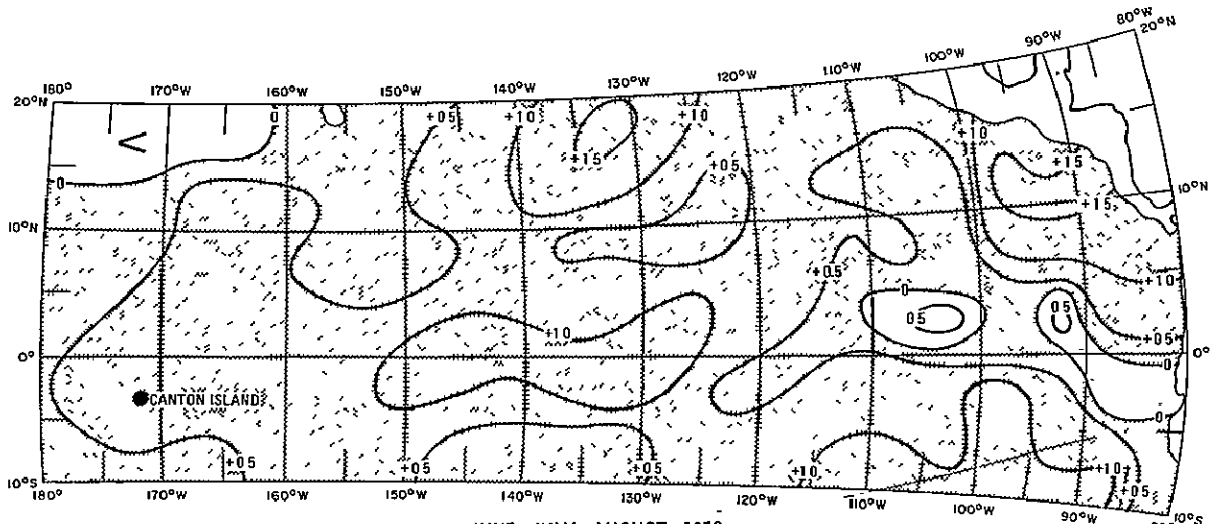
CANTON ISLAND
JUNE, JULY, AUGUST, 1958

Figure A-19

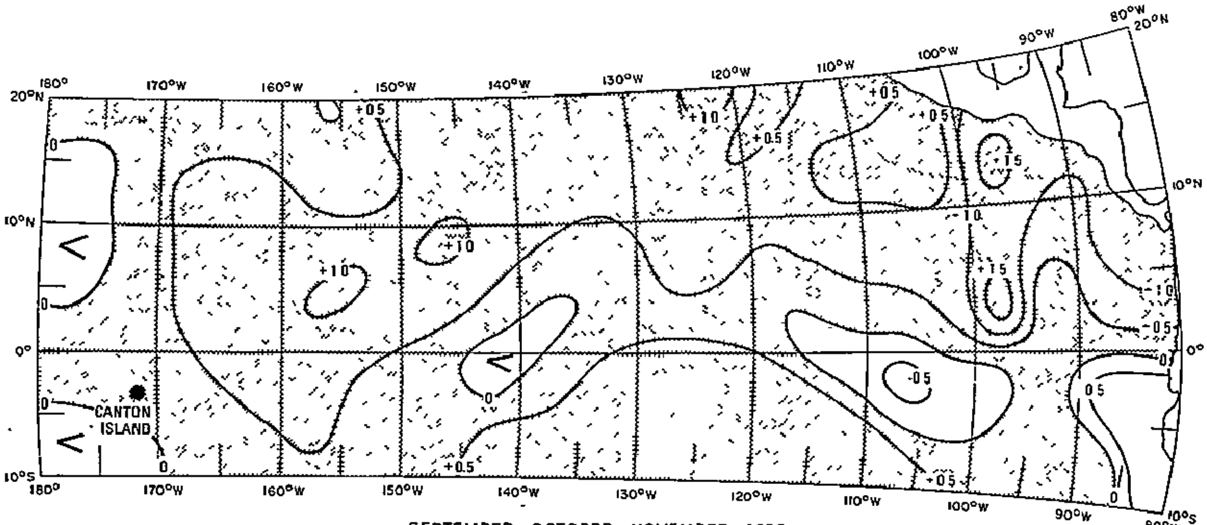

SEPTEMBER, OCTOBER, NOVEMBER, 1958

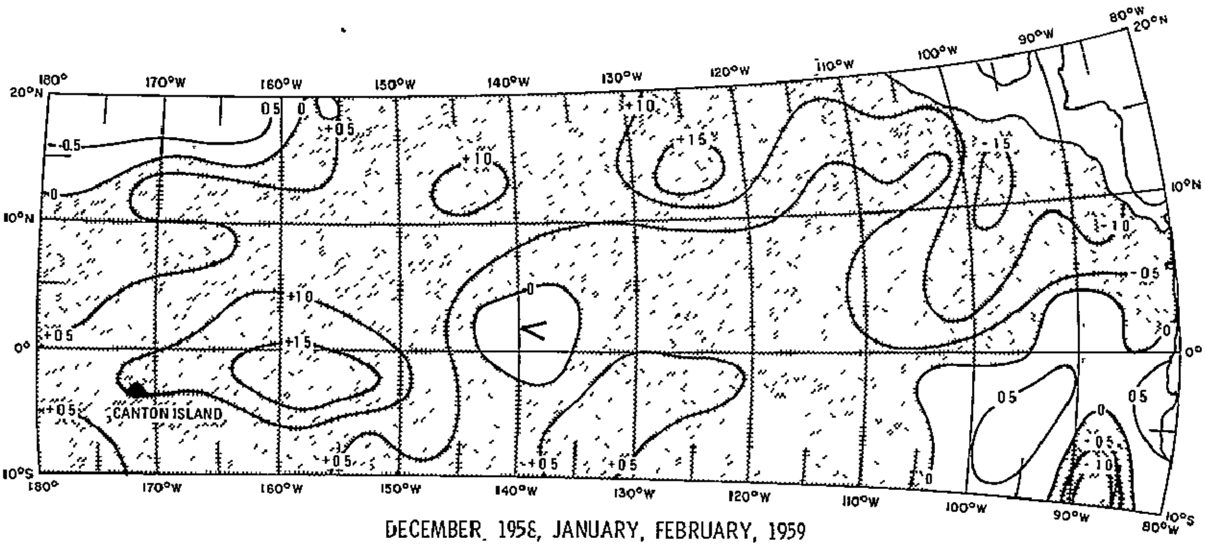

DECEMBER, 1958, JANUARY, FEBRUARY, 1959

Figure A-20

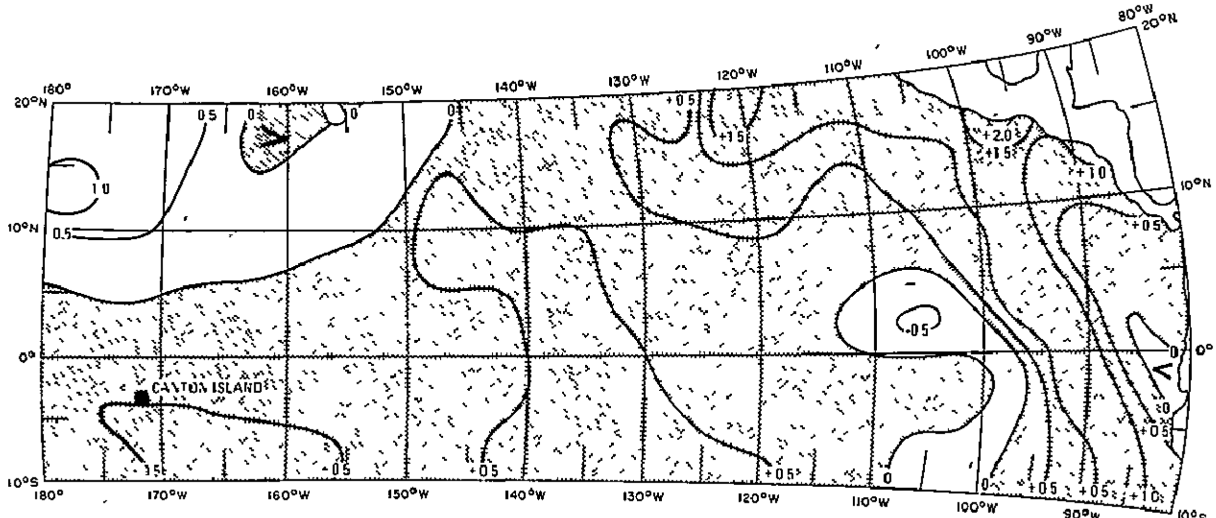

MARCH, APRIL, MAY, 1959

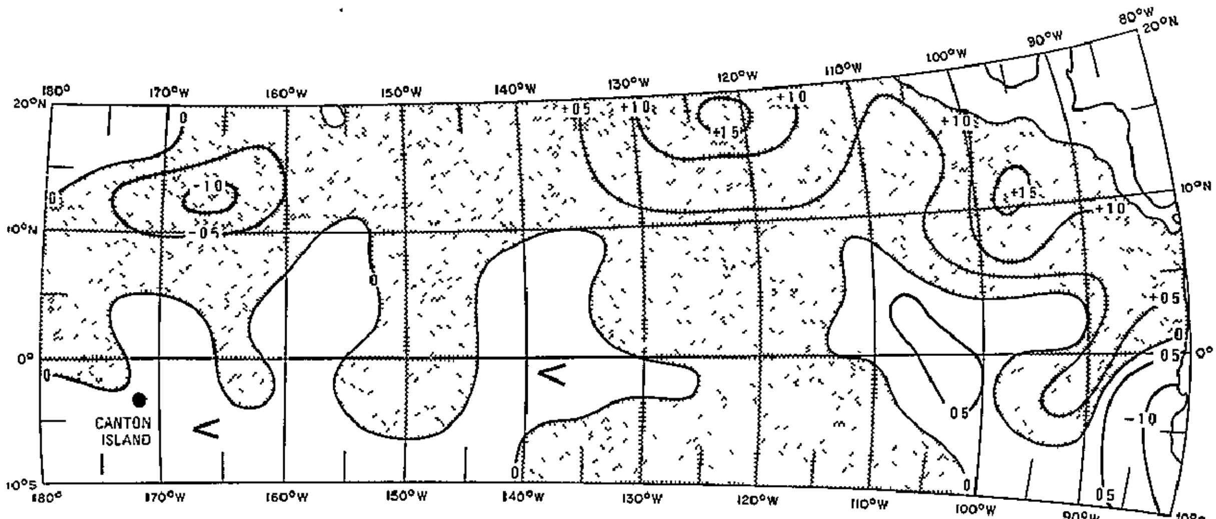

JUNE, JULY, AUGUST, 1959

Figure A-21

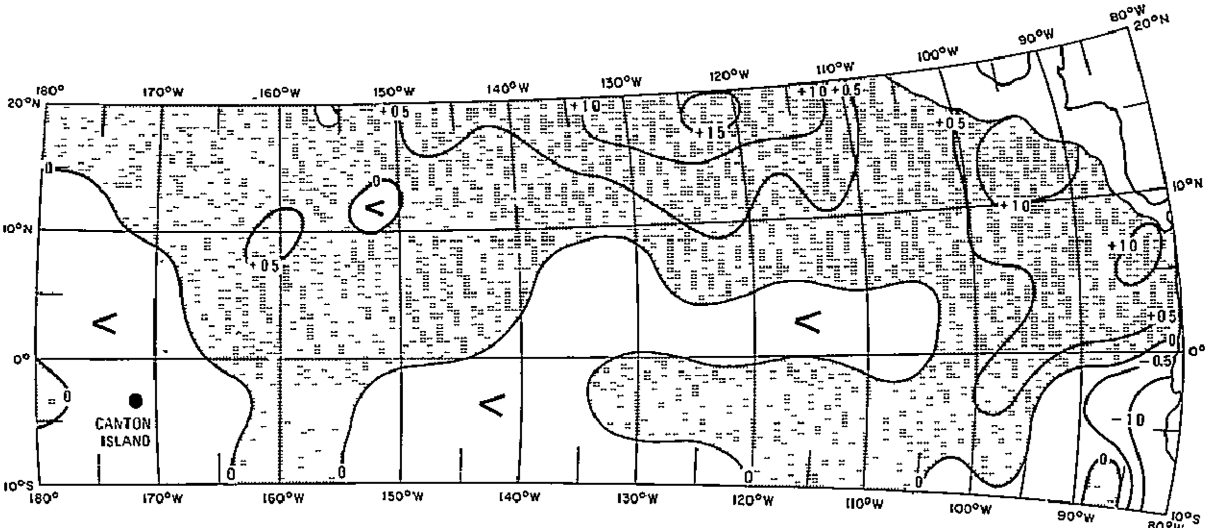

SEPTEMBER, OCTOBER, NOVEMBER, 1959

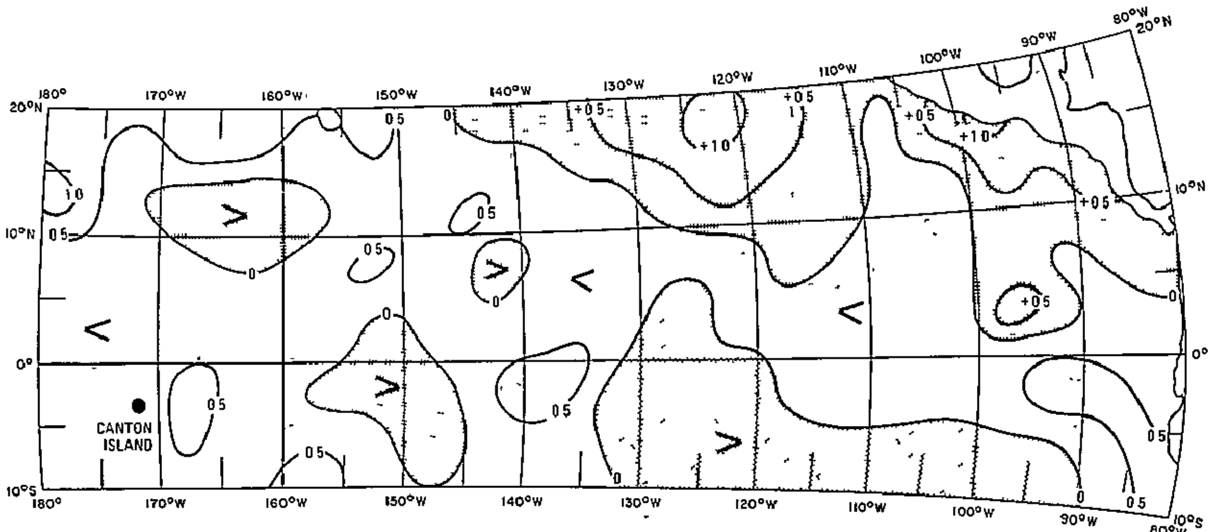

DECEMBER, 1959, JANUARY, FEBRUARY, 1960

Figure A-22

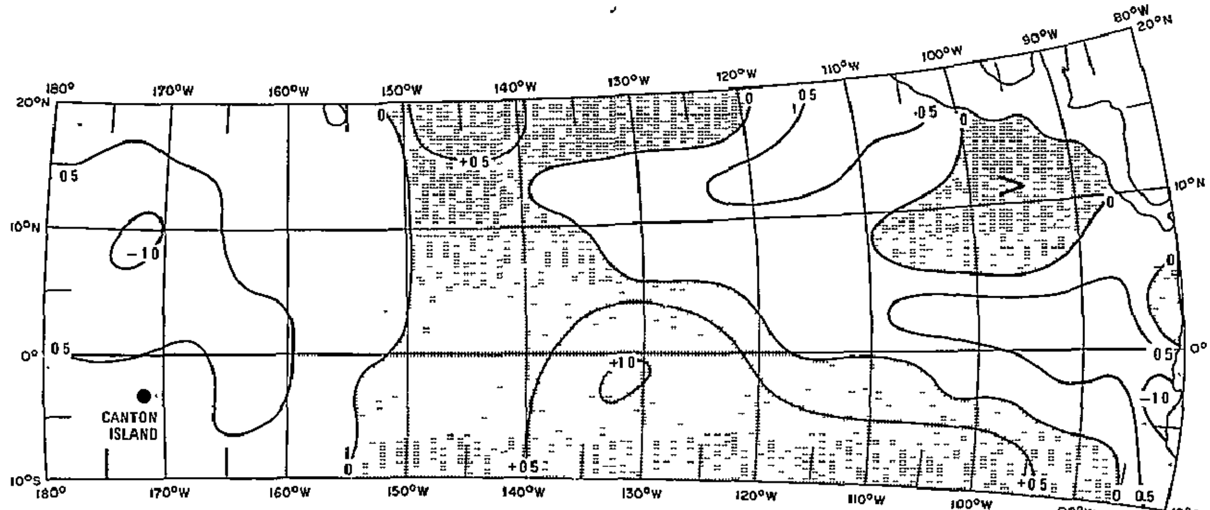

MARCH, APRIL, MAY, 1960

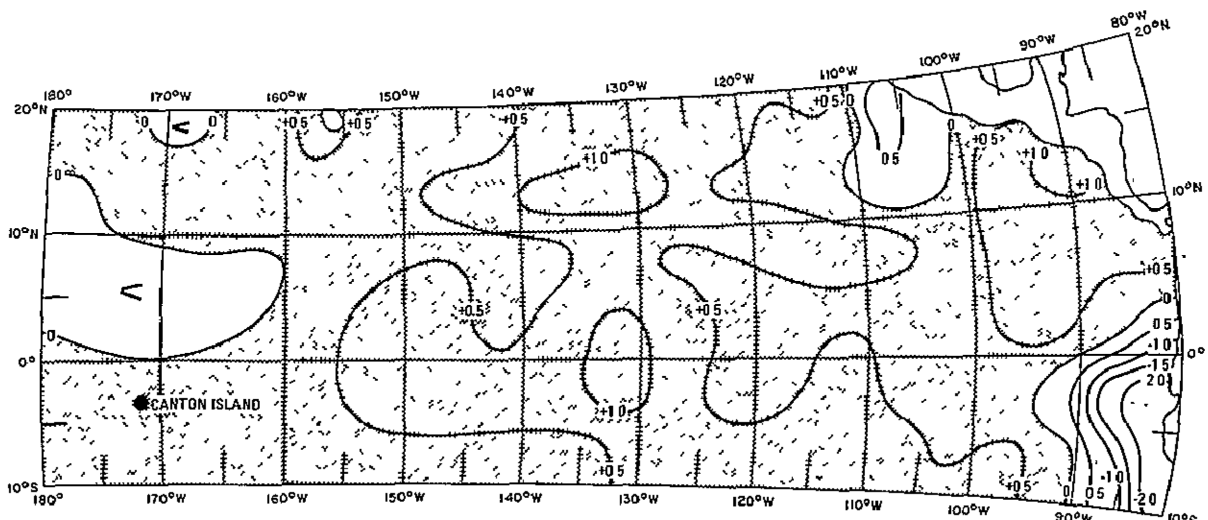

JUNE, JULY, AUGUST, 1960

Figure A-23

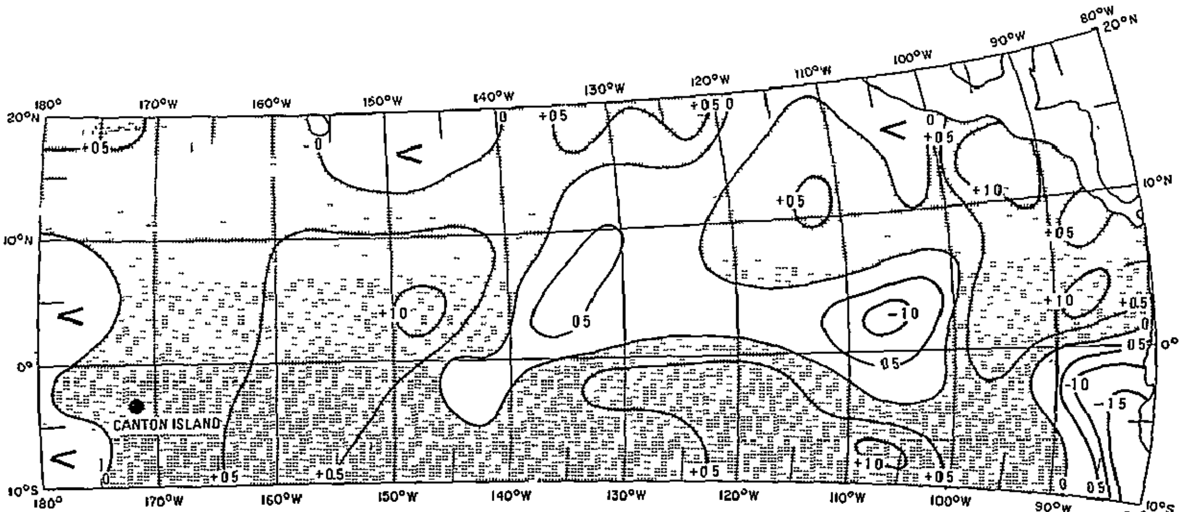

SEPTEMBER, OCTOBER, NOVEMBER, 1960

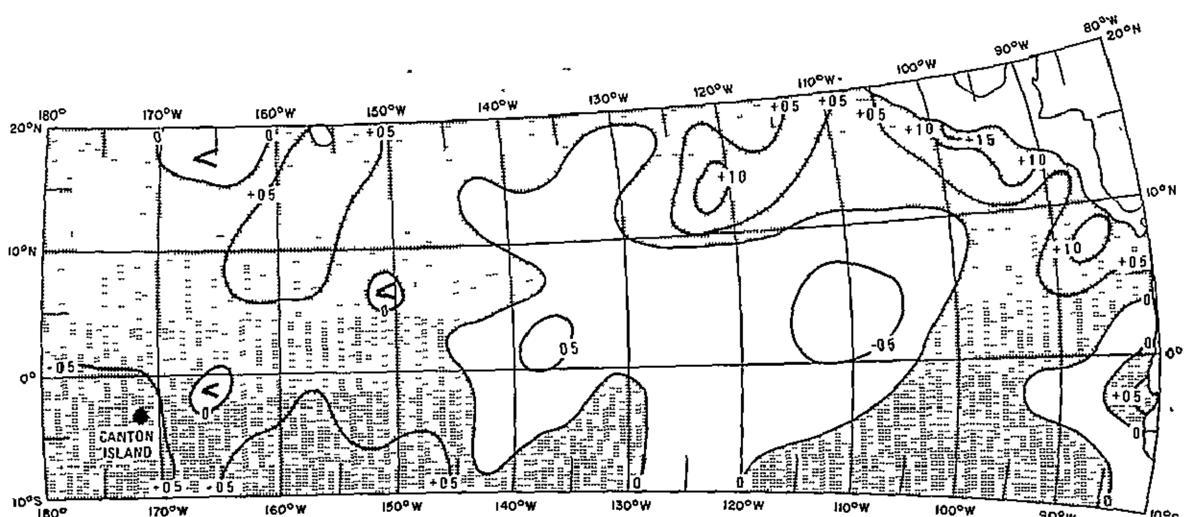

DECEMBER, 1960, JANUARY, FEBRUARY, 1961

Figure A-24

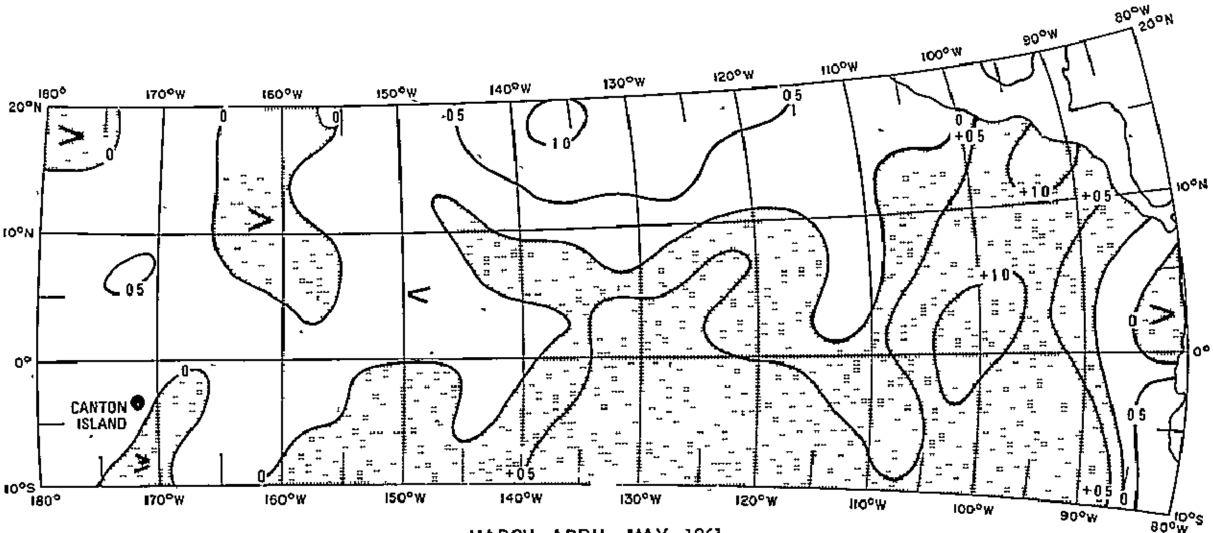

MARCH, APRIL, MAY, 1961

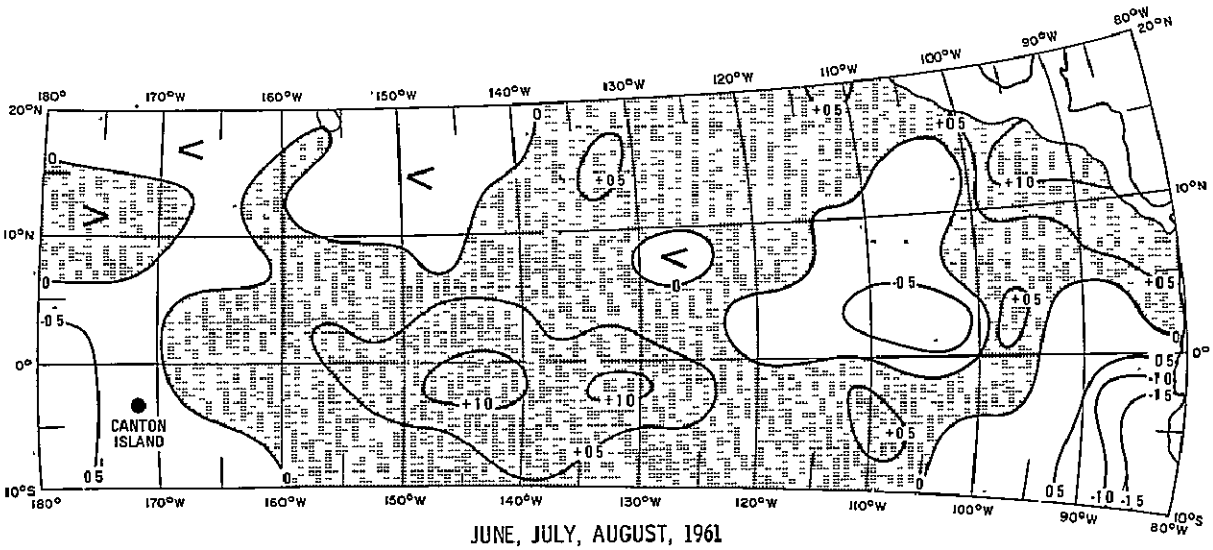

JUNE, JULY, AUGUST, 1961

Figure A-25

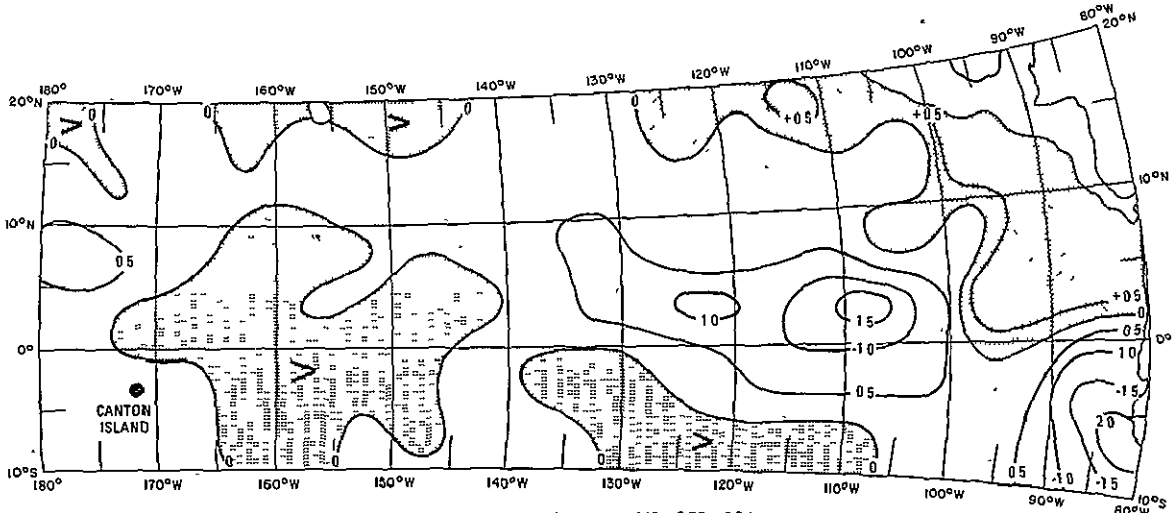

SEPTEMBER, OCTOBER, NOVEMBER, 1961

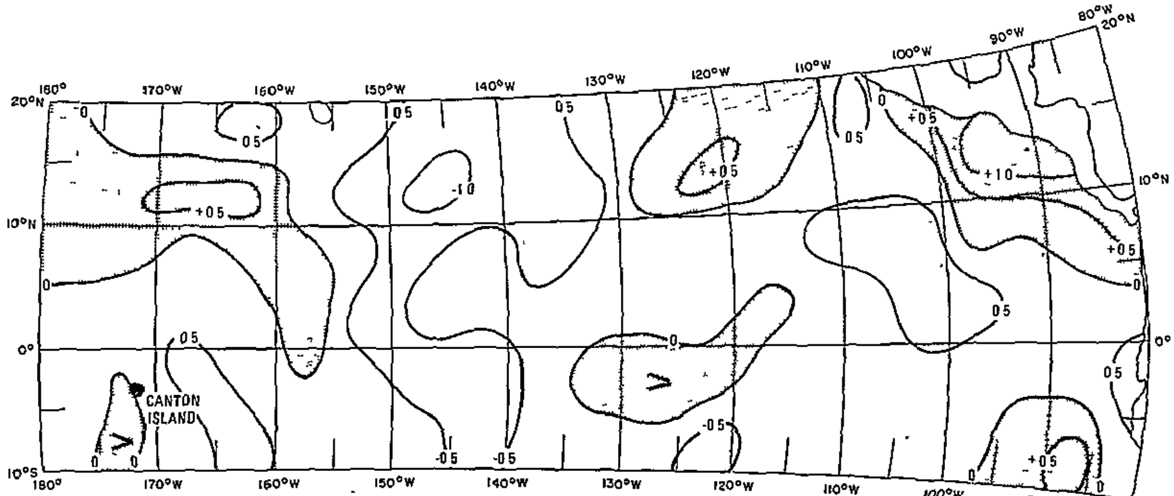

DECEMBER, 1961, JANUARY, FEBRUARY, 1962

Figure A-26

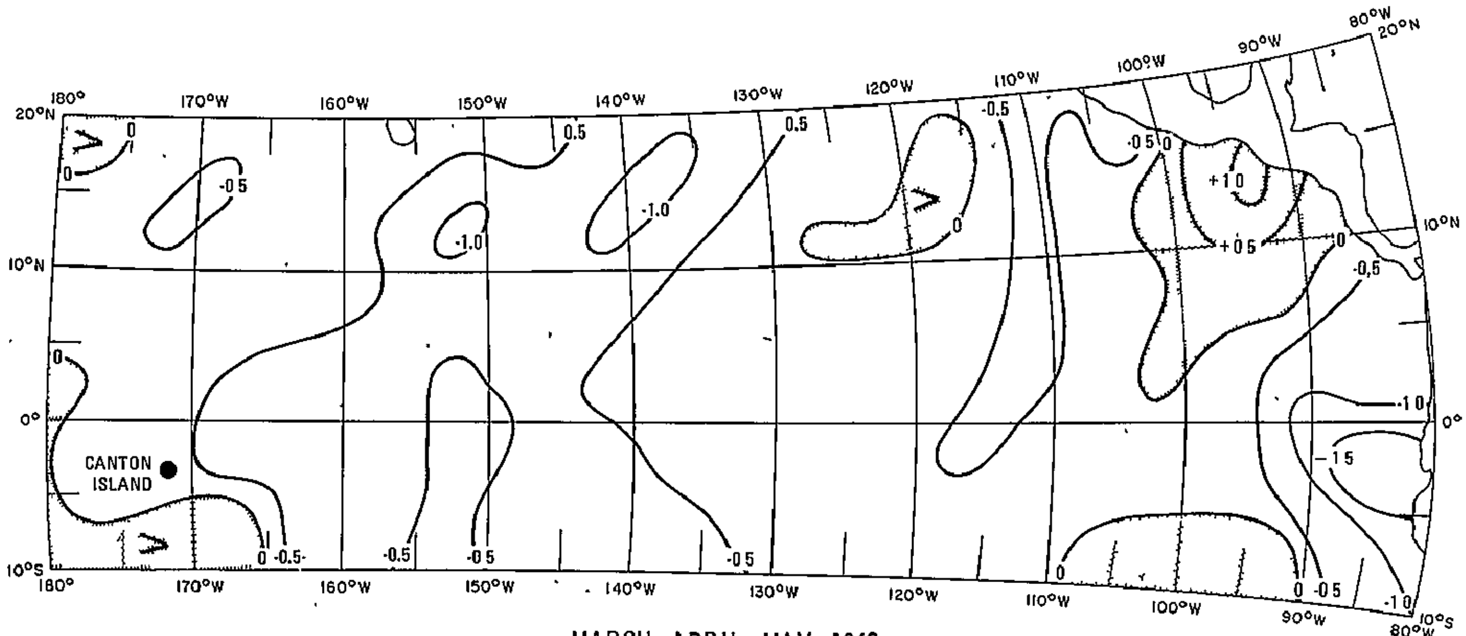

MARCH, APRIL, MAY, 1962

Figure A-27

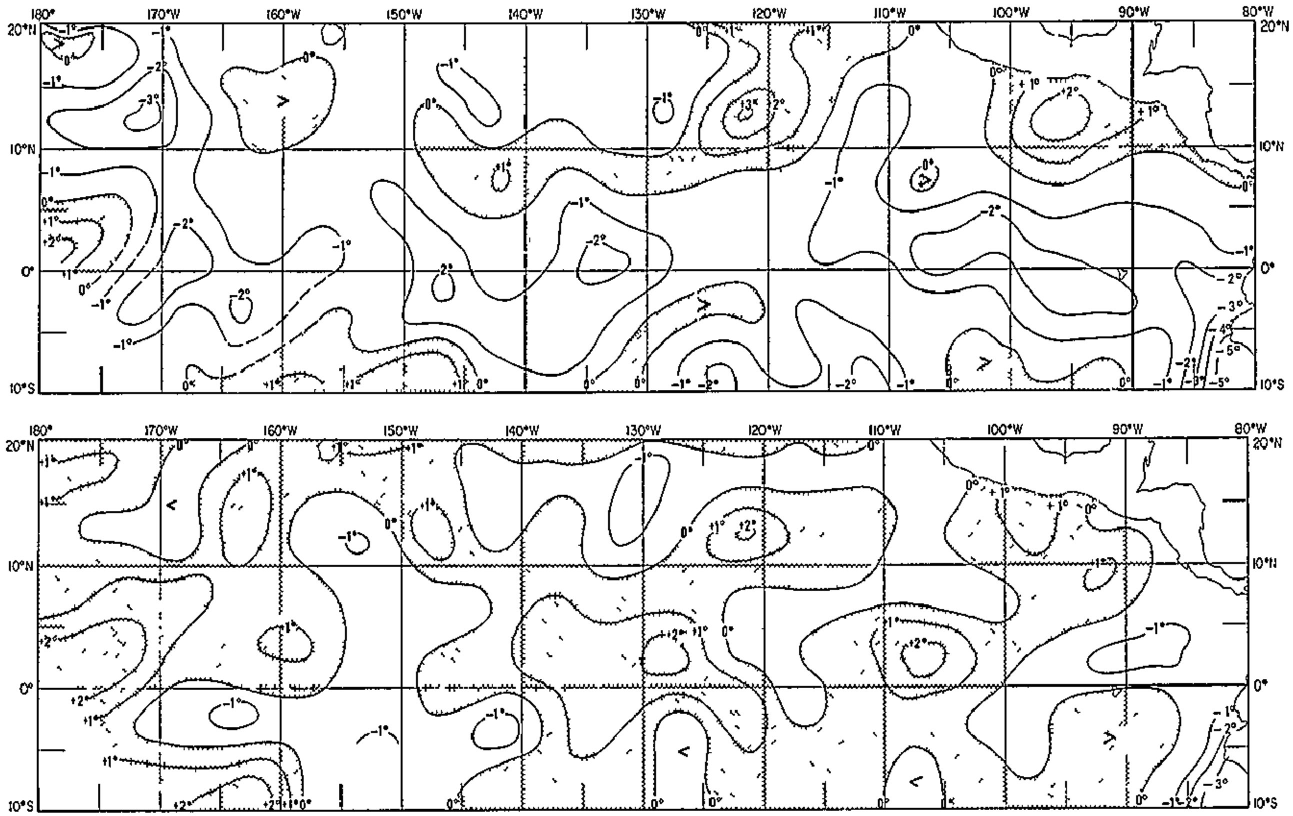

DECEMBER-1962
JANUARY
FEBRUARY
1963

MARCH
APRIL
MAY
1963

Figure A-29

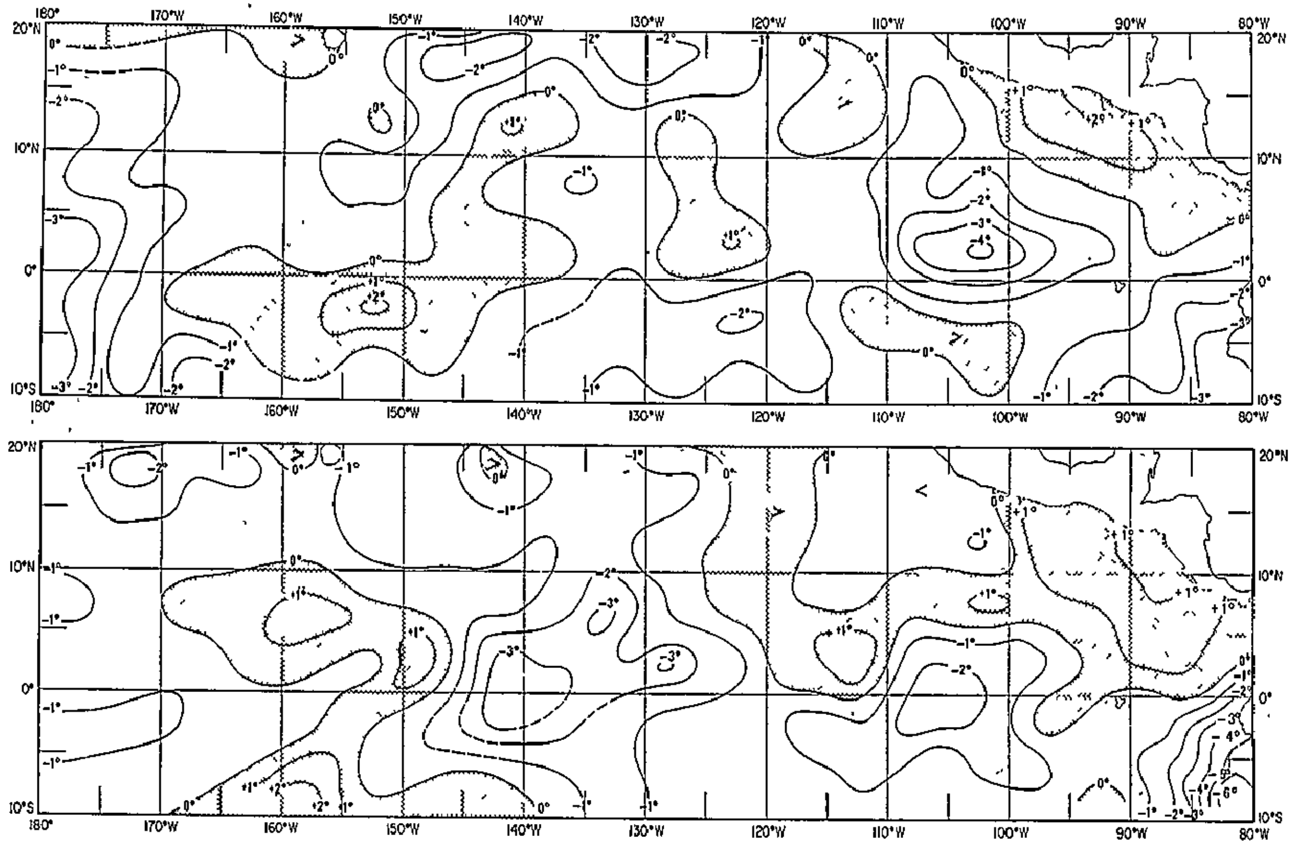

JUNE
JULY
AUGUST
1962

SEPTEMBER
OCTOBER
NOVEMBER
1962

Figure A-28

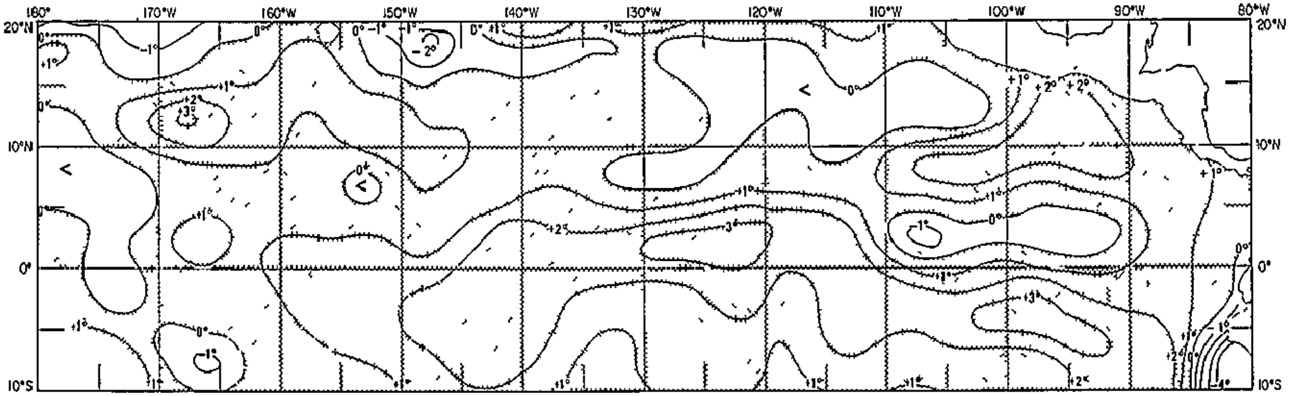

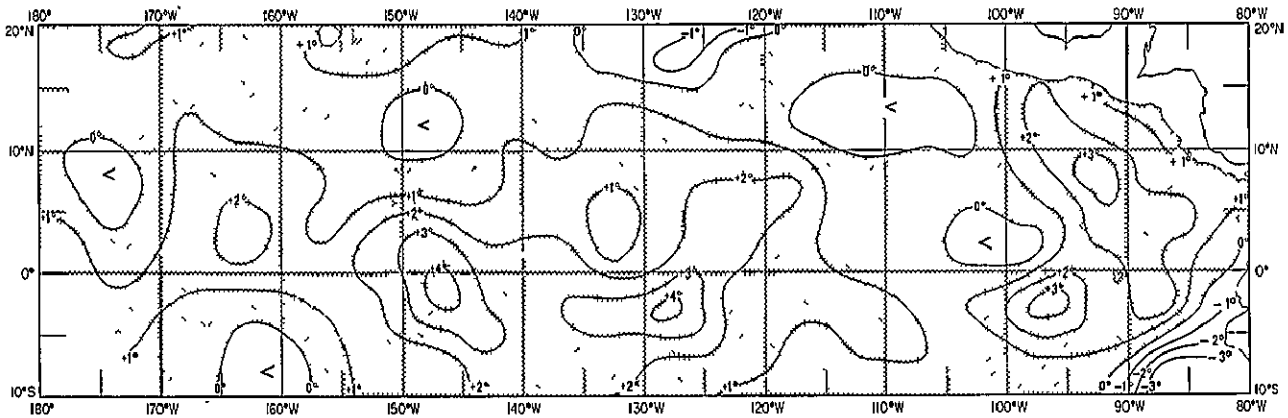

Figure A-30

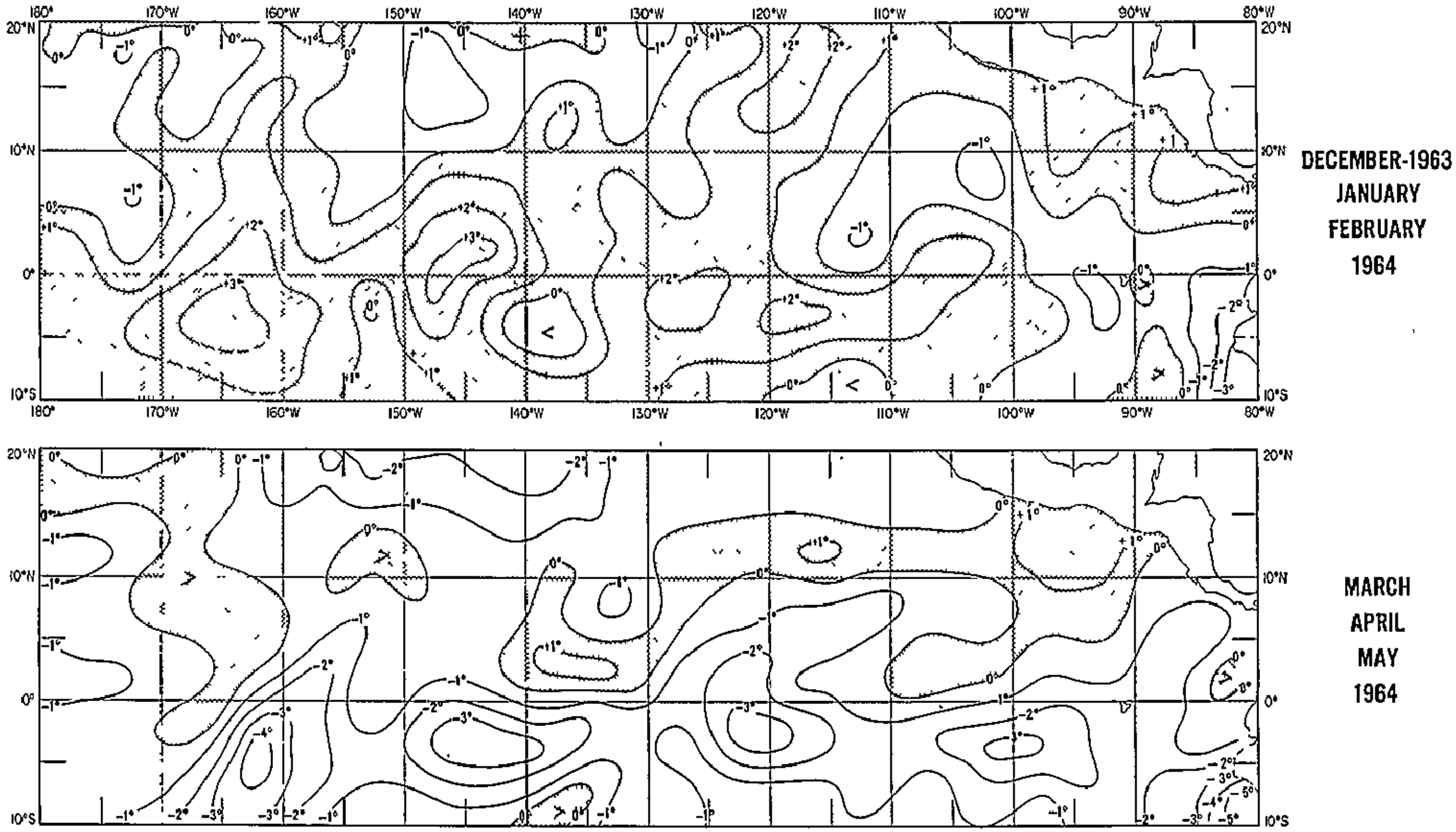

Figure A-31

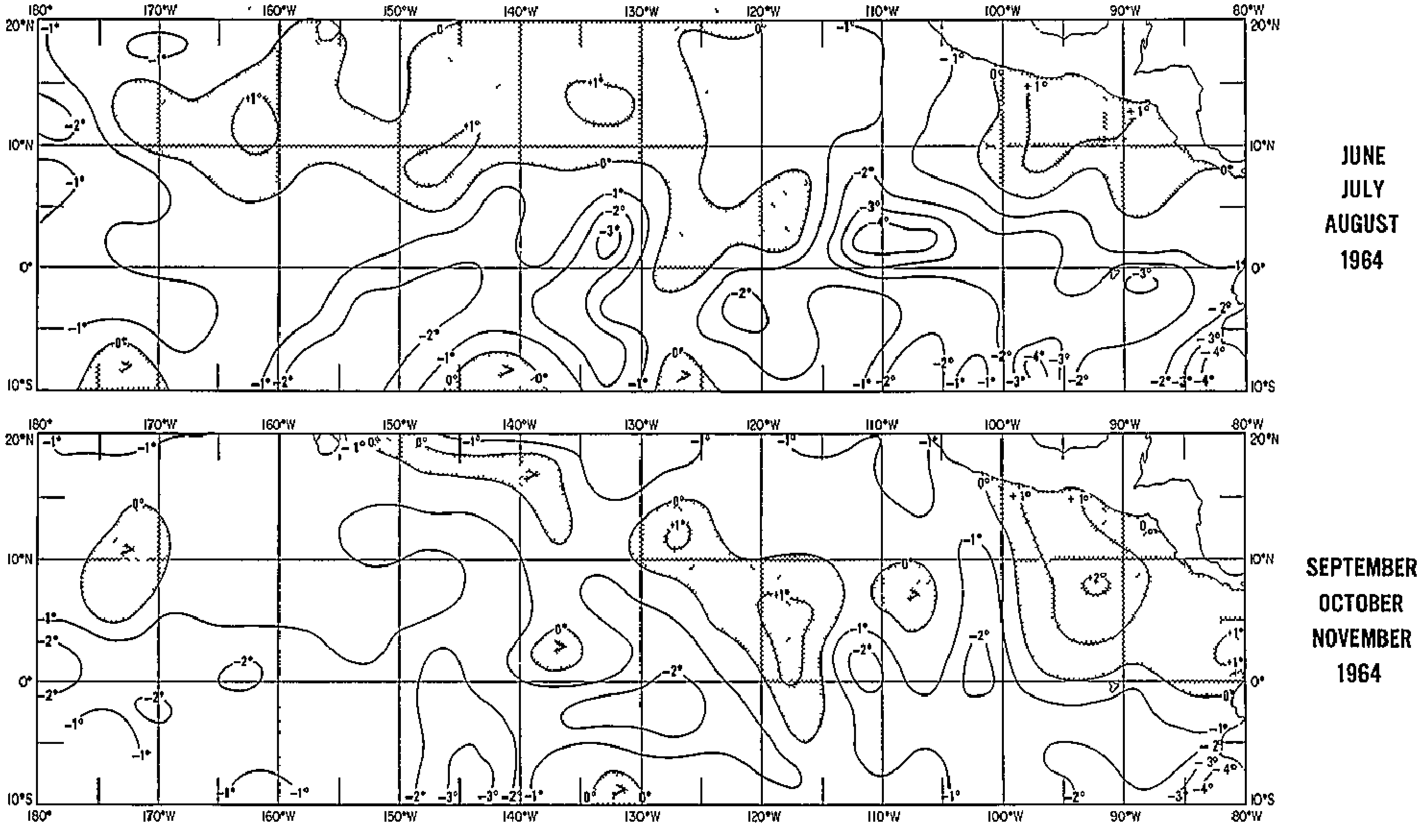
180°
170°W
160°W
150°W
140°W
130°W
120°W
110°W
100°W
90°W
80°W
20°N
10°N
0°
10°S
JUNE
JULY
AUGUST
1964
SEPTEMBER
OCTOBER
NOVEMBER
1964

Figure A-32

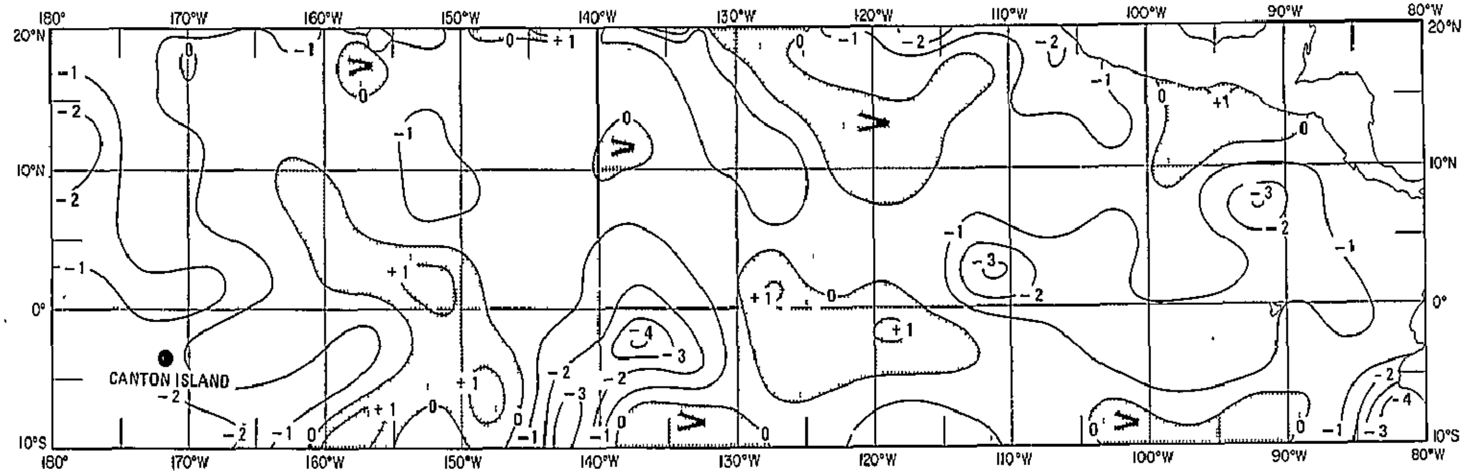

DECEMBER 1964, JANUARY, FEBRUARY 1965

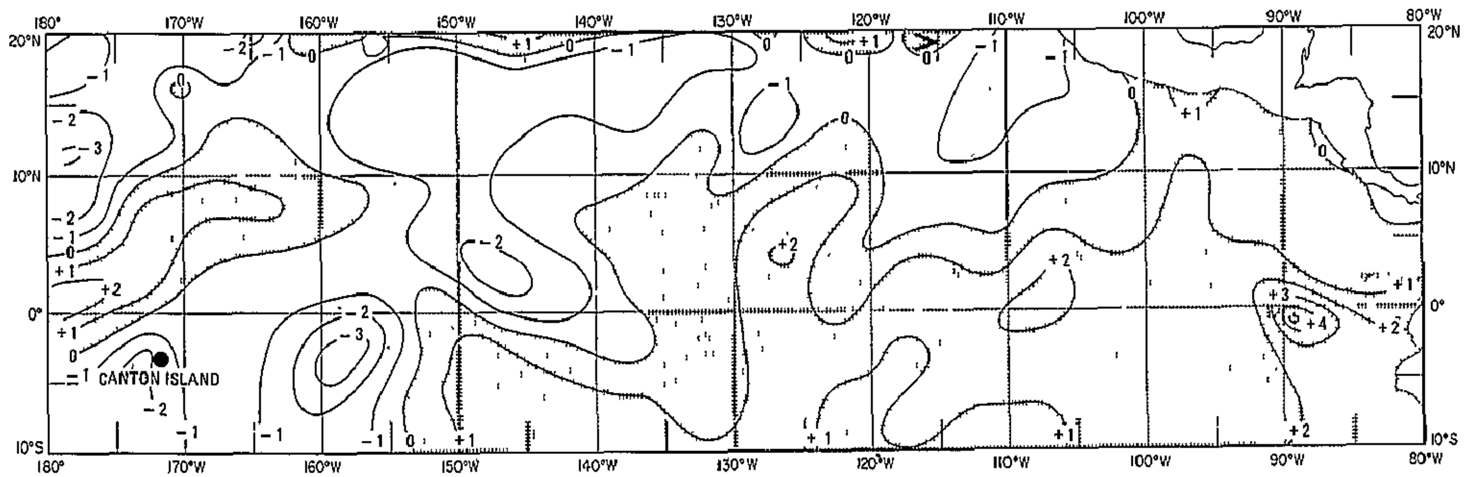

MARCH, APRIL, MAY 1965

Figure A-33

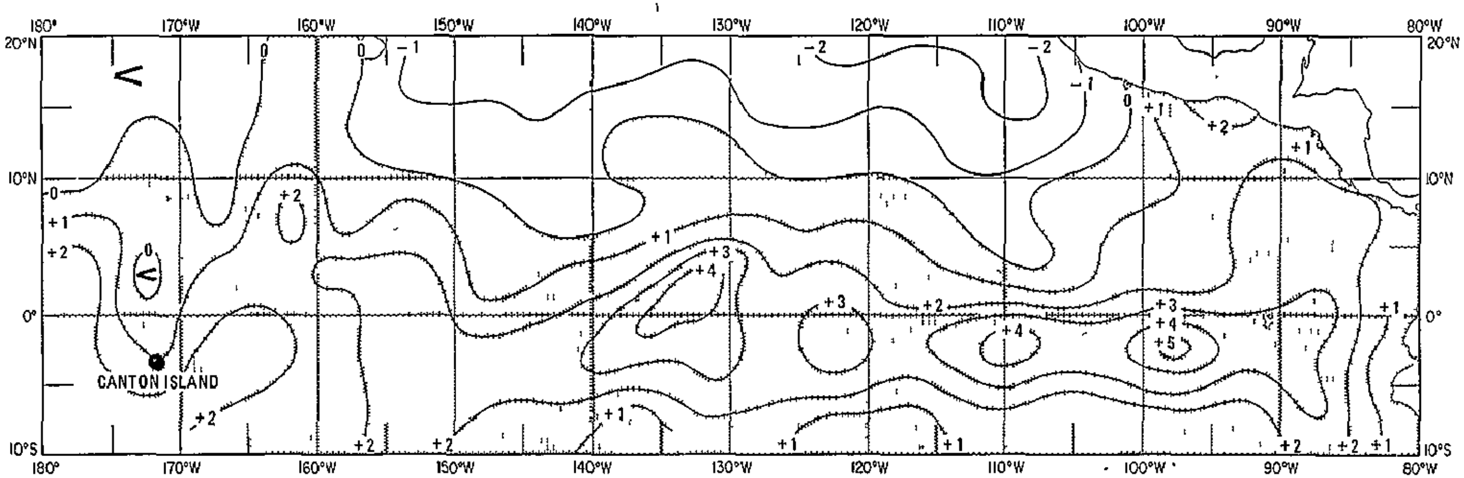

JUNE, JULY, AUGUST 1965

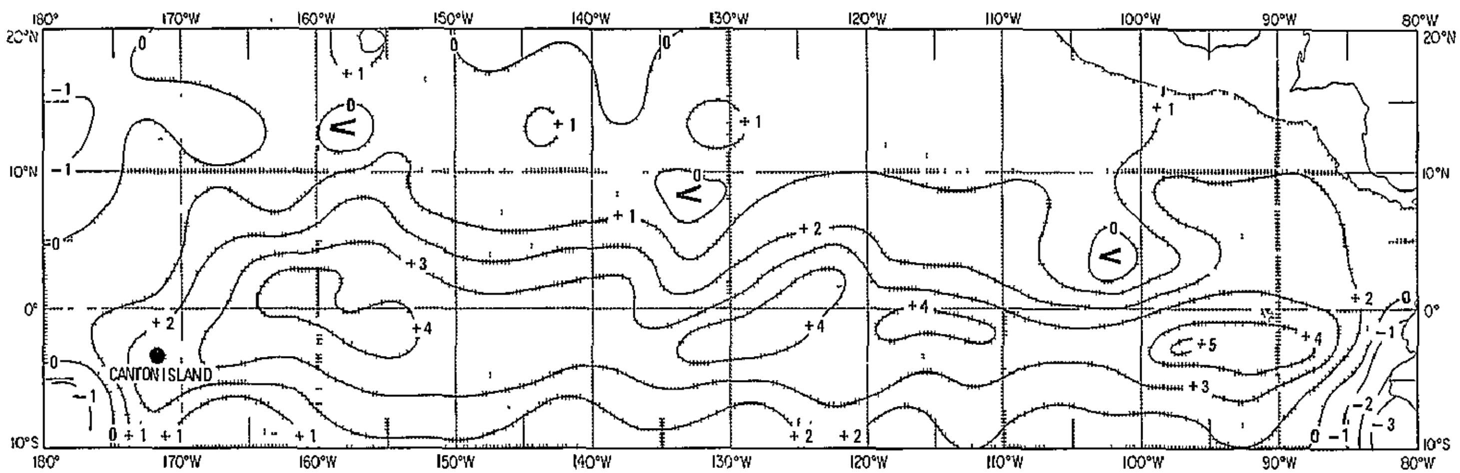

SEPTEMBER, OCTOBER, NOVEMBER 1965

Figure A-34

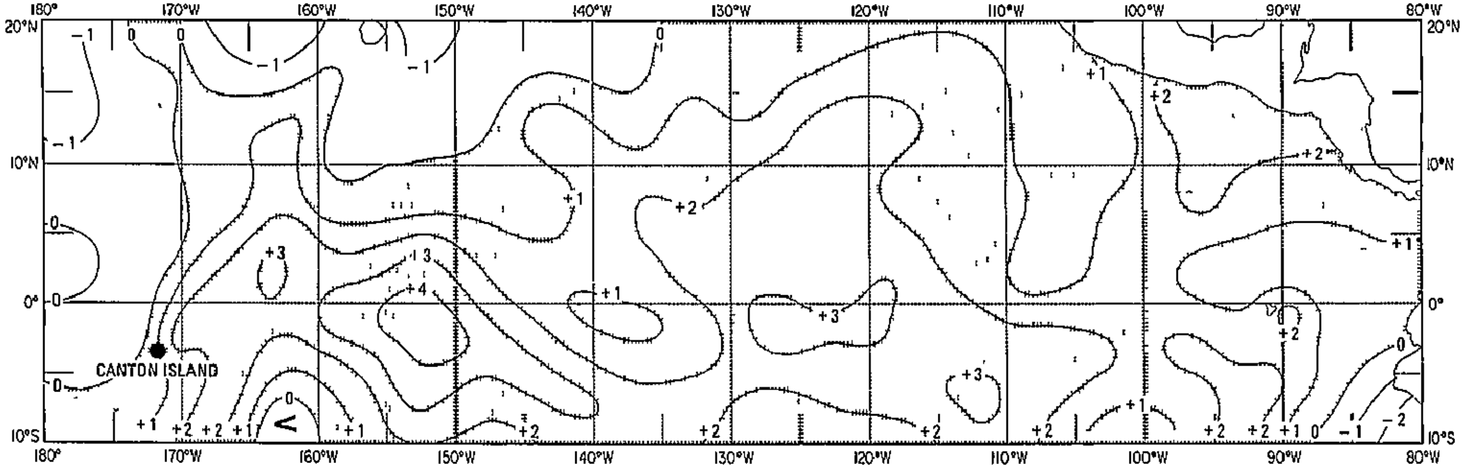

DECEMBER 1965, JANUARY, FEBRUARY 1966

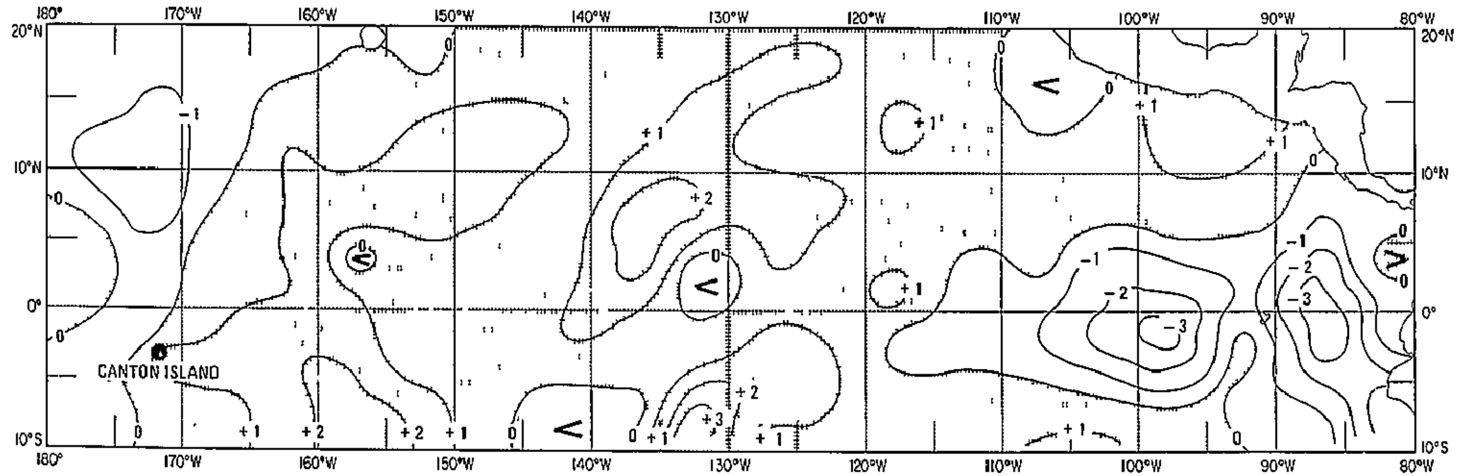

MARCH, APRIL, MAY 1966

Figure A-35

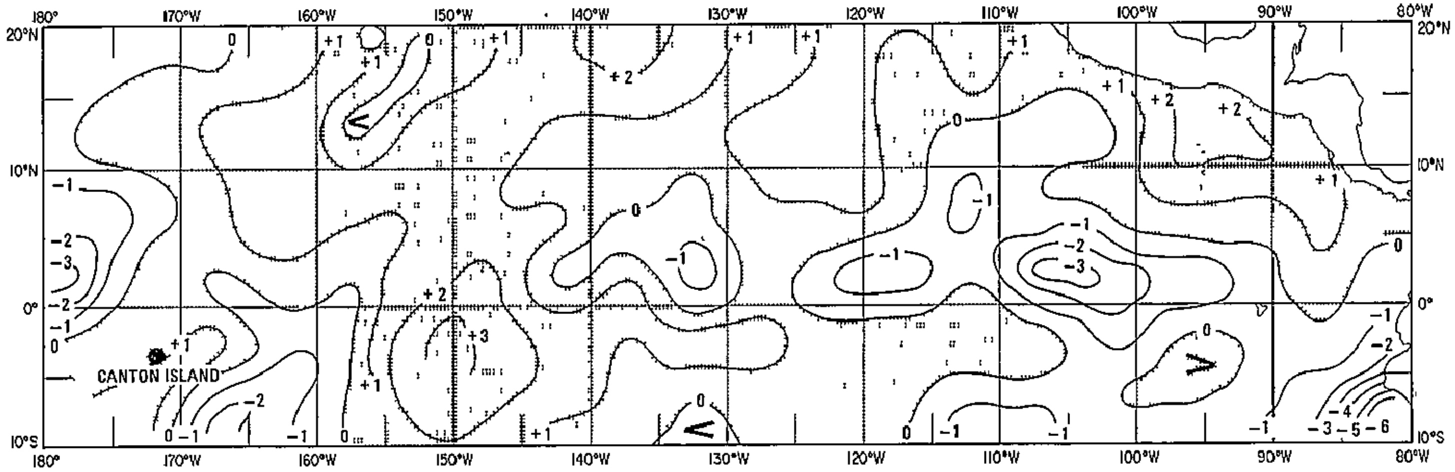

JUNE, JULY, AUGUST 1966

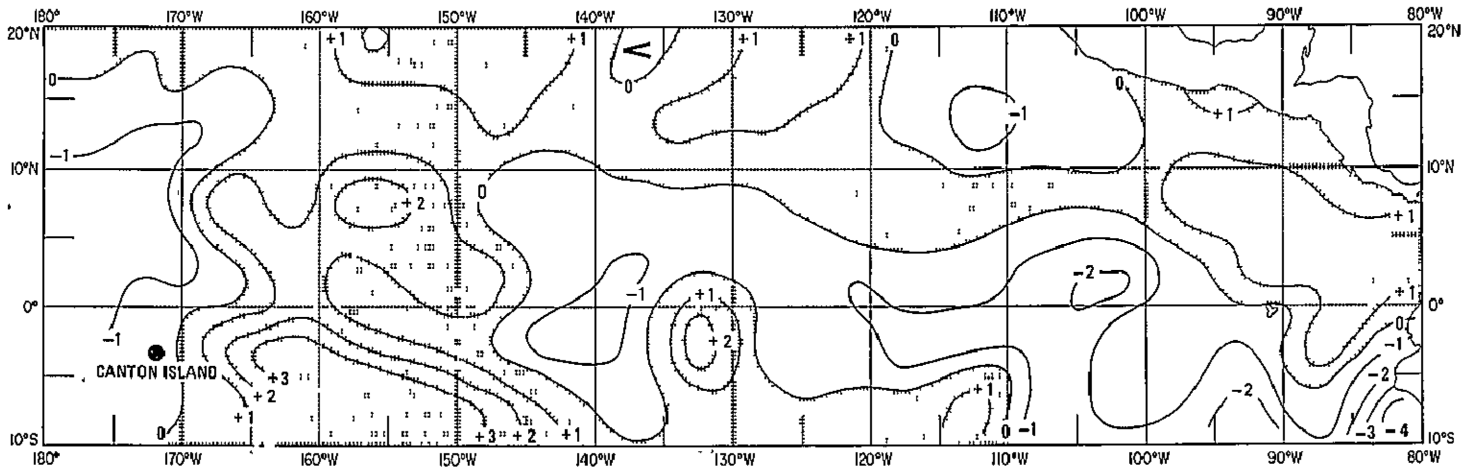

SEPTEMBER OCTOBÉR, NOVEMBER 1966

Figure A-36

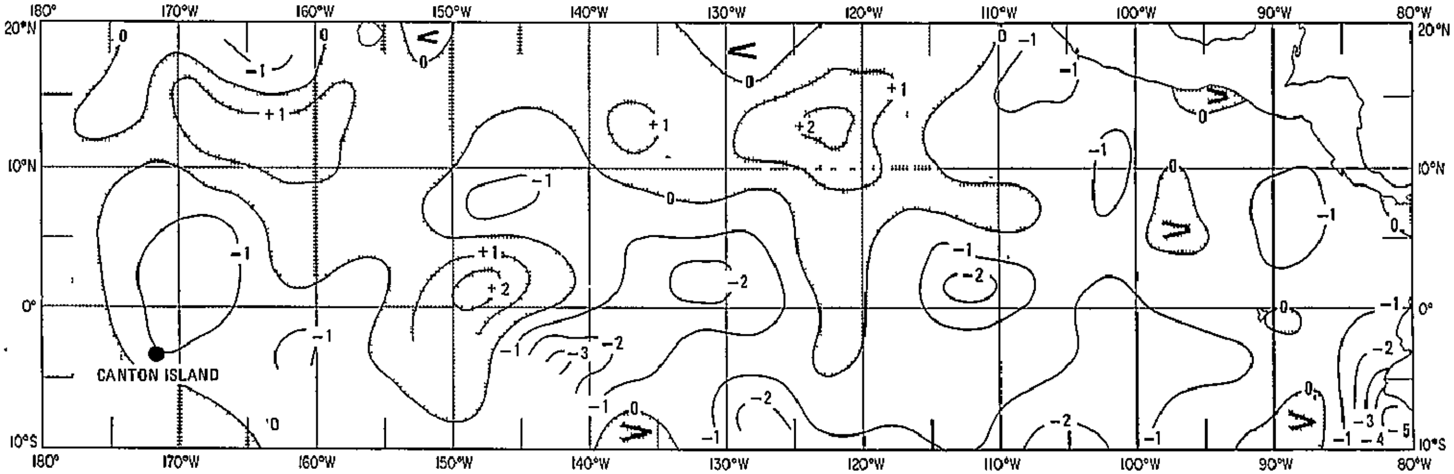

DECEMBER 1966, JANUARY, FEBRUARY 1967

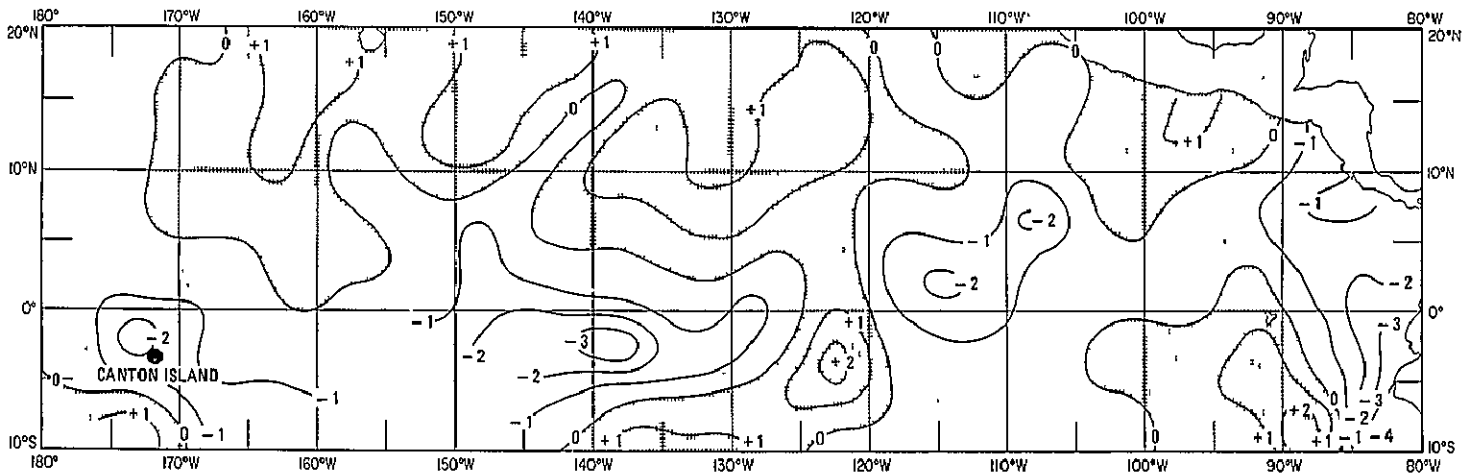

MARCH, APRIL, MAY 1967

Figure A-37

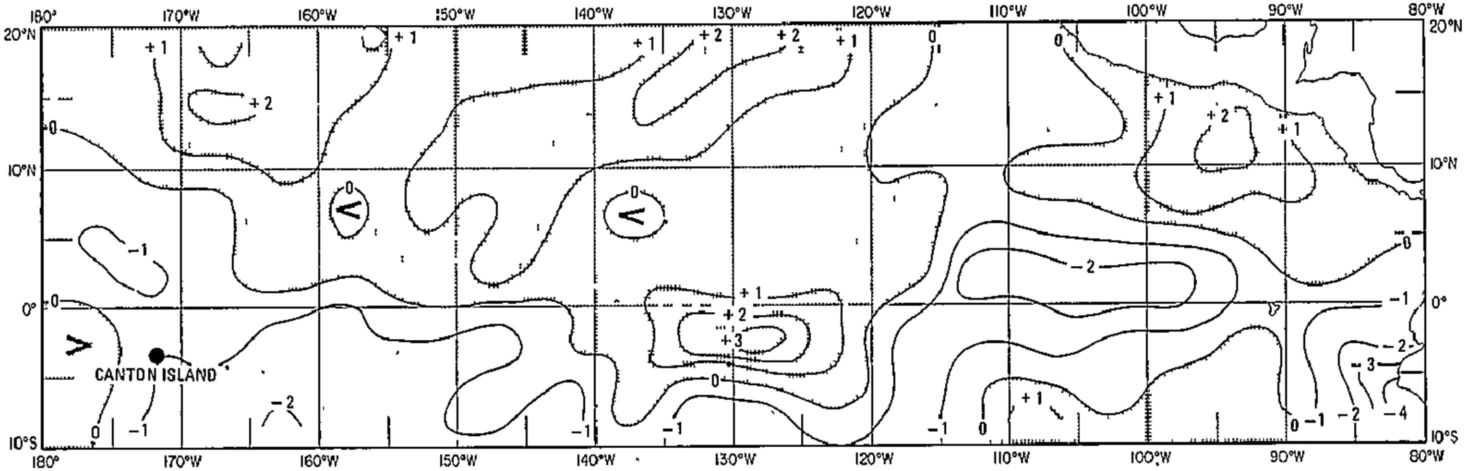

JUNE, JULY, AUGUST 1967

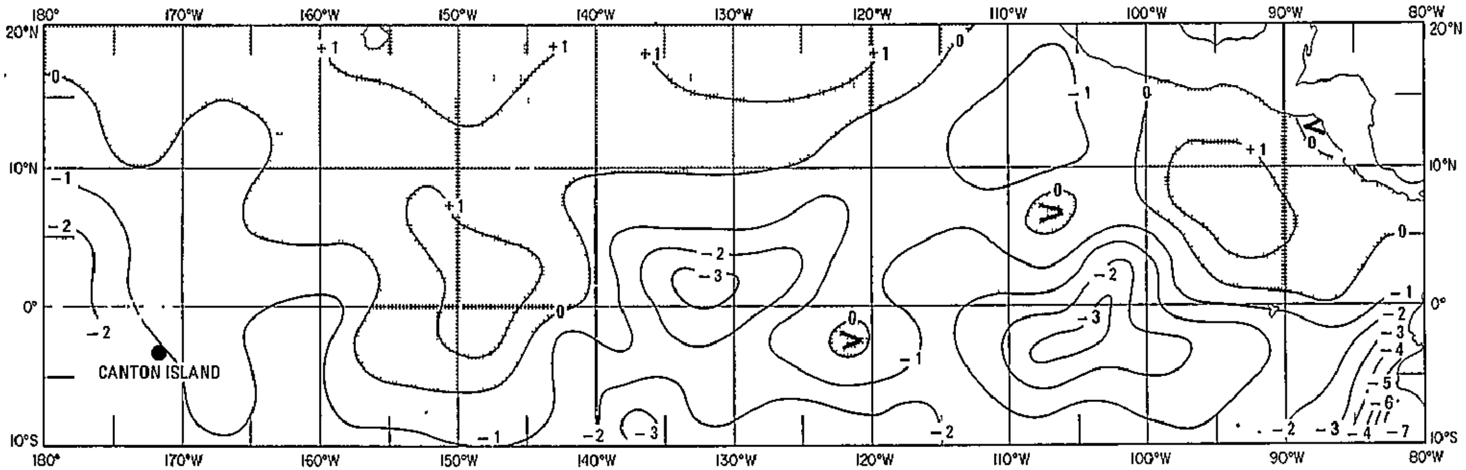

SEPTEMBER, OCTOBER, NOVEMBER 1967

Figure A-38

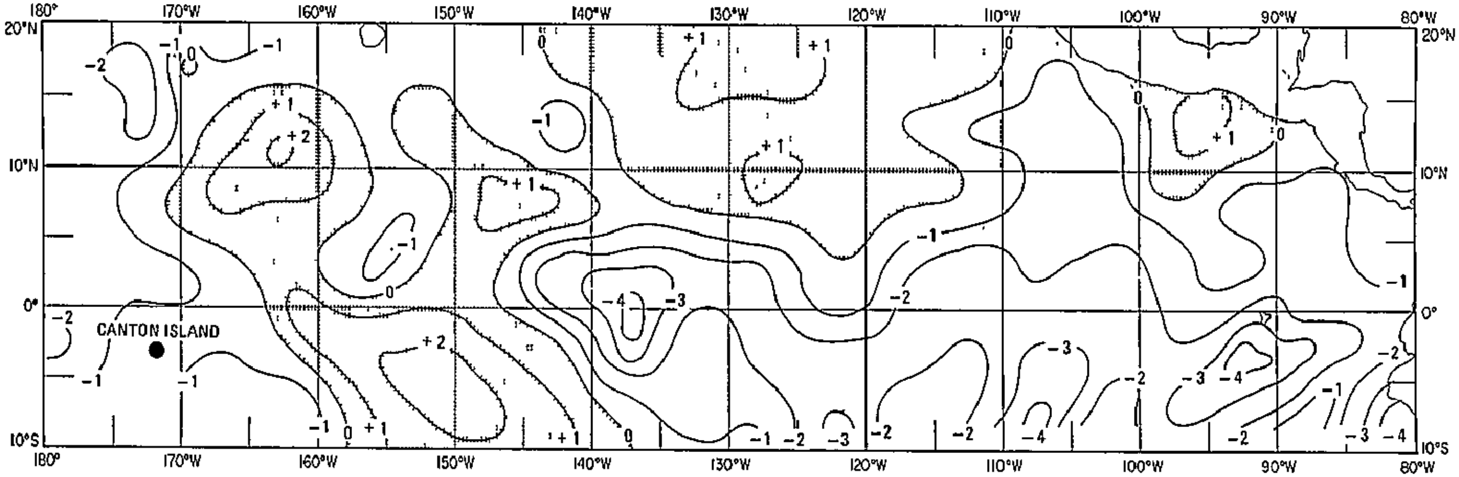

DECEMBER 1967, JANUARY, FEBRUARY 1968

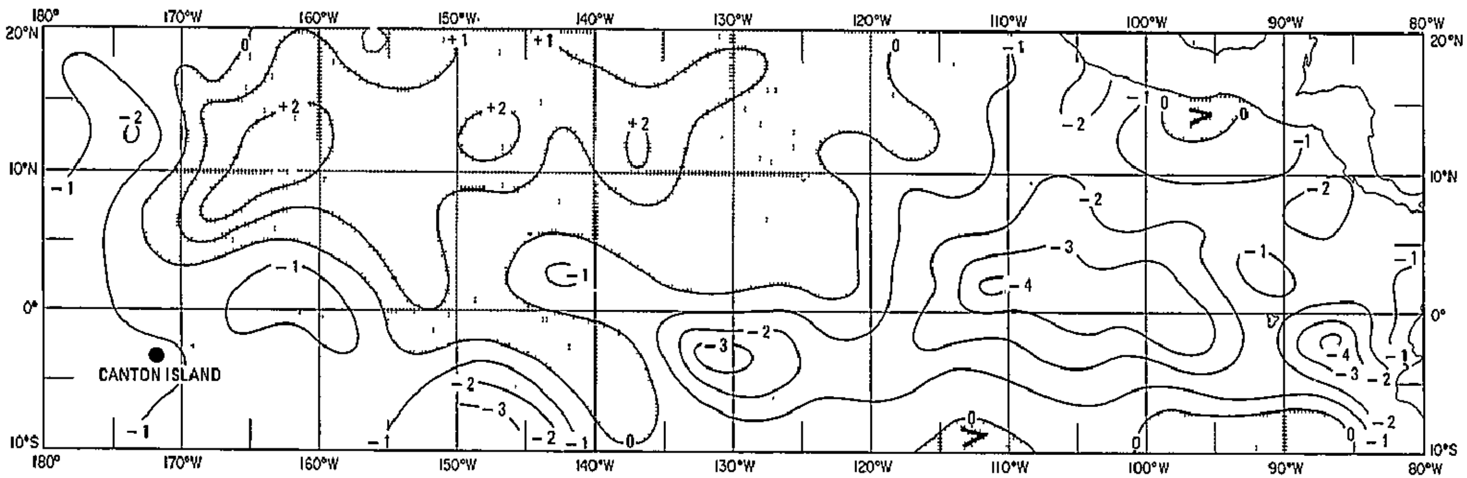

MARCH, APRIL, MAY 1968

Figure A-39

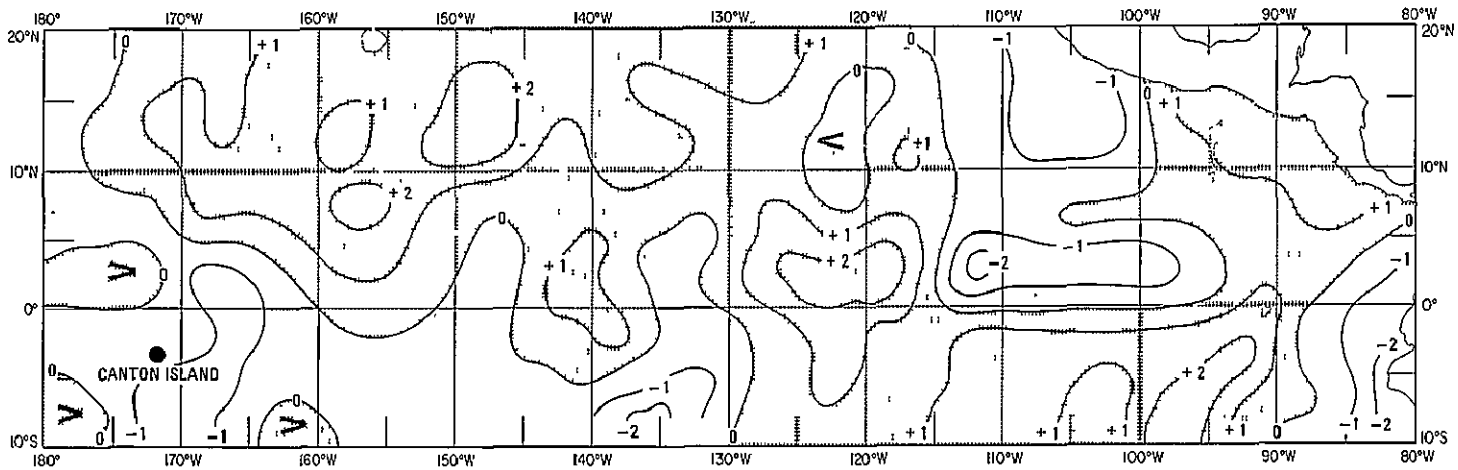

JUNE, JULY, AUGUST 1968

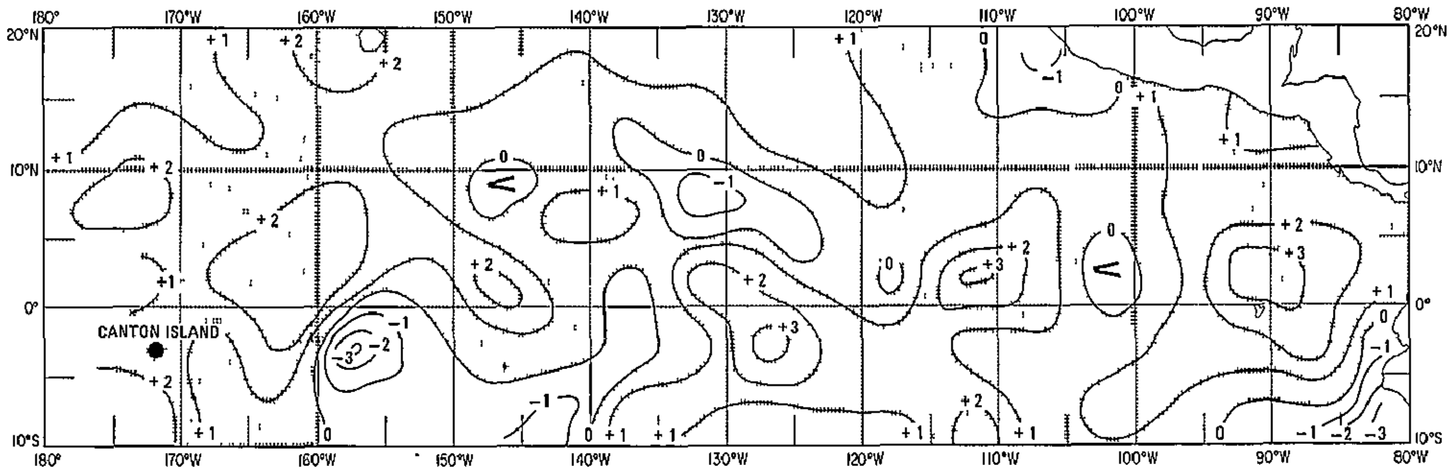

SEPTEMBER, OCTOBER, NOVEMBER 1968

Figure A-40

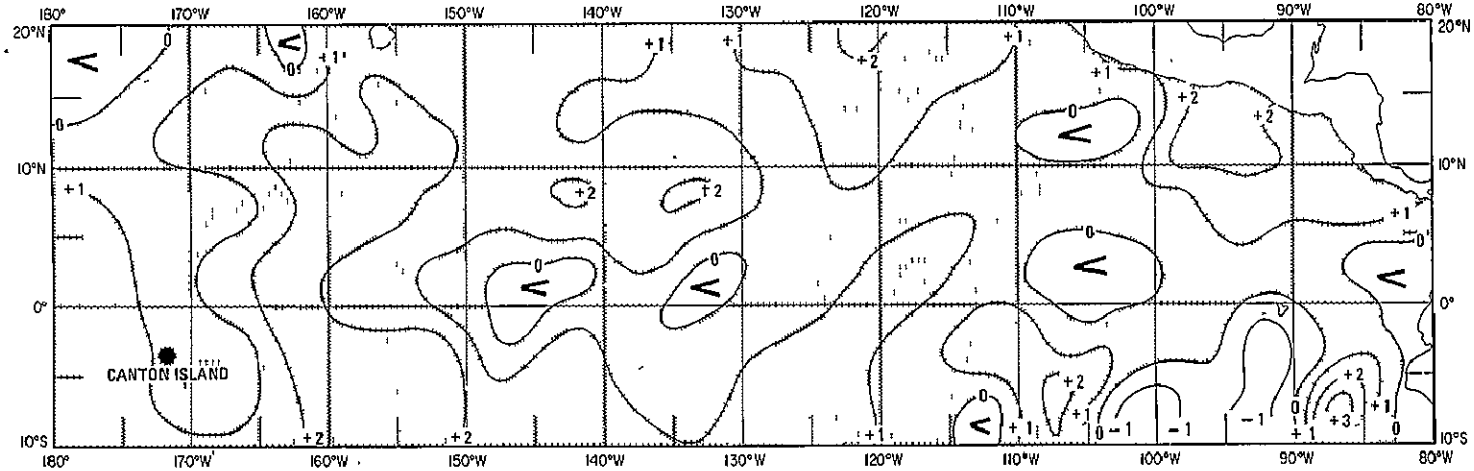

DECEMBER 1968, JANUARY, FEBRUARY 1969

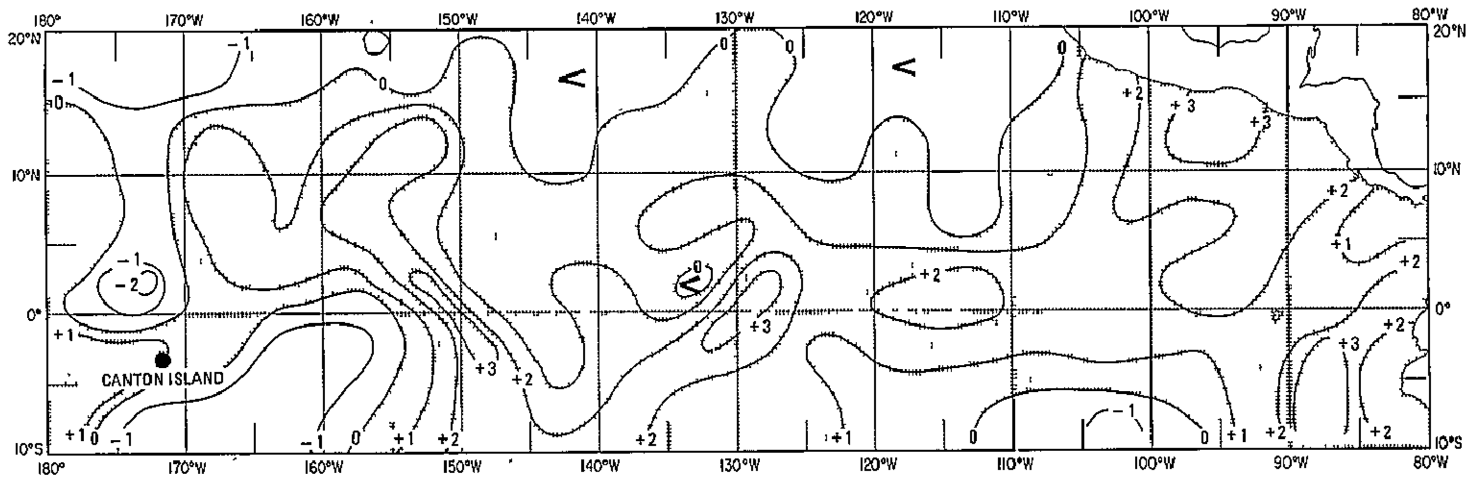

MARCH, APRIL, MAY 1969

Figure A–41

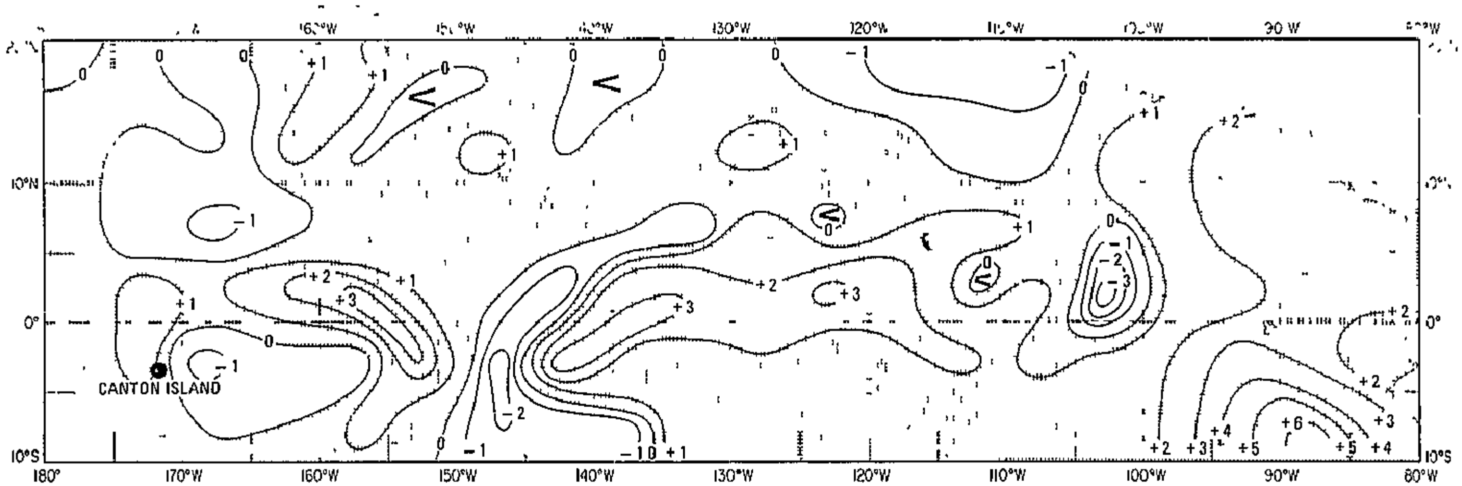

JUNE, JULY, AUGUST 1969

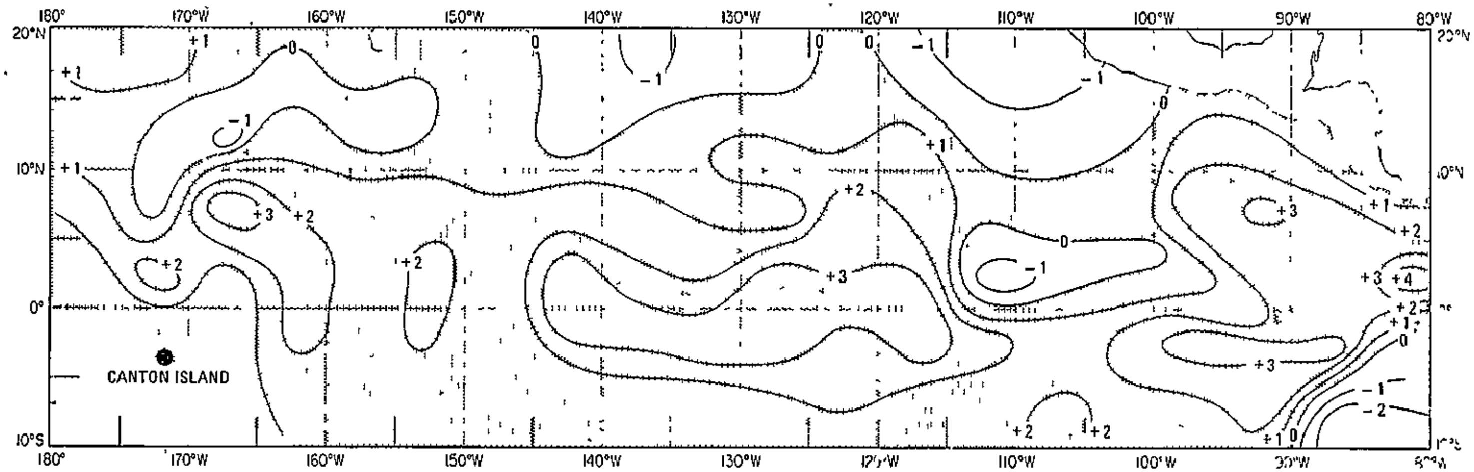

SEPTEMBER, OCTOBER, NOVEMBER 1969

Figure A-42

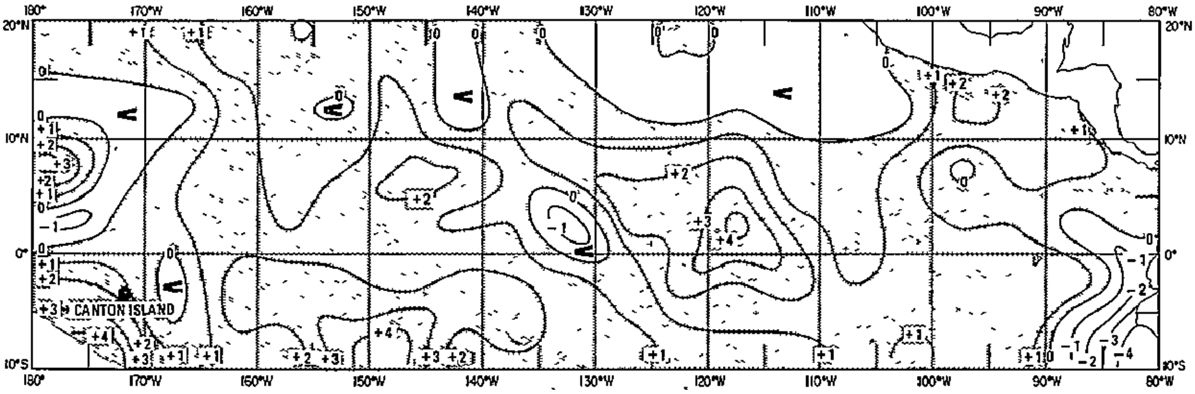

DECEMBER 1969, JANUARY, FEBRUARY 1970

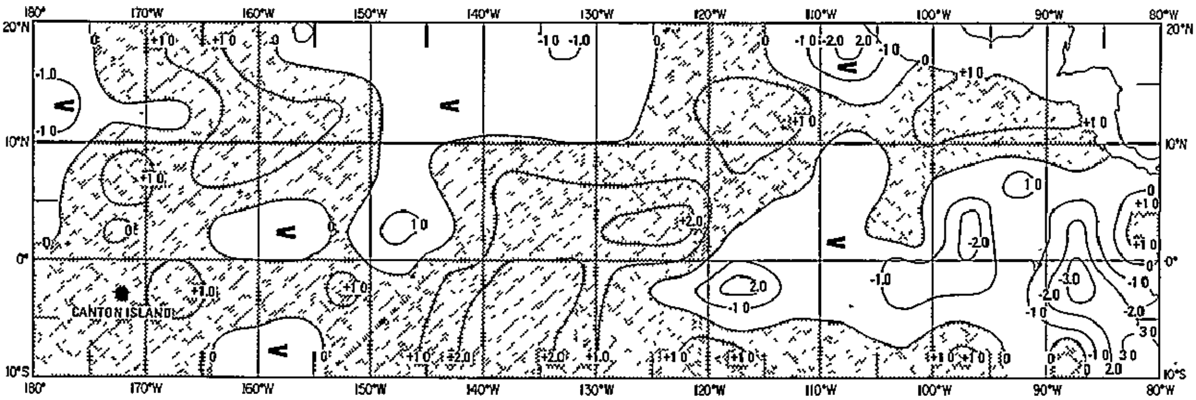

MARCH, APRIL, MAY 1970

Figure A-43

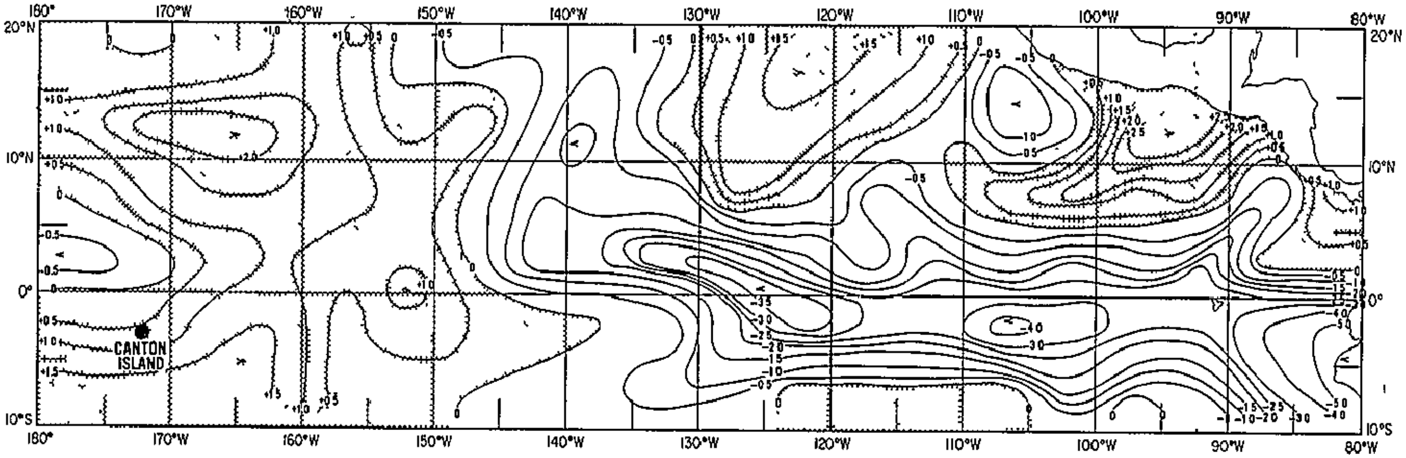

JUNE, JULY, AUGUST, 1970

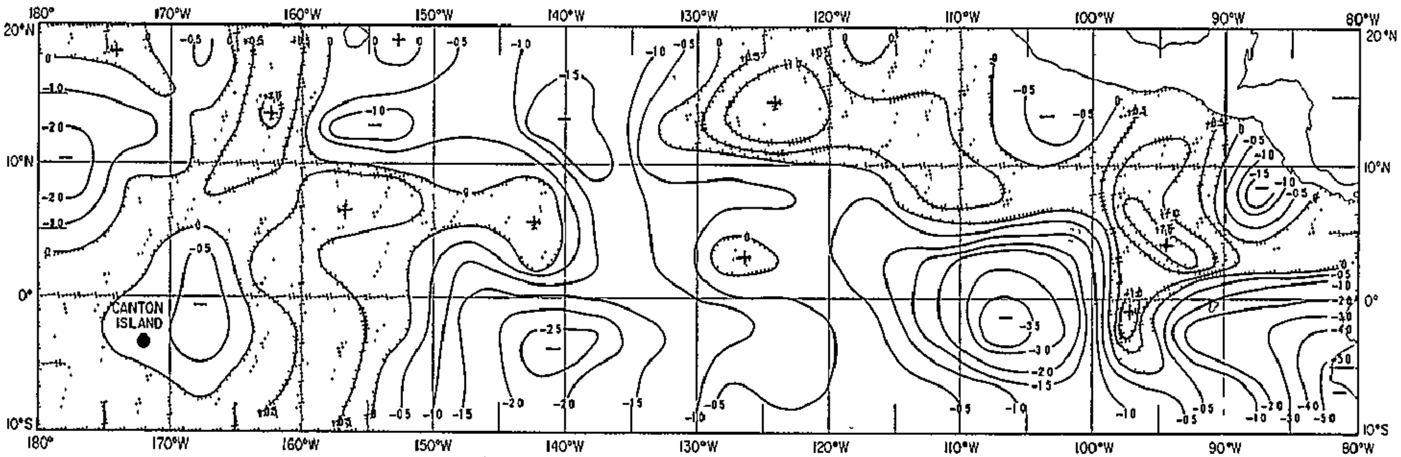

SEPTEMBER, OCTOBER, NOVEMBER, 1970

Figure A-44

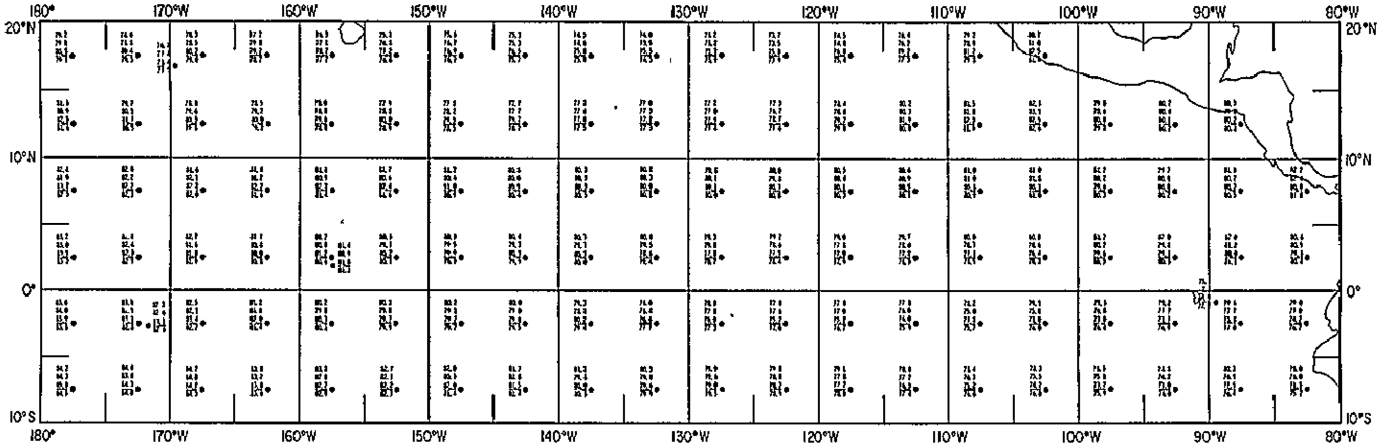

DECEMBER, JANUARY, FEBRUARY

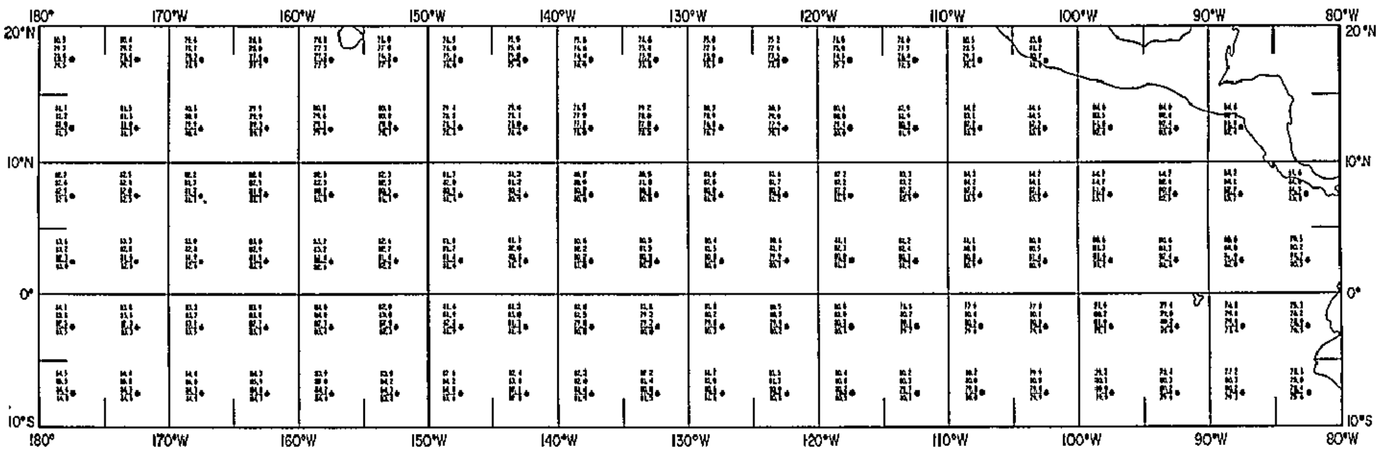

MARCH, APRIL, MAY

Figure A-45

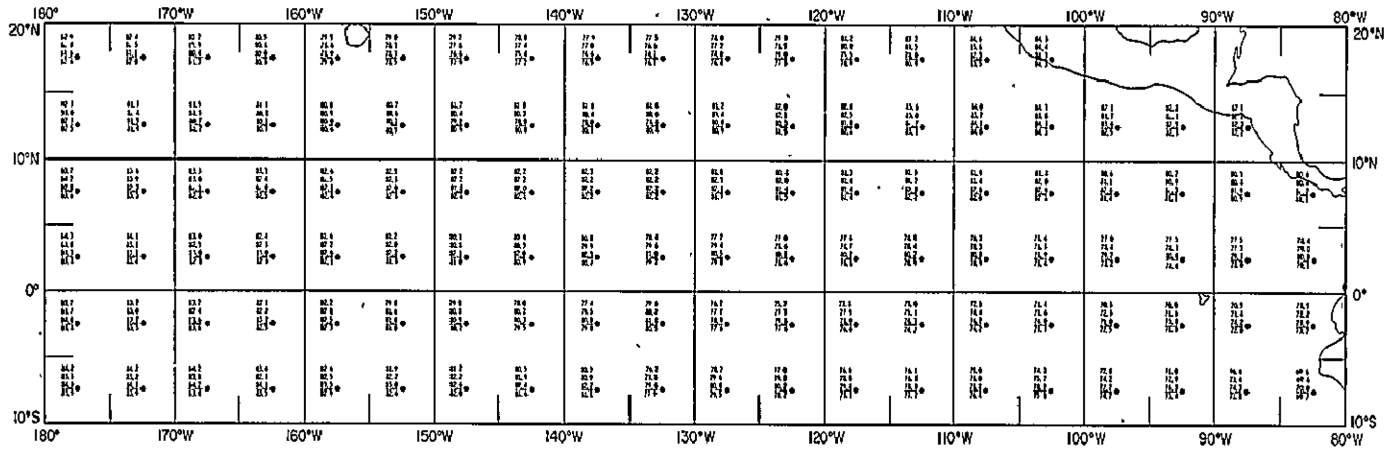

JUNE, JULY, AUGUST

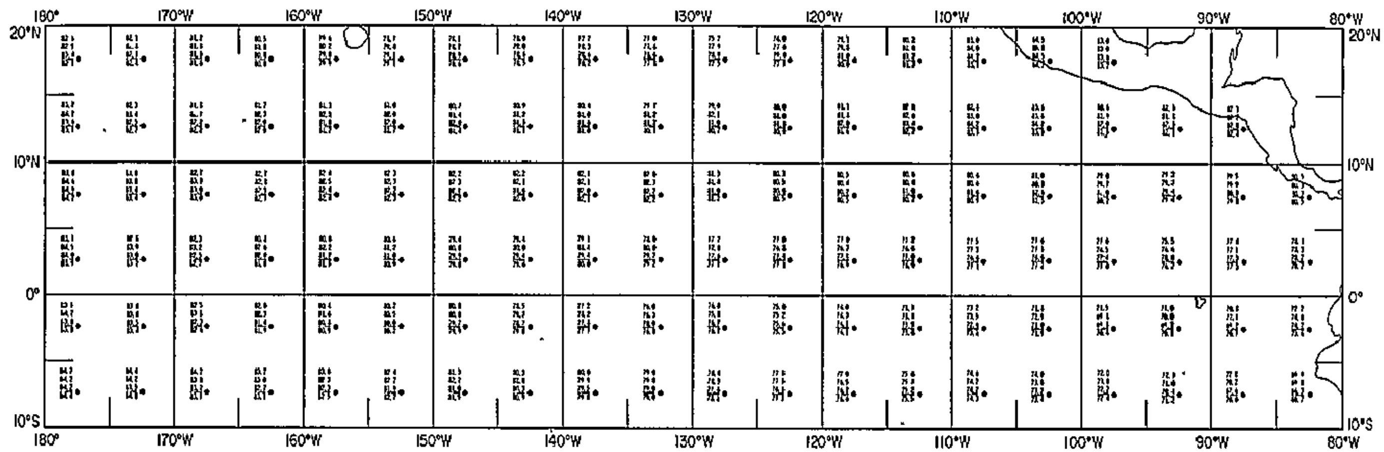

SEPTEMBER, OCTOBER, NOVEMBER

Figure A-46

APPENDIX B

SATELLITE-DERIVED CLOUDINESS AND SEA SURFACE TEMPERATURE ANOMALIES OVER THE TROPICAL PACIFIC OCEAN (1962-1970)

A comparison of satellite-derived monthly cloudiness (in percent of area covered by ≥ 6/10 clouds) and 3-monthly sea surface temperature anomalies (weighted) from 1962 to 1970 for the following regions:

Figure B-1. 20°-30°N, 100°W-180° (clouds), 20°-30°N, 100°-180° (sea)

Figure B-2. 10°-20°N, 100°W-180°(clouds), 10°-20°N, 90°W-180°(sea)

Figure B-3. 5°-15°N, 100°W-180° (clouds), 5°-15°N, 90°W-180°(sea)

Figure B-4. 0°-10°N, 100°W-180°(clouds), 0°-10°N, 80°W-180°(sea)

Figure B-5. 5°N-5°S, 100°W-180°(clouds), 5°N-5°S, 80°W-180°(sea)

Figure B-6. 0°-10°S, 100°W-180°(clouds), 0°-10°S, 80°W-180°(sea)

Figure B-7. 10°-20°S, 100°W-180°(clouds), 20°-25°S, 100°W-180°(clouds)

Figure B-8. 20°-30°N, 180°-130°E(clouds)
10°-20°N, 180°-130°E(clouds)

Figure B-9. 5°-15°N, 180°-130°E(clouds)
0°-10°N, 180°-130°E(clouds)

Figure B-10. 5°N-5°S, 180°-130°E(clouds)
0°-10°S, 180°-130°E(clouds)

Figure B-11. 10°-20°S, 180°-130°E(clouds)

Figure B-12. 0°-30°N, 100°W-180°(clouds)
0°-30°N, 180°-130°E(clouds)
0°-25°S, 100°W-180°(clouds)
0°-25°S, 180°-130°E(clouds)

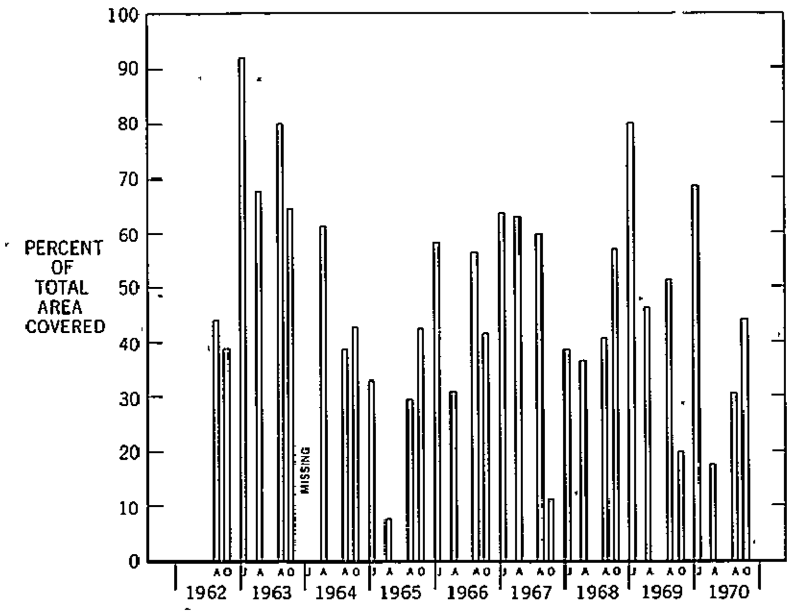

EASTERN PACIFIC
% OF AREA COVERED BY ≥ 6/10 CLOUD COVER
20°–30°N 100°W–180°

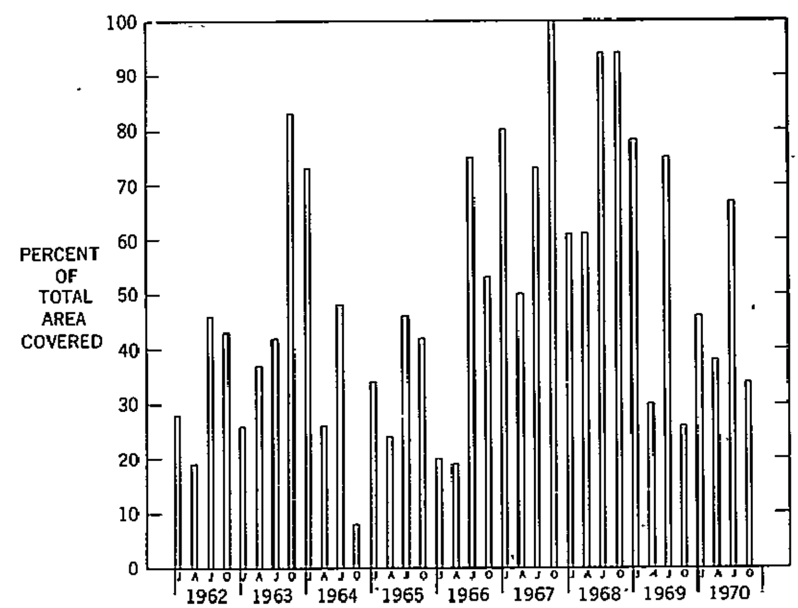

EASTERN PACIFIC
% OF AREA COVERED BY A POSITIVE
SEA SURFACE TEMPERATURE ANOMALY (WEIGHTED)
20°–30°N 100°W–180°

Figure B-1

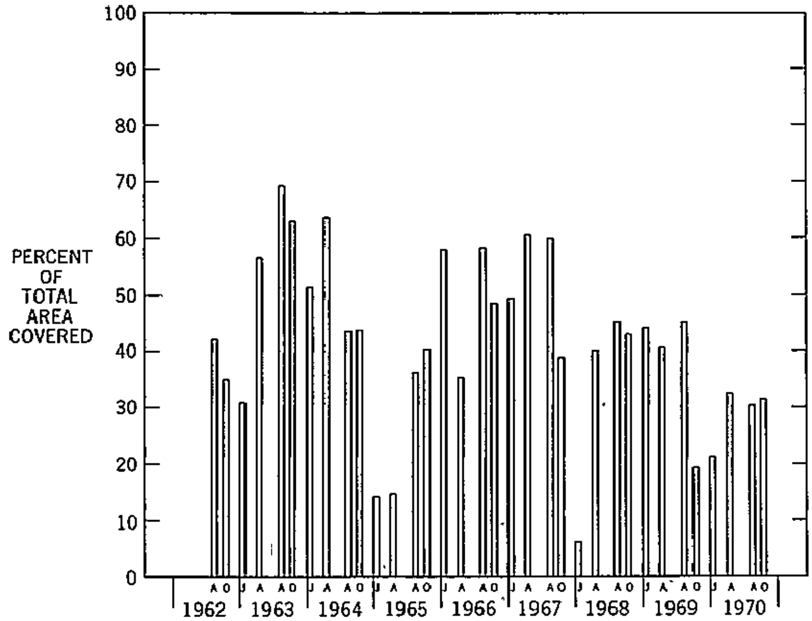

EASTERN PACIFIC
% OF AREA COVERED BY ≥ 6/10 CLOUD COVER
10°–20°N 100°W–180°

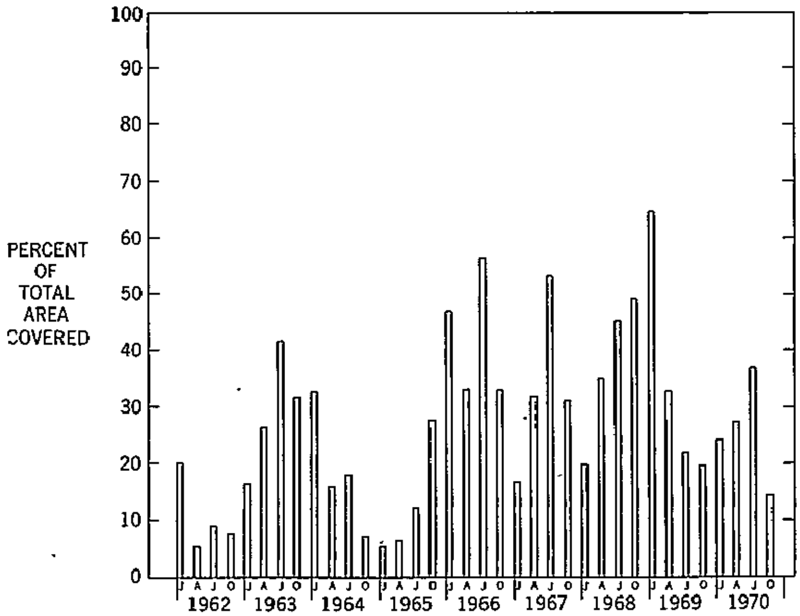

EASTERN PACIFIC
% OF AREA COVERED BY A POSITIVE
SEA SURFACE TEMPERATURE ANOMALY (WEIGHTED)
10–20°N 90°W–180°

Figure B-2

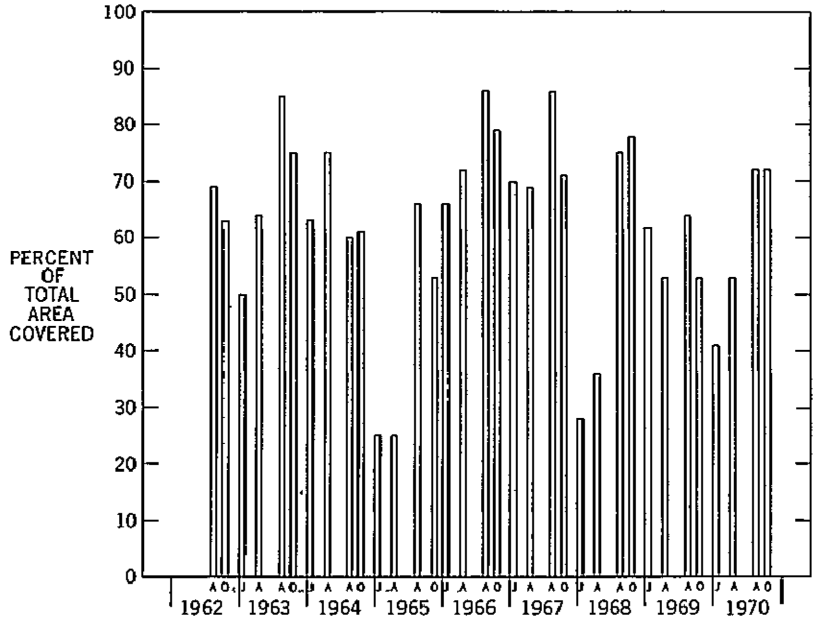

EASTERN PACIFIC
% OF AREA COVERED BY ≥ 6/10 CLOUD COVER
5°N–15°N 100°W–180°

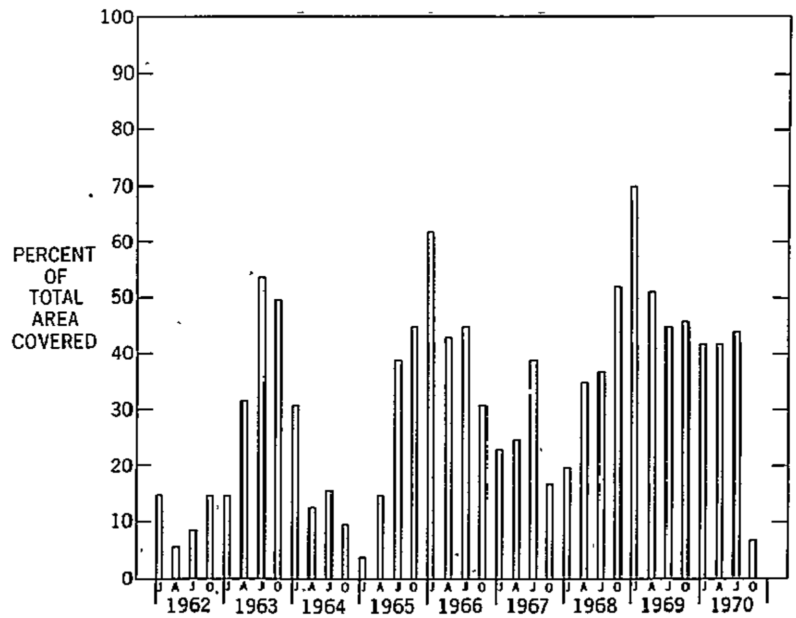

EASTERN PACIFIC
% OF AREA COVERED BY A POSITIVE
SEA SURFACE TEMPERATURE ANOMALY (WEIGHTED)
5°N–15°N 90°W–180°

Figure B-3-

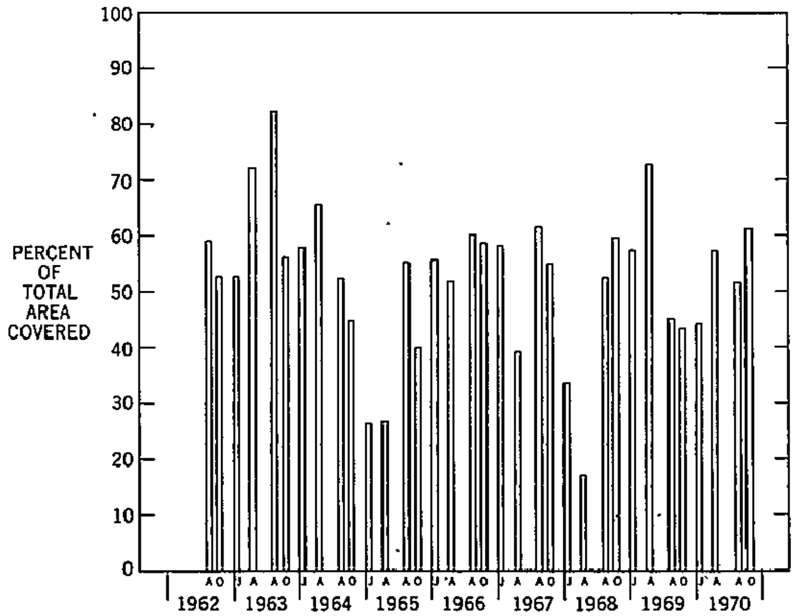

EASTERN PACIFIC
% OF AREA COVERED BY ≥ 6/10 CLOUD COVER
0°–10°N 100°W–180°

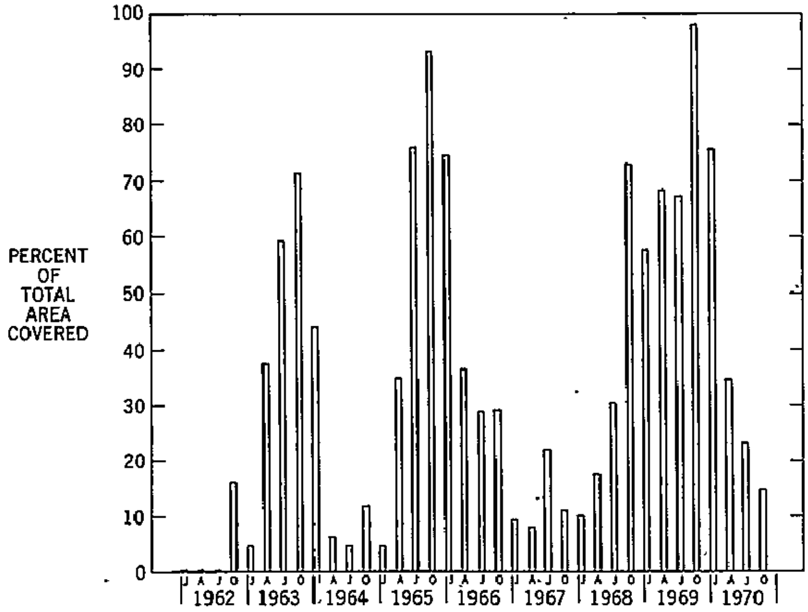

EASTERN PACIFIC
% OF AREA COVERED BY A POSITIVE
SEA SURFACE TEMPERATURE ANOMALY (WEIGHTED)
0–10°N 80°W–180°

Figure B–4

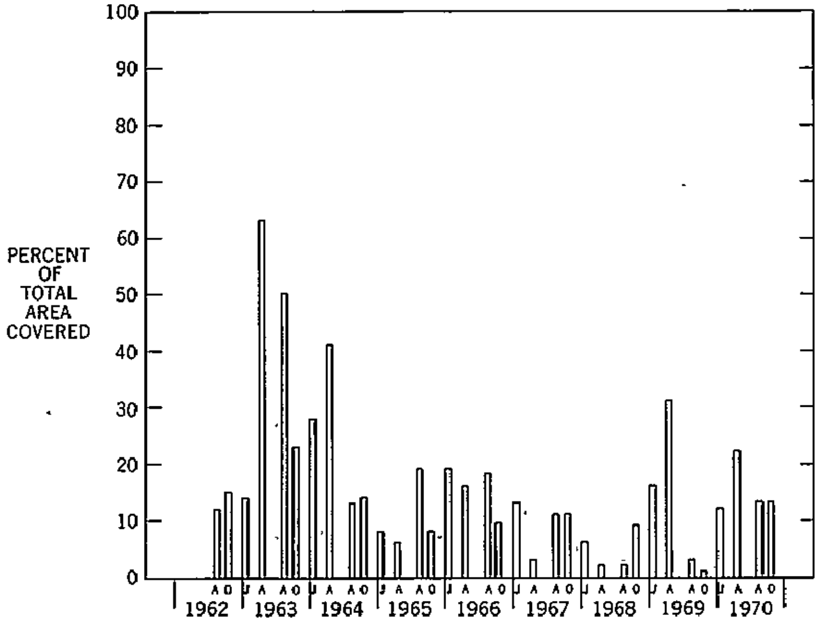

EASTERN PACIFIC
% OF AREA COVERED BY ≥ 6/10 CLOUD COVER
5°N–5°S 100°W–180°

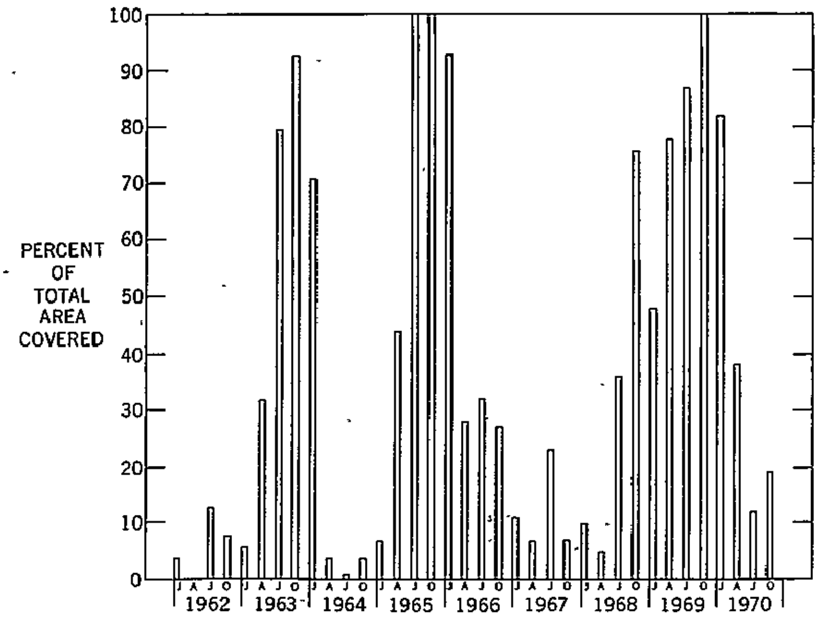

EASTERN PACIFIC
% OF AREA COVERED BY ≥ 0°C
SEA SURFACE TEMPERATURE ANOMALY (WEIGHTED)
5°N–5°S 80°W–180°

Figure B-5

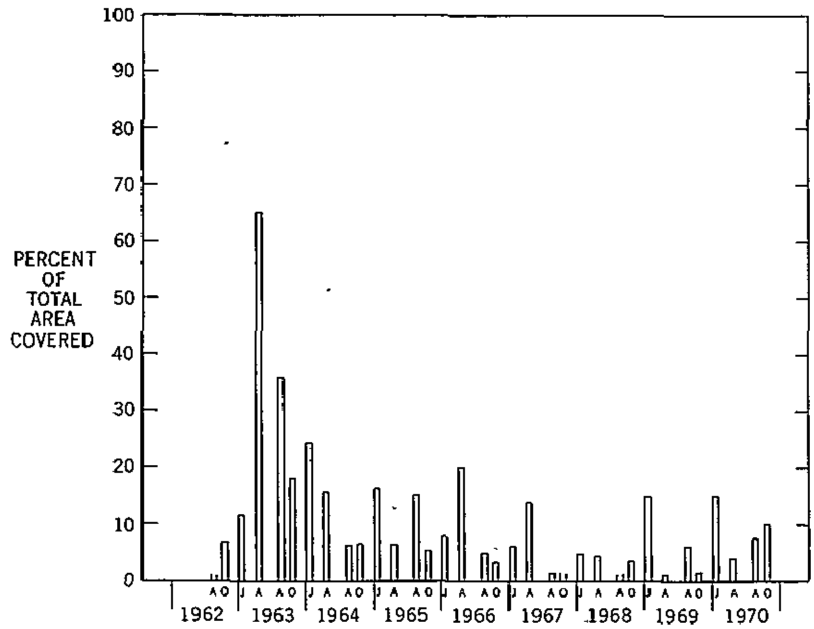

EASTERN PACIFIC
% OF AREA COVERED BY ≥ 6/10 CLOUD COVER
0°–10°S 100°W–180°

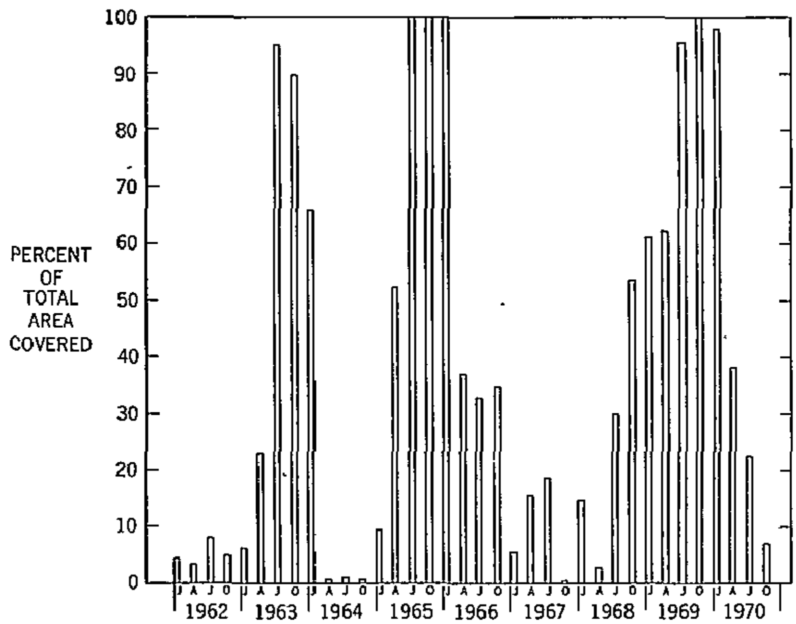

EASTERN PACIFIC
% OF AREA COVERED BY A POSITIVE SEA SURFACE TEMPERATURE ANOMALY (WEIGHTED)
0–10°S 80°W–180°

Figure B-6

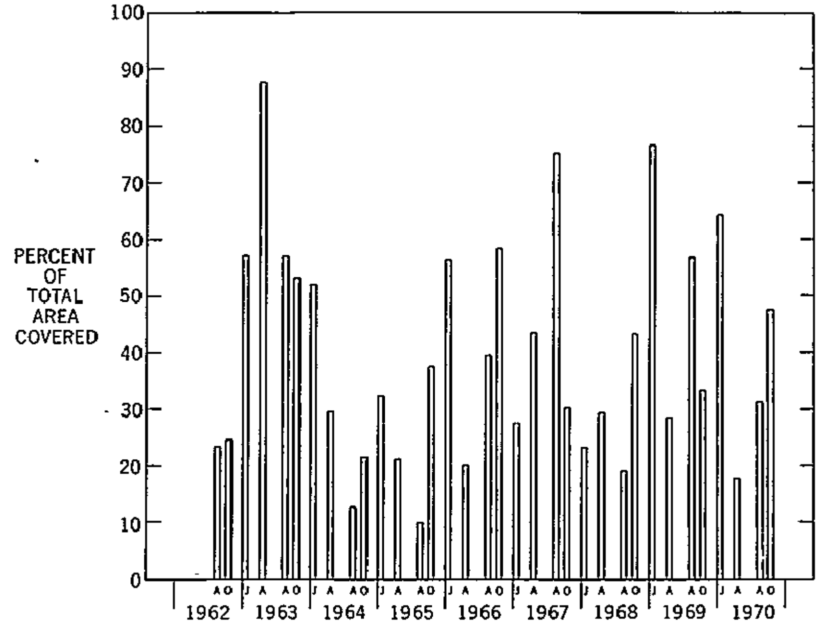

EASTERN PACIFIC
% OF AREA COVERED BY ≥ 6/10 CLOUD COVER
10°–20° S 100°W–180°

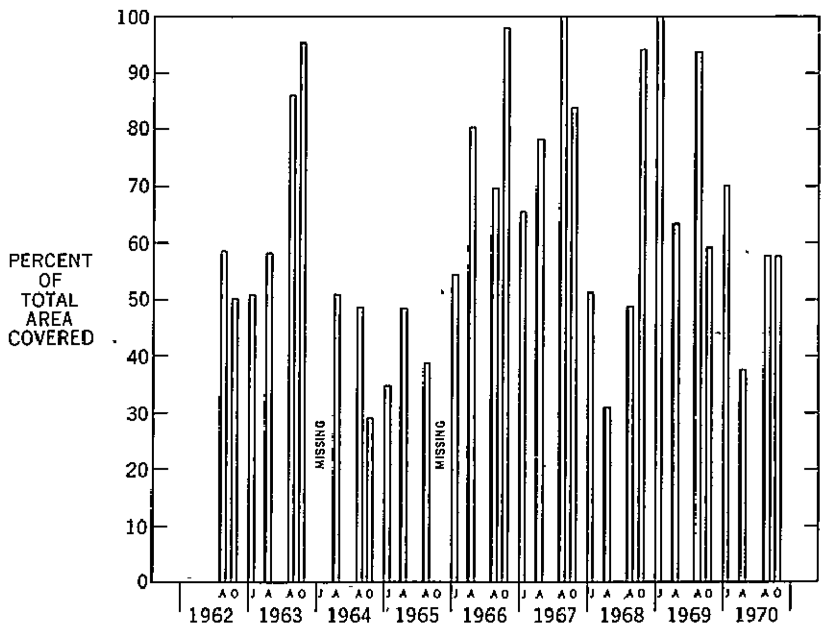

EASTERN PACIFIC
% OF AREA COVERED BY ≥ 6/10 CLOUD COVER
20°–25°S 100°W–180°

Figure B-7

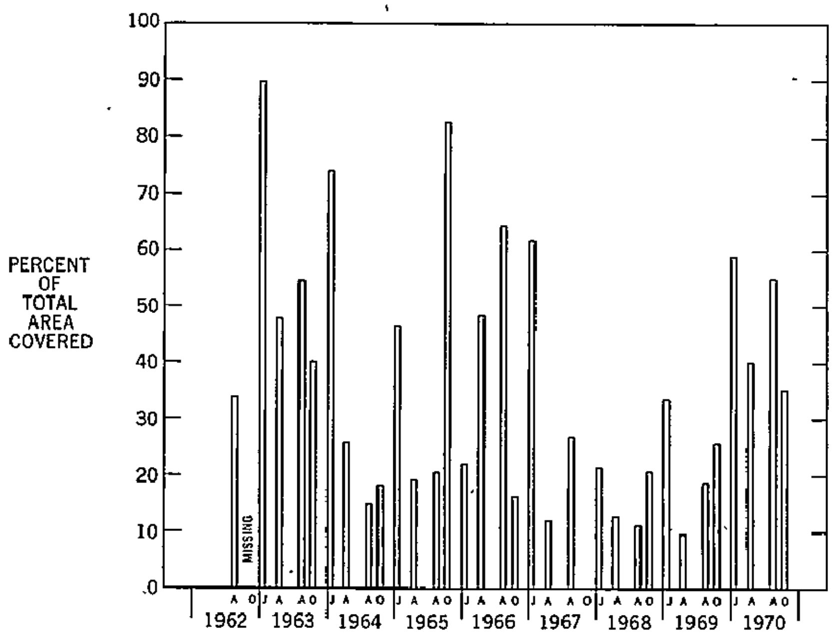

WESTERN PACIFIC
% OF AREA COVERED BY ≥ 6/10 CLOUD COVER
20°–30°N 180°–130°E

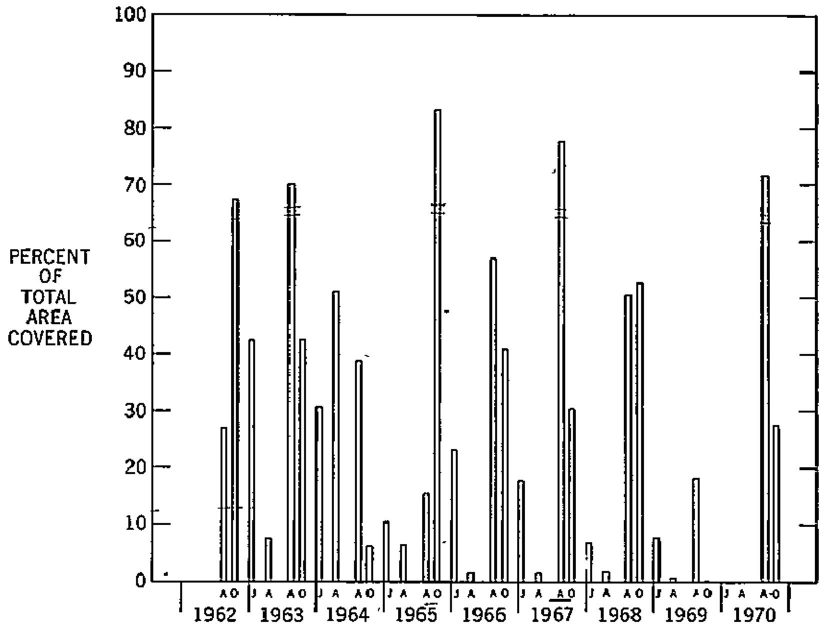

WESTERN PACIFIC
% OF AREA COVERED BY ≥ 6/10 CLOUD COVER
10°–20°N 180°–130°E

Figure B-8

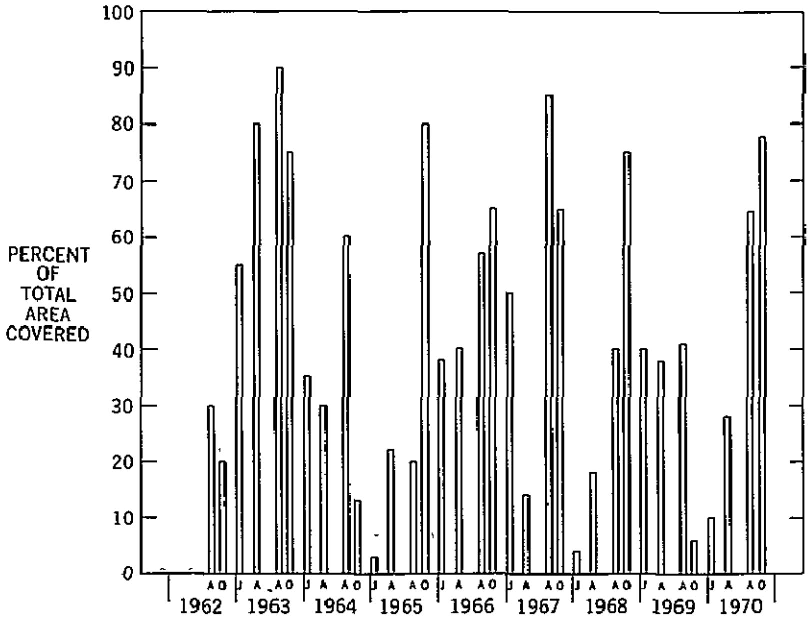

WESTERN PACIFIC
% OF AREA COVERED BY ≥ 6/10 CLOUD COVER
5°–15°N 180°–130°E

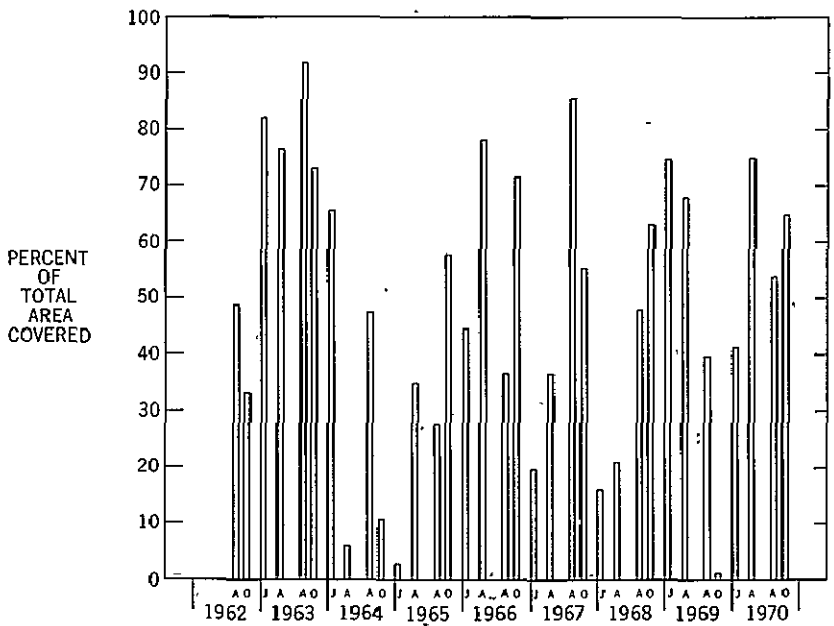

WESTERN PACIFIC
% OF AREA COVERED BY ≥ 6/10 CLOUD COVER
0°–10°N 180°–130°E

Figure B-9

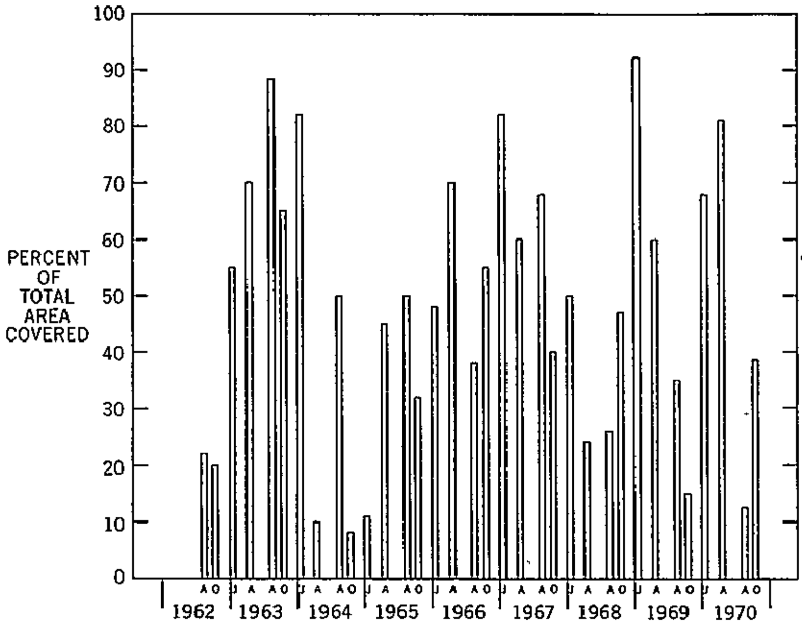

WESTERN PACIFIC
% OF AREA COVERED BY ≥ 6/10 CLOUD COVER
5°N–5°S 180°–130°E

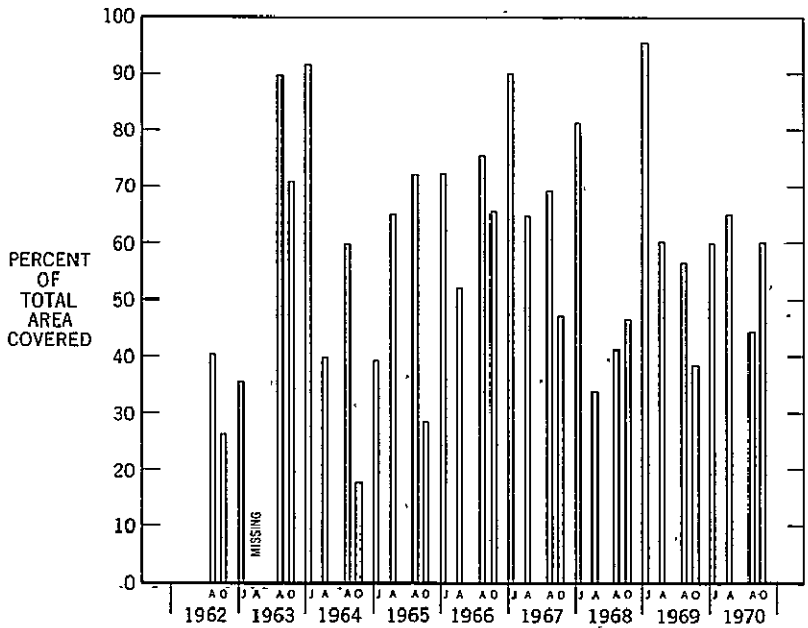

WESTERN PACIFIC
% OF AREA COVERED BY ≥ 6/10 CLOUD COVER
0°–10°S 180°–130°E

Figure B-10

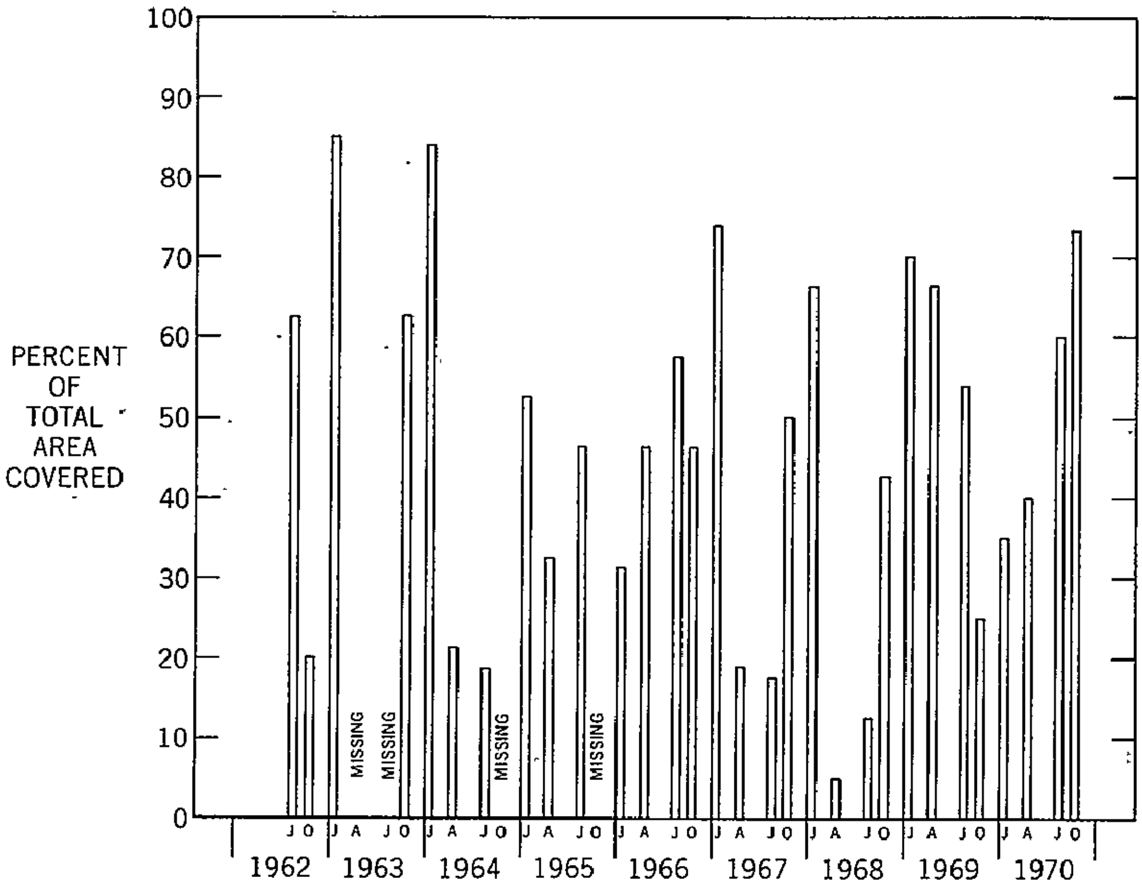

WESTERN PACIFIC
% OF AREA COVERED BY ≥ 6/10 CLOUD COVER
10°–20°S 180°–130°E

Figure B-11

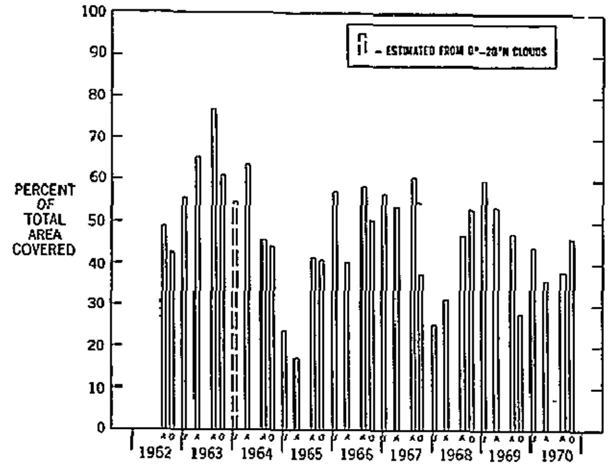

EASTERN PACIFIC
% OF AREA COVERED BY ≥ 6/10 CLOUD COVER
0°–30°N 100°W–180°

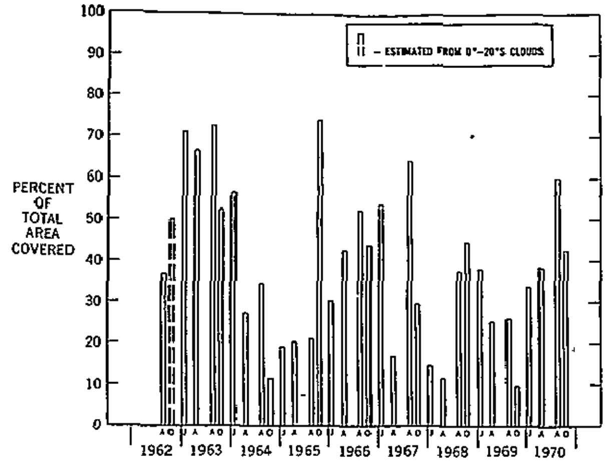

WESTERN PACIFIC
% OF AREA COVERED BY ≥ 6/10 CLOUD COVER
0°–30°N 180°–130°E

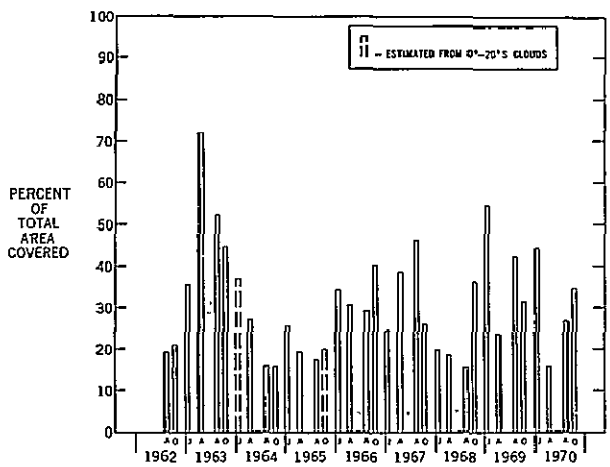

EASTERN PACIFIC
% OF AREA COVERED BY ≥ 6/10 CLOUD COVER
0°–25°S 100°W–180°

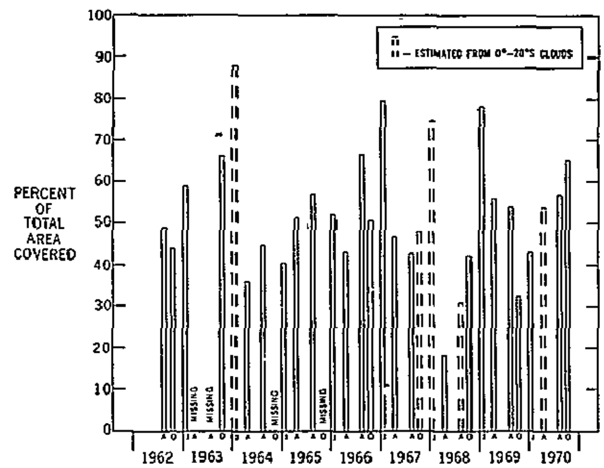

WESTERN PACIFIC
% OF AREA COVERED BY ≥ 6/10 CLOUD COVER
0°–25°S 180°–130°E

Figure B-12